Remote substituent effects on methyl torsional barriers and Pi electron density in stilbenes
by Brian Scott Metzger

A thesis submitted in partial fulfillment of the requirements for the degree of Doctor of Philosophy in Chemistry
Montana State University

Abstract:
Jet-cooled fluorescence excitation spectra and single vibronic level fluorescence spectra are presented for several substituted trans-stilbenes. Nearly complete assignments of the low-frequency skeletal modes and methyl torsional transitions are given. The methyl rotor barrier is used as a probe of the local μ electron density and is found to be very sensitive to the nature of the electronic state, along with substituents ten carbons away.

An extended conjugated system allows for the removal of possible steric interactions and the changes in the methyl barrier will be influenced by μ electronic effects. The trans-stilbenes examined are: p-hydroxy-trans-stilbene, p-methoxy-trans-stilbene, p-trifluoromethyl-trans-stilbene, p-dimethylamino-trans-stilbene, p'-hydroxy-p-methyl-trans-stilbene, p'-cyano-p-methyl-trans- stilbene, p'-trifluoromethyl-p-methyl-trans-stilbene, p'-dimethylamino-p-methyl-trans-stilbene, and p'-p-dimethyl-trans-stilbene. The molecules were chosen for the electron donating and withdrawing capabilities of the substituents. Jet expansion has been used to remove some of the spectral congestion arising from thermal population of low frequency vibrations. The methyl torsional barriers were measured and the substituent induced differences are discussed. The methyl barrier decreases with substitution of remote substituents.

Two electronic origins were found in the spectra of p-hydroxy-trans-stilbene and p-hydroxy-p'-methyl-trans-stilbene, and these origins are due to the two preferred conformers of the hydroxy group. The hydroxy functional group and the methoxy functional group act similarly in the excited state but differ as Van der Waals complexes with H2O.

A vibrational state mixing which accompanies methyl substitution is manifested as a Fermi resonance in the excitation spectrum and the positions and intensities of the coupled levels along with an approximate coupling matrix element are discussed.

REMOTE SUBSTITUENT EFFECTS ON METHYL TORSIONAL BARRIERS AND PI ELECTRON DENSITY IN STILBENES

by

Brian Scott Metzger

A thesis submitted in partial fulfillment

of the requirements for the degree

of

Doctor of Philosophy

in

Chemistry

MONTANA STATE UNIVERSITY
Bozeman, Montana

August 1996

APPROVAL

of a thesis submitted by

Brian Scott Metzger

This thesis has been read by each member of the thesis committee and has been found to be satisfactory regarding content, English usage, format, citations, bibliographic style, and consistency, and is ready for submission to the College of Graduate Studies.

Dr. Lee H. Spangler _____ 4/24/96
Date

Approved for the Department of Chemistry

Dr. David M. Dooley _____ 9/25/96
Date

Approved for the College of Graduate Studies

Dr. Robert H. Brown _____ 10/22/96
Date

STATEMENT OF PERMISSION TO USE

In presenting this thesis in partial fulfillment of the requirements for a doctoral degree at Montana State University-Bozeman, I agree that the Library shall make it available under rules of the Library. I further agree that copying of this thesis is allowable only under scholarly purposes, consistent with "fair use" as prescribed in the U.S. Copyright Law. Requests for extensive copying or reproduction of this thesis should be referred to University Microfilms International, 300 North Zeeb Road, Ann Arbor, Michigan 48106, to whom I have granted "the exclusive right to reproduce and distribute my dissertation in and from microform along with the non-exclusive right to reproduce and distribute my abstract in any format in whole or in part."

Signature Brian Mcgee

Date 9/30/96

ACKNOWLEDGEMENTS

I want to express my sincere gratitude to all of the people who supported me during my graduate career at Montana State University. I thank my advisor, Dr. Lee Spangler, for the opportunity to work with him on this research project and for giving his insight and energies to this work. I must acknowledge the many who read through the manuscript and offered valuable suggestions and criticisms. These include Dr. Pat Callis, Dr. David Singel, Dr. Jan Sunner, Dr. Eric Grimsrud, Mr. Bruce Fender, Mr. Kurt Short, and Mr. Kevin McMindes. I benefited greatly from the extremely valuable research assistance of Mr. Dave Duncan, Mr. Tim Kercher, Mr. Kendal Ryter, and many other academic colleagues within the chemistry department.

I would like to thank my parents and family for their encouragement during my time in Bozeman. Most of all I thank my wife, Krista, for supporting me in this endeavor and for her patience, loving encouragement, and overwhelming support.

TABLE OF CONTENTS

TABLE OF CONTENTS-Continued

LIST OF TABLES

LIST OF TABLES: continued

LIST OF TABLES: continued

LIST OF FIGURES

LIST OF FIGURES: continued

LIST OF FIGURES: continued

LIST OF FIGURES: continued

ABSTRACT

Jet-cooled fluorescence excitation spectra and single vibronic level fluorescence spectra are presented for several substituted trans-stilbenes. Nearly complete assignments of the low-frequency skeletal modes and methyl torsional transitions are given. The methyl rotor barrier is used as a probe of the local π electron density and is found to be very sensitive to the nature of the electronic state, along with substituents ten carbons away.

An extended conjugated system allows for the removal of possible steric interactions and the changes in the methyl barrier will be influenced by π electronic effects. The trans-stilbenes examined are: p-hydroxy-trans-stilbene, p-methoxy-trans-stilbene, p-trifluoromethyl-trans-stilbene, p-dimethylamino-trans-stilbene, p'-hydroxy-p-methyl-trans-stilbene, p'-cyano-p-methyl-trans- stilbene, p'-trifluoromethyl-p-methyl-trans-stilbene, p'-dimethylamino-p-methyl-trans-stilbene, and p'-p-dimethyl-trans-stilbene. The molecules were chosen for the electron donating and withdrawing capabilities of the substituents. Jet expansion has been used to remove some of the spectral congestion arising from thermal population of low frequency vibrations. The methyl torsional barriers were measured and the substituent induced differences are discussed. The methyl barrier decreases with substitution of remote substituents.

Two electronic origins were found in the spectra of p-hydroxy-trans-stilbene and p-hydroxy-p'-methyl-trans-stilbene, and these origins are due to the two preferred conformers of the hydroxy group. The hydroxy functional group and the methoxy functional group act similarly in the excited state but differ as Van der Waals complexes with H_2O.

A vibrational state mixing which accompanies methyl substitution is manifested as a Fermi resonance in the excitation spectrum and the positions and intensities of the coupled levels along with an approximate coupling matrix element are discussed.

CHAPTER ONE

INTRODUCTION

The importance of molecular conformation to chemical activity can not be understated since there is a direct link between the physical properties of a molecule and its structure. From simple atomic structures to the complex folding of proteins, scientists have long sought to understand the source behind structural preference. A simple case long studied by scientists is the internal rotation about a single bond and the resulting conformational preference in ethane. The hindrance to free rotation about the C-C bond in ethane was discovered because of discrepancies between the experimental determined entropy and the calculated entropy from statistical mechanics[1]. The internal rotation of a methyl group has now become a classic subject and spectroscopic studies have made it possible to develop a well accepted explanation for the origin of barriers in the ground state[2].

Spectroscopy is the study of the interactions between matter and electromagnetic radiation[3]. Spectroscopic investigations give chemists detailed information about specific molecular processes, such as vibrations, rotations, and electronic transitions. Information concerning the barriers to internal rotation

in the ground state can come from a number of sources including infrared, microwave, NMR, IR and Raman spectroscopy measurements[4-7].

Through comprehensive studies, the hindered internal rotation of the methyl group is well known for its extreme sensitivity to its local steric and electronic environment[8]. Any changes in molecular structure or the pi electronic density show up in the form of different barriers for the methyl group. Thus, when the methyl torsional transitions are observed in the spectrum, the methyl rotor can be used as a probe to study electronic features of the molecule.

Considering the methyl groups sensitivity to the local electron density, physical chemists anticipated a dramatic change in the potential for internal rotation by electronic excitation[9]. However, spectroscopy at room temperature is complicated by the inevitable hot band excitation originating from higher populated vibrational and torsional states. Consequently, there had been little information available for the internal rotation in electronically excited states[10]. With the advent of supersonic jet expansion, evidence of torsional motion in toluene, fluorotoluenes, and other substituted benzenes has been used to infer a relationship between changes in the torsional potential upon excitation and pi electron density within the molecule[11,12]. The supersonic expansion prepares isolated ultracold molecules with reduced spectral congestion and complex partners depending on expansion conditions[13].

The dramatic changes in the barrier heights for the methyl group upon electron excitation is generally discussed in terms of hyperconjugation and intramolecular hydrogen bonding[12]. Ab initio calculations confirm that

hyperconjugation is the dominant interaction in determining the methyl behavior in aliphatic systems containing a methyl group adjacent to an sp^2 carbon[14]. Since hyperconjugation involves an overlap of the methyl group orbitals with those of the ring, the sensitivity to local π electron density and observed conformational changes can be rationalized.

Work on p-methyl-trans-stilbene (CH_3-Ph-CH=CH_2-Ph) suggests the effects due to hyperconjugation extend further than the intermediate π system, where substitution of remote functional groups affects motion at the other end of the molecule. Spangler presented spectral evidence in p-methyl-trans-stilbene of methyl rotor activity characteristic of a three-fold barrier, which indicates that the two meta positions are inequivalent[15]. P-methyl-styrene (CH_3-Ph-CH=CH_2), similar in structure to p-methyl-trans-stilbene, has a small six-fold barrier similar to toluene[16]. Given this, the three fold barrier to methyl internal rotation is probably due to the remote phenyl ring six carbons away. The large distance separating the remote ring from the methyl bearing ring in p-methyl-trans-stilbene rules out simple steric interaction and the threefold barrier is most likely an electronic effect interacting through the conjugated system.

The idea of remote interactions dictated by through-bond electron transfer is intriguing since the usefulness of this concept can easily be seen in the field of organic chemistry and molecular electronics. A slow decrease in the interaction as a function of distance is especially important in the field of electronics[17]. Current research in such diverse areas as molecular electronics, protein-folding kinetics, and applied regioselectivity is the driving force behind the desire to

understand the nature of the excitation process on the π electron density in conjugated systems[18-21].

Statement of the problem

The aim of this research is to examine the effect of remote substituents on methyl torsional barriers in molecules where the substituted-phenyl ring is attached to a methyl bearing ring by means of a vinylene (-CH=CH-) linking group. Steric effects can be a strong factor in hindering the methyl torsion in single ring systems. Therefore, an extended conjugated system allows for the removal of possible steric interactions and the changes in the methyl barrier will be influenced by π electronic effects. The extended conjugated system of methyl substituted trans-stilbenes makes it ideal to measure these electronic effects.

Previous research in this group has found that the strong donating character of remote functional groups, such as the amino and methoxy functional groups, reduce the barrier of the methyl group ten atoms away on the stilbene skeletal frame[22,23]. Moreover, there is a pattern in the reduction of the barrier suggesting that the stronger the electron-donating group, the lower the barrier. More evidence is desirable to solidify the difficult task of understanding the mechanism for the remote substituent effects on the methyl torsional barrier. Presently, there has been no unified viewpoint for the intramolecular interaction responsible for the rotational barrier in electronically excited states[11]. This thesis

presents a study of the analysis of the barrier to internal rotation for the methyl group as a function of different remote substituents for several stilbenes.

A comprehensive data set should include at least two donors, two halogens, CH_3, H, and one acceptor to cover the wide range of substituent inductive properties. This study seeks to fulfill the above requirement by selecting previously uninvestigated functional groups shown in Figure 1 which are: p-hydroxy-trans-stilbene, p-methoxy-trans-stilbene, p-trifluoromethyl-trans-stilbene, p-dimethylamino-trans-stilbene, p'-hydroxy-p-methyl-trans-stilbene, p'-cyano-p-methyl-trans- stilbene, p'-trifluoromethyl-p-methyl-trans-stilbene, p'-dimethylamino-p-methyl-trans-stilbene, and p'-p-dimethyl-trans-stilbene. In these molecules, the perturbation to the methyl barrier is due to electronic effects and not steric effects from the remote substituent since the large distance between the methyl and remote ring and the rigidity of the stilbene frame prevent any through-space interaction. Comparison of the remote substituent effects on the methyl torsional barriers in the stilbenes mentioned here will allow for a sophisticated understanding to the origin of the methyl barrier in the stilbene system.

Also, the comparison of the slight differences in electronic effects of the remote substituent in these stilbenes furnishes an interesting look at a vibrational state mixing which accompanies methyl substitution. This coupling is manifested as a Fermi resonance in the excitation spectrum and the positions and intensities of the coupled levels along with an approximate coupling matrix element will be discussed.

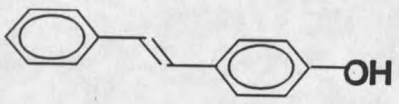

p-hydroxy-trans-stilbene

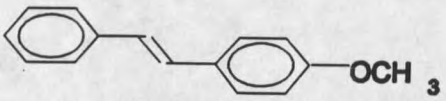

p-methoxy-trans-stilbene

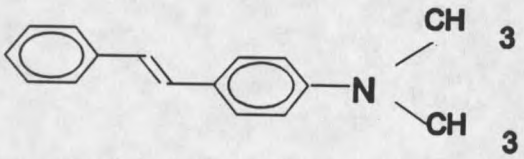

p-dimethylamino-trans-stilbene

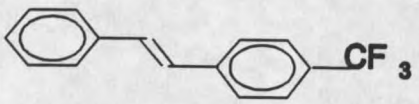

p-trifluoromethyl-trans-stilbene

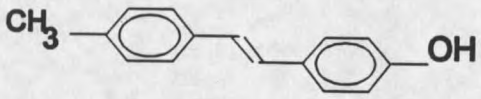

p'-hydroxy-p-methyl-trans-stilbene

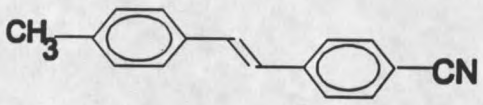

p'-cyano-p-methyl-trans-stilbene

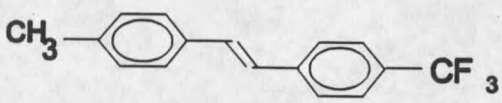

p'-trifluoromethyl-p-methyl-trans-stilbene

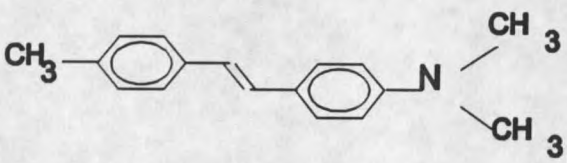

p'-dimethylamino-p-methyl-trans-stilbene

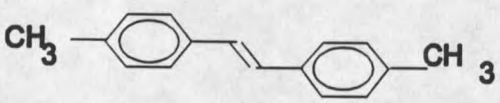

p'-p-dimethyl-trans-stilbene

Figure 1. The stilbene analogues examined in this study.

Finally, It would be expected that the methyl group's tendency to couple with ring vibrations and the observed changes in the torsional barrier should perform an important role in the relaxation processes of the excited-state trans-stilbene. Experimental evidence and theoretical arguments suggest that the methyl rotor is an accelerating functional group for intramolecular vibrational redistribution (IVR) within an isolated molecule[24-26]. Recent studies concerning the photochemistry of trans-stilbene discuss possible isomerization mechanisms, including IVR, that occur in the excited state[27-30]. In light of our current research focus on methyl torsional barriers, it would be appropriate to comment on our observations of possible isomerization dynamics in the excited state of trans-stilbene in relation to different methyl rotor behavior caused by remote substitution.

CHAPTER TWO

METHYL ROTOR THEORY AND HISTORY

Information about molecular structure and bonding can be retrieved by considering the nature of the energy levels of the methyl group. In usual harmonic approximations, the vibrational modes of the molecules are assumed to be small amplitude and are uncoupled from each other. The low frequency and large amplitude motion of the methyl torsion make it unlike other normal modes of vibrations. The methyl rotor may be interpreted as a rigid body rotating in a plane or a mass point moving in a circle of radius r. In the case of a rigid, free internal rotation, the potential energy is taken to be zero. The appropriate wave function describing the motion would then be the orthonormal particle-in-a-ring functions shown here:

$$\Psi = \frac{1}{\sqrt{2}} e^{im\phi} \text{ , } m = 0, \pm 1, \pm 2, \ldots .$$

The free rotor model above is incomplete for most molecules since a barrier generally hinders the internal rotation. This hindrance displays itself in the spectrum because the observed energy spacings are much larger than those

predicted by the free rotor model. Due to the three equivalent C-H bonds, the potential well will possess three minima, or some integer multiple of three, and the appropriate form for the potential function for hindered internal rotation is:

$$V=\Sigma_n[\ (V_n/2)*\ (1-\cos(nf))]. \qquad n= 3, 6, 9 \ldots$$

where n is an integer > 0 and *f* is the torsional angle[31]. The dominant component in this summation is usually the lowest component possessing the correct symmetry. The relative signs of V_3 and V_6 are valuable in identifying the shape of the potential. With a small positive V_6 and larger positive V_3, the total potential well appears to be sharper at the base and broader at the top. The reverse is true for a small negative V_6 relative to a positive V_3.

As the barrier increases, the internal rotation becomes highly hindered and takes on pseudo vibrational motion in the states well below the top of the potential well. If the system is in a state below the barrier, it is classically locked in that configuration and does not have enough energy to move to another equivalent configuration on the other side of the barrier.

Quantum mechanically, the system can tunnel through the barrier from one conformer to another. Tunneling represents an exchange, or permutation of nuclei, a symmetry operation not adequately treated by point group symmetry. The molecular symmetry groups of Bunker and Longuet-Higgins are used allowing classification of the spin states, the states of nuclear motion, and

electronic states of non-rigid molecules[32,33]. G_6 is the appropriate molecular symmetry group for single methylated trans-stilbenes since the frame to which the methyl group is attached has no symmetry about the torsional axis.

Table 1. The G_6 molecular symmetry table.

G_6	E [1]	(123) (321) [2]	(23)* (12)* (31)* [3]
A_1	1	1	1
A_2	1	1	-1
E	2	-1	0

In the G_6 molecular symmetry group shown in table 1, E is the identity operation, (123) and (321) are permutations of the nuclei, and the * signifies inversion of the spatial coordinates of the entire molecule through its center of mass[34].

To determine the electronic spectrum emerging from these energy states shown in Table 2, the torsion-rotation wavefunctions must be classified according to the symmetry species of the molecular symmetry group. The total wave function must observe the Pauli exclusion principle for the exchange of fermions and can have either even or odd parity for inversion[32]. This restriction applies to the * column in the G_6 molecular symmetry group. The direct product

$$\Gamma_{tot} = \Gamma_e \otimes \Gamma_v \otimes \Gamma_{tor} \otimes \Gamma_{rot} \otimes \Gamma_{ns} \subset A_1, A_2$$

for the total symmetry of p-methyl-trans-stilbene must be either A_1 or A_2, as expressed in the above equation. The use of supersonic expansion, discussed in Chapter Three, should create molecules in their zero point (skeletal) vibrational state. Hence, the electronic and vibrational symmetries will be A_1, and the methyl torsional levels are A_1 and E symmetry. The rotational symmetries are either A_1 (ee, oe), or A_2 (eo, oo)[35]. The symmetries of the torsional levels in p-methyl-trans-stilbene are resolved from how the torsional angles and basis functions transform under the operations of G_6 and are given in Table 2.

Table 2. The internal rotation angular momentum quantum number relating to the symmetry of the torsional state with G_6 symmetry.

m	E $\tau_{\Theta=0}$ 2cosmΘ	(123) τ+240 2cosmΘ	(23)* τ	
0	1	1	1	A_1
±1	2	-1	0	E
±2	2	-1	0	E
±3	2	2	0	A_1+A_2
±4	2	-1	0	E
±5	2	-1	0	E
±6	2	2	0	A_1+A_2

In p-methyl-trans-stilbene, the nuclear spin wavefunctions are either A_1 or E symmetry. From Table 3, we find all the rotational levels within a particular torsional band have the same nuclear spin symmetry. In G_6, A_1 and A_2 torsions

have A_1 nuclear spin symmetry and have a statistical weight of 8. Torsions with E symmetry must have a E nuclear spin symmetry and a statistical weight of 4.

Table 3. The symmetry species for G_6 p-methyl-trans-stilbene.

Γ_{tor}	$\Gamma_e \otimes \Gamma_v$	Γ_{rot}	Γ_{ns}	Γ_{tot}
A_1	A_1	A_1	A_1	A_1
E	A_1	A_1	E	A_1
E	A_1	A_2	E	A_2
A_2	A_1	A_1	A_1	A_2
A_1	A_1	A_2	A_1	A_1

One of the effects of the different nuclear spin symmetries of the A and E torsional levels is the rigorous selection rule in electronic spectra. The A_1 and E spin isomers result in the observance of both $A \leftrightarrow A$ and $E \leftrightarrow E$ transitions in the excitation spectrum. On the other hand, transitions starting in E levels can only go to other E levels, and A_1 to A_1 levels. Consequently, the selection rules help with the identification of transitions by greatly simplifying the dispersed emission spectra. The statistical weight ratios of the torsional transitions affect their relative intensities directly and partly explains the electronic origin intensity ratio seen in the spectra for the methylated trans-stilbenes investigated in this thesis.

For the methyl substituted trans-stilbene compounds studied in this thesis, the energy levels of a methyl rotor are labeled $0a_1$, 1e, 2e, $3a_2$, $3a_1$, 4e, 5e, $6a_2$, $6a_1$... in order of increasing energy[15]. The dependence of the energy of each internal rotational transition as a function of a V_3 barrier height is illustrated in

Figure 2. By identifying some of the low torsional levels in the spectrum, higher transitions can often be located by a comparison with the calculated frequencies.

The geometric structure of an excited electronic state usually differs from that of the ground state[36]. The rotational fine structure of the vibrational bands is the basic way to yield information about the moments of inertia and hence the molecular structure. The experimental methods used in this thesis do not have the resolution necessary to observe rotational fine structure, thus the Franck-Condon principle offers the only other method of obtaining information about the geometrical structure of an electronic state.

A qualitative picture of The Franck-Condon principle has the sluggish nuclei retaining their position and momentum while the electrons quickly make a transition[37]. The nuclei experience new forces since they are usually displaced relative to the equilibrium geometry of the new potential surface. A change in the conformational preference, displacement of the potential energy surface, and barrier shape all contribute to the observed vibronic band intensities. The Franck-Condon principle does not influence the absolute intensity, but only affects its distribution among vibrational components[38].

The quantitative application of the Franck-Condon principle requires a brief quantum-mechanical discussion. The probability that an electronic transition between two states will occur is proportional to the square of the transition moment integral having the form: $M = \int \psi'^{*} \mu \psi \, d\tau$, where the prime

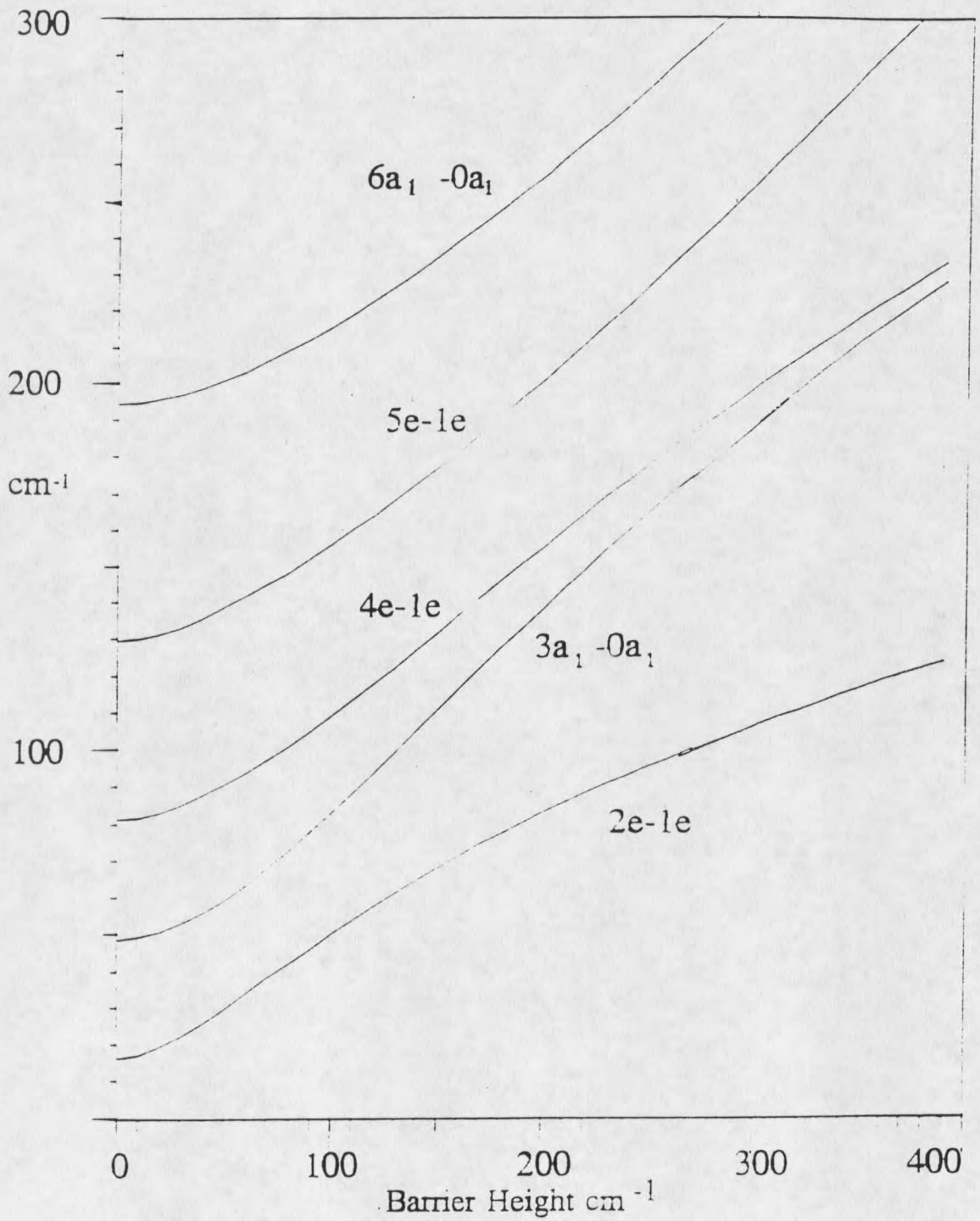

Figure 2. Methyl rotor splitting as a function of V_3 barrier height.

denotes an excited state and μ is the dipole moment operator. For most spectroscopic purposes the nuclei are assumed to be stationary and the dipole moment operator depends only on electronic motion. Since the nuclei move much more slowly than the electrons, the Born-Oppenheimer approximation states that it is reasonable to factor the total wave function for a molecule into a product of wave functions as follows:

$$\psi = \psi_e \psi_v$$

where ψ_e is the electronic wave function, and ψ_v is the vibrational wave function. In the Born-Oppenheimer approximation, transitions between torsional levels in two different electronic states can be described by an electronic transition moment integral times a vibrational overlap integral,

$$M = \int \psi^*_{e'} \mu_e \psi_e \, d_e \int \psi^*_{v'} \psi_v \, d_v \ .$$

The square of the vibrational integral on the right is commonly referred to as the Franck-Condon factor. This integral represents the overlap of the vibrational wave functions of the ground and excited states. The magnitude of this integral affects the relative intensities among vibrational components.

The first step in determining the potential barrier for a methyl group from experimental data is to use the fortran program, VNCOS, written by Laane and coworkers[39]. This program calculates the eigenvalues for a potential function of

the type Σ_n $(V_n/2)(1-\cos nx)$. The V_3 and V_6 terms are optimized to reflect the barriers that generate the proper frequency differences of the rotor levels observed in the spectrum.

VNCOS was written to calculate vibrational levels for the potential energy surface of a single electronic state, but lacks the ability to calculate the band intensities in the excitation or dispersed emission spectra. A program written by Spangler, known as INROT, calculates the frequency of a transition and its intensity based on the barriers previously calculated from VNCOS for the ground and excited states[40]. The intensities are calculated from the Franck-Condon factors. The values for the rotational barrier and conformational change of the methyl group can then be optimized to yield the observed intensities and frequencies.

As mentioned before, supersonic expansion cools the molecules down to its lowest a_1 and e levels. Thus transitions to the a_2 levels in the electronically excited state will be symmetry forbidden and only a_1 and e levels will be accessible. If the conformation of the methyl group was the same for both the ground and excited state, only the a_1-a_1 and e-e transitions would be observed, since only these transitions would have appreciable Franck-Condon overlaps. If many transitions in the methyl rotor progression have intensity in a spectrum, the conformation change is typically 30-60°.

Molecular Orbital Explanation for the Barrier to Internal Rotation

The conformational preferences in molecules can be traced to the nature of interactions between molecular orbitals. Barriers to internal rotation in molecules are among the most interesting properties that are amenable to qualitative molecular orbital theory. The acceptance of a simple qualitative molecular orbital explanation for the staggered preference and resulting barrier to internal rotation in ethane has led scientists to extend the model to more sophisticated molecules[2].

For example, the preferred eclipsed conformation for aliphatic systems in which one of the methyl hydrogens of a methyl group eclipses the double bond can be explained by the interaction between the occupied methyl group orbitals of π symmetry and the π and π^* orbitals of the unsaturated linkage[9]. The origin of the rotational barrier is similarly related to that of ethane[14]. The highest occupied and lowest unoccupied orbitals of the methyl rotor and the π system of a double bond are shown in Figure 3. The first of the four interactions are between filled valence shells. The overlap between the two fragments is greatest when the two methyl hydrogens are positioned directly over the double bond. The interaction between these filled orbitals (labeled A) is repulsive since they are both occupied, and the staggered conformation is more destabilized by closed-shell repulsion than the eclipsed one. This destabilization is most likely

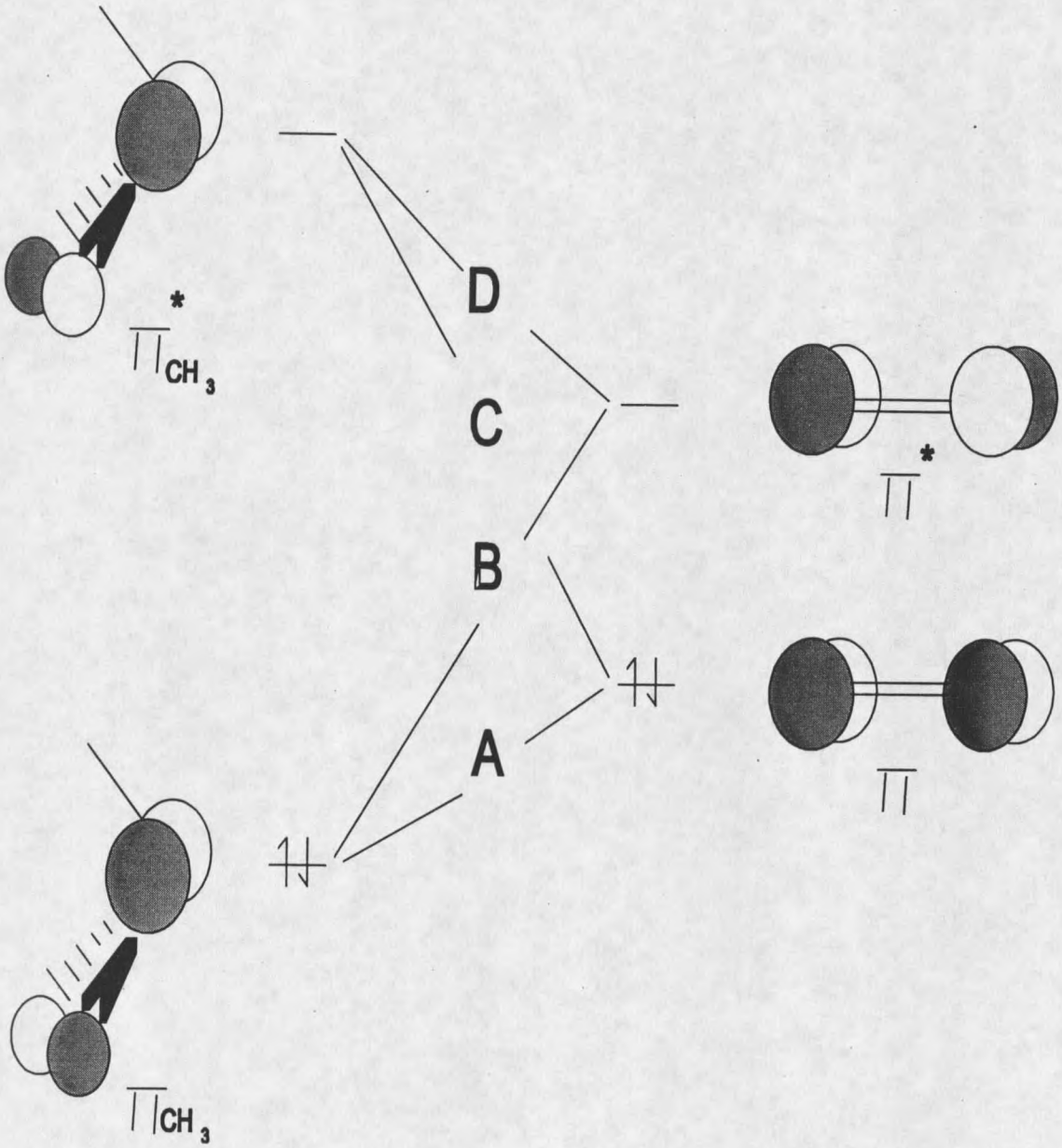

Figure 3. Interaction of the π system of a nonpolar double bond with the π and π* orbitals of a methyl group.

the main factor responsible for the preference for the eclipsed methyl group conformation. If the four electron interaction is eliminated by the promotion of an electron to a higher orbital; e.g., by $\pi\pi^*$ excitation, then other factors may dictate a different preferred conformation of the methyl group in an electronically excited state. For example, the methyl group has been found to prefer a staggered conformation of C-H bonds with respect to carbonyl functionality in the excited states of carbonyl compounds[14]. Thus the conformation having minimum π electron overlap is favored in the ground state and the conformation of maximum π overlap is favored in the excited state.

A particular carbonyl compound, acetaldehyde, has a considerably smaller barrier to rotation (1.16 kcal/mole) than does propene (2.0 kcal/mole)[41]. A qualitative description of a methyl group attached to a polar double bond has been proposed to explain this reduction in the barrier between propene and acetaldehyde[9]. The reduction in the barrier mainly involves a secondary overlap contribution involving the methyl hydrogens and the far end of the double bond. A general illustration of this secondary overlap contribution and brief discussion is presented here. Since the left atom in the polar double bond is more electronegative in Figure 4, the empty π^* double bond orbital will be heavily localized on the right atom. According to simple electronegativity perturbations, interaction B takes on added importance at the same time interaction C is diminished[9]. Figure 4 shows the dominating interaction between the π_{CH_3} and π^* fragment orbitals (labeled B in Figure 3). Thus the total positive overlap between

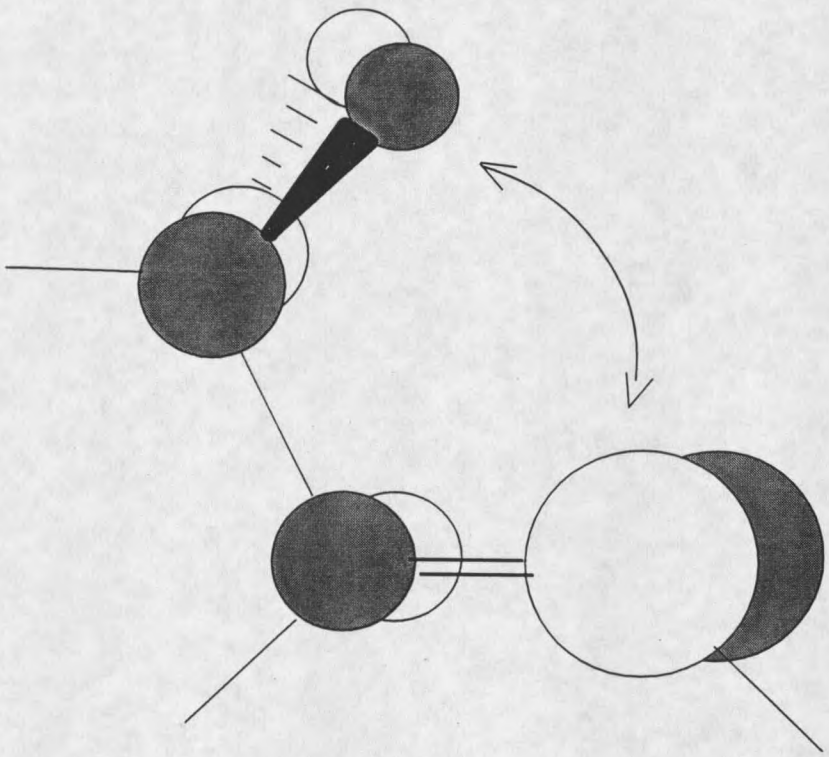

Figure 4. The secondary overlap contribution involving the out-of-plane methyl hydrogens (π_{CH3}) and the far end of the π^* system of a polar double bond.

these fragments is decreased and the stabilization is less. Interaction B should increase the preference for the eclipsed arrangement and should increase the rotational barrier. In the case of acetaldehyde, the double bond is polarized in the opposite manner and interaction B for acetaldehyde is depicted in Figure 5. Interaction B loses some of its ability to distinguish between the staggered and eclipsed conformers. A reduction in conformational preference for the eclipsed arrangement is observed since the rotational barrier for acetaldehyde has decreased. The point to be emphasized is the importance of this secondary overlap contribution to the sensitivity of the methyl group to its local environment.

The secondary overlap contribution can also be illustrated in molecules with a methyl group attached to a symmetrical local environment. An example of this can be seen in molecules such as nitromethane, toluene, p-xylene, p-fluorotoluene, and 2-methylpyrimidine[42-46]. The barrier to internal rotation in all these molecules was found to be small. Although the interactions present in the aliphatic compounds are also present in these aromatic compounds, the symmetric, uniform π electron distribution on the atoms on either side of the methyl group in the aromatic compounds makes the interaction between the orbitals nearly equal at all torsional angles. This symmetric π electron density causes the forces due to hyperconjugation to nearly cancel and gives rise to the observed small barriers. It is generally accepted that substitution in a symmetric local environment renders the methyl group a nearly free rotor[46].

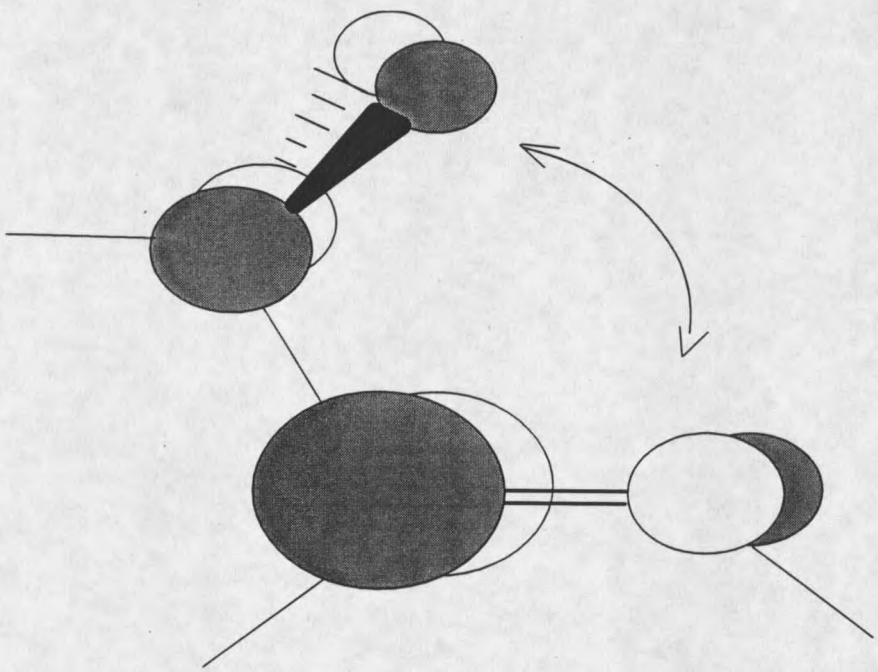

Figure 5. The generalized description of the interaction between π_{CH3} and π^* fragment orbitals for acetaldehyde.

If the aromatic ring is substituted in a position that breaks the symmetry, the electron densities can become unbalanced causing changes in the nature and the magnitude of the barrier. This reasoning has a significant impact on the results found for p-methyl-trans-stilbene. Despite the qualitative similarity of the two adjacent C sites in this molecule, a large three fold barrier was found in the excited state[15]. This result suggests a significant asymmetry in the electron distribution in the stilbene molecule in the excited state.

The simple orbital picture briefly discussed in this chapter should be able to provide qualitative information about the variation in torsional barriers for methylated stilbenes as a function of detailed molecular environment. We feel these ideas best represent the origin of the sensitivity of the methyl group to π electronic effects from the functionality of substituent effects, as will be shown in this thesis for substituted stilbenes.

CHAPTER THREE

EXPERIMENTAL PROCEDURES

At room temperature, spectroscopy of non-rigid molecules is a very difficult process due to the inevitable hot band excitation originating from higher populated vibrational and torsional states. Supersonic free expansions have been widely known to produce extensive cooling of translational and partial cooling of rotational and vibrational degrees of freedom of molecular gases[47]. Since supersonic free expansion is used to cool the molecules studied in this thesis, the nature of the cooling process will be briefly discussed.

The heated sample is entrained in helium and the gas mixture is flowed through a pulsed nozzle. As the gas expands from the high pressure region at 3-5 bar into the low pressure chamber around 10^{-5} torr, the binary collisions of the sample and the carrier gas produce extensive cooling in the transitional, vibrational, and rotational degrees of freedom. The collisional energy transfer occurs until the gas density becomes too low to support collisions and ends the cooling process. High backing pressures allow for more efficient cooling, while low backing pressures can not cool the molecule down to the zero vibrational level completely, resulting in hot bands. The supersonic jet expansion process results in molecules at nearly 0 K (0.1 K translational temperature, 3-5 K

rotational temperature, and 10 K ca. Vibrational temperature)[48]. Supersonic expansion may also produce weakly bound molecular complexes formed between the seeded molecule and the helium carrier gas[47]. Therefore, different backing pressures were used to identify possible hot bands and helium complexes that might appear along with low frequency transitions.

The experimental methods used in obtaining excitation spectra are shown in Figure 6. The molecular beam is generated in a six-inch nominal six-way cross evacuated by a Varian Vhs-6 diffusion pump backed by a Varian sd-450 mechanical pump. The samples are solids of low volatility near room temperature and are susceptible to decomposition if heated above about 300 °C. The stilbenes were heated to 130-180°c and entrained with 2-5 bar high purity helium before supersonic expansion through a General Valve Series 9 pulsed nozzle into the vacuum chamber. The nozzle pin hole diameter was 0.8 mm except for a 0.1 mm orifice to produce further cooling in p-trifluoromethyl-trans-stilbene and p'-trifluoromethyl-p-methyl-trans-stilbene.

For our water complexation experiment, a dual gas flow line apparatus was constructed to control the concentration of water in complexation of the stilbenes. This allowed us to study the concentration dependence of the spectra by splitting the helium flow and leading one branch through a flow controller and a container with water before recombining it with the main flow. HPLC grade water was used without further purification.

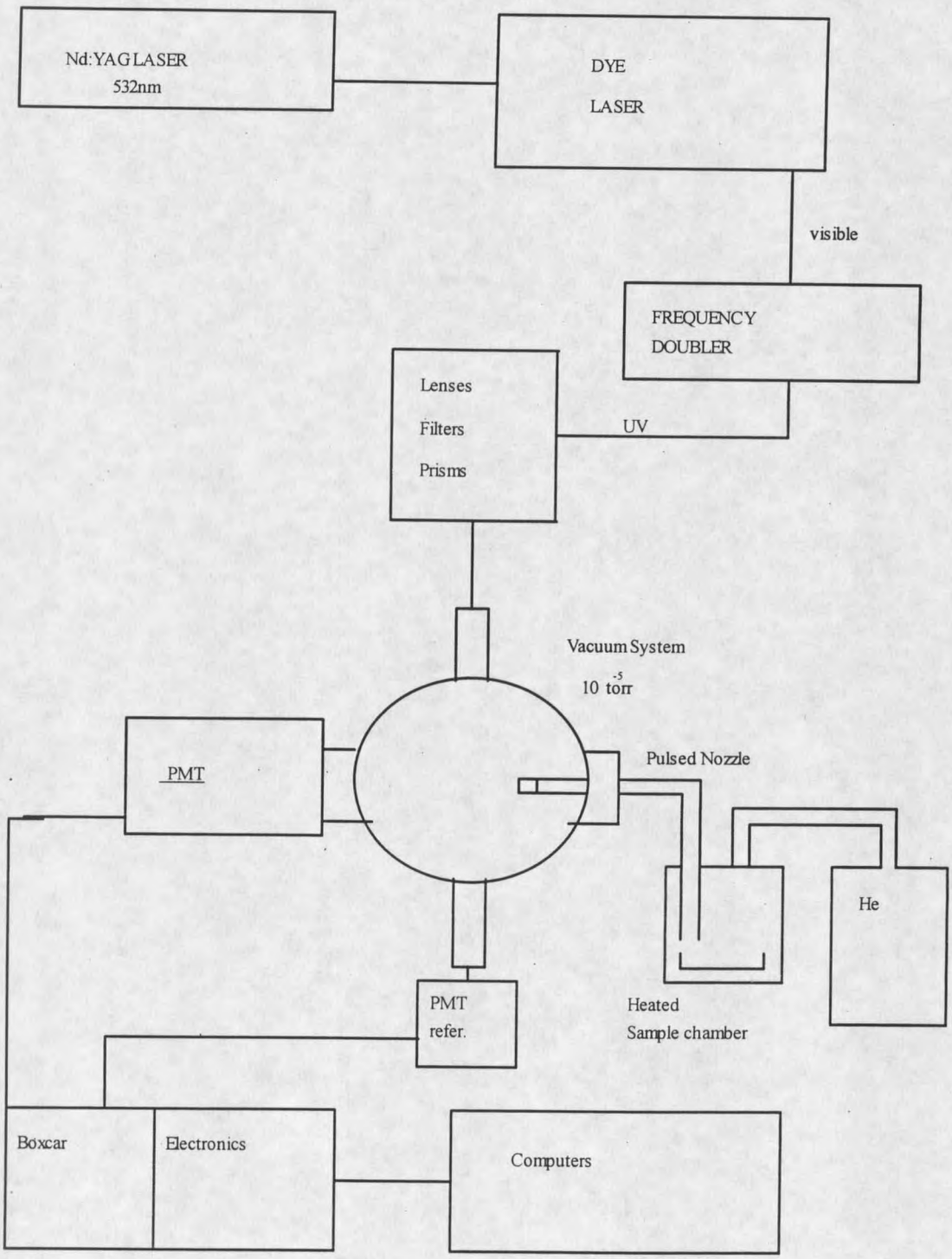

Figure 6. The apparatus for one-photon fluorescence excitation experiments.

The source is a Lumonics Hyperdye pulsed dye laser capable of 0.07 cm^{-1} resolution and has a Bethune amplifier cell which greatly improves beam quality. The dye laser is pumped by a Lumonics HY750 Nd:YAG laser operated at 532 nm with a 20Hz repetition rate and a pulse duration of 8 ns. The stilbenes analyzed in this thesis cover a broad wavelength region from 28,500 to 32,500 cm^{-1} requiring several different dyes including DCM, R640, and LDS 698 mixed in 100% pure methanol.

The visible light is frequency doubled to the UV with a Lumonics Hypertrack 1000 Doubler using a BBO crystal. The appropriate Schott filters were used to remove visible light before passing through a spatial filter and a focusing lens. The UV light crosses the jet expansion at right angles, and the intersection is at one focal point of a Melles Griot REM 014 ellipsoidal reflector. An EMI 9813qb photomultiplier tube (PMT) collects the fluorescence at the other focal point. The resulting signal is averaged by a Stanford Research Systems boxcar integrator, digitized, and stored on an IBM compatible computer. The spectra presented are normalized for laser intensity by passing the UV beam through a solution of Rhodamine 590 and detecting the solution fluorescence with a second PMT.

Dispersed emission (DE) experiments were performed to measure ground state energy levels and are conducted with the same experimental apparatus described previously with only slight modifications. The laser is fixed at a specific absorption frequency of the molecule, and the emission takes place to

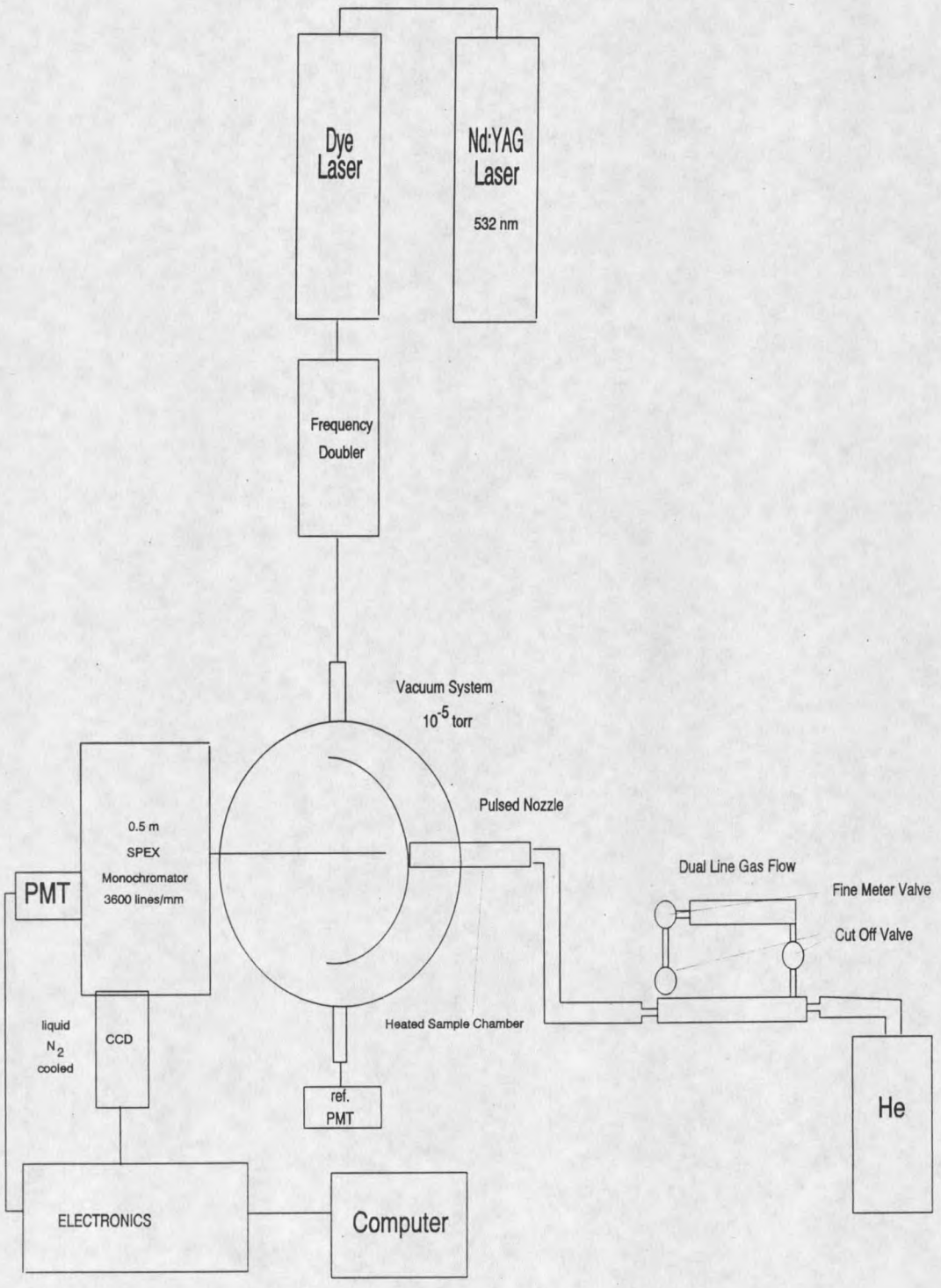

Figure 7. The apparatus for dispersed emission experiments utilizing the CCD detection system.

symmetry allowed ground state energy levels. This can also be used for identification of the methyl torsional transitions, such as "a" and "e" levels which have different nuclear spin symmetries. Specifically, if an "a" transition is excited, the emission will go only to "a" levels in the ground state. A Spex monochromator with a 0.05m focal length and a 3600 lines/mm grating collects the emission at the other focal point. The monochromator disperses the fluorescence and focuses it onto a Princeton Instruments liquid nitrogen cooled charged coupled device (CCD) detector. CSMA software allows the user to collect, store, process, and plot data from the CCD detector. The CCD virtues include it's high sensitivity, high fill factor, and large format capability. Additionally, the CCD's imaging capabilities eliminate the need for scanning the monochromator over the frequency range, cutting the data collection time from days to hours.

Finally, it should be noted that the excitation spectra offer far greater sensitivity than the dispersed emission spectra since total fluorescence is collected in the former case. Furthermore, the resolution in the excitation data is limited by the laser bandwidth; the dispersed emission resolution is limited by the monochromator where it is achieved at the expense of sensitivity. Thus, the vibrational frequencies are generally more accurate in the excited state than the ground state.

Preparation of Stilbenes

The chemistry of stilbene is straightforward and allows for the creation of many functional derivatives. The main method in preparing the para-substituted stilbene molecules is a Wittig reaction between the appropriately substituted aldehyde and the ylid[48]. The ylid was either purchased commercially from Lancaster Chemical Co. or made in an Arbusov reaction[49]. The Wittig synthesis is known for high product yield and is advantageous due to the absence of skeletal rearrangements during carbon-carbon double bond formation in trans-stilbene. The preparation of the anion consisted of adding the ylid to a strongly basic reagent, sodium hydroxide, in 1,2-dimethoxyethane. The elevated temperatures during the reaction prevent any cis-stilbene isomer from being present and only the stable trans isomer would be expected[49]. The compounds were collected using vacuum filtration and recrystalized in pure ethanol. Identity and purity of compounds were assessed by 300mhz ^{1}H NMR, FTIR, and gas chromatography.

P'-p-dimethyl-trans-stilbene was synthesized by first generating the ylid in an Arbusov reaction between 12.38 ml of triethylphosphite and 10.75 ml α-chloro-para-xylene. The mixture was heated gently for 1 hour. Four grams (0.0217 moles) of the ylid were dissolved in 80ml of 1,2-dimethoxyethane (DME) and added to 1.30 grams of NaH. The crude "ylid" product was used without further purification in most cases. It was invariably contaminated with starting material, but this proved easier to remove at the next stage. After refluxing for

several minutes, the solution was combined with 2.61 grams (0.0217 moles) of p-tolualdehyde. The solution was heated to boiling and refluxed for 1 hour. The solution was white in color and semi-transparent white crystals formed upon addition of distilled water. The crystals were collected using vacuum filtration and recrystalized in 100% ethanol. This procedure was also used for the synthesis of p'-methoxy-p-methyl-trans-stilbene, p-dimethylamino-trans-stilbene, p'-dimethylamino-p-methyl-trans-stilbene, p-trifluoromethyl-trans-stilbene, and p'-trifluoromethyl-p-methyl-trans-stilbene.

P'-cyano-p-methyl-trans-stilbene was synthesized by adding 2 equivalents of NaH in 80 ml of DME to 5 grams (0.0121 moles) of 4-cyano-benzyl-triphenylphosphonium chloride, purchased from Lancaster Chemical and used without further purification. After refluxing for several minutes, 1.828 grams (0.0121 moles) of p-tolualdehyde were added to the mixture followed by one hour of additional refluxing. The solution was dark orange in color and white crystals formed upon addition of distilled water. The crystals were collected using vacuum filtration and recrystalized in 100% ethanol.

P'-hydroxy-p-methyl-trans-stilbene was synthesized in a deakylation reaction by first preparing p'-methoxy-p-methyl-trans-stilbene following the procedure outline for p'-p-dimethyl-trans-stilbene[50]. P'-methoxy-p-methyl-trans-stilbene was added to 4 equivalents of boron tribromide methyl sulfide in 30 ml of 1,2-dichloroethane under an atmosphere of pure nitrogen. Boron trihalides are used to cleave aliphatic methyl ethers. The reaction mixture was refluxed until

the starting material had disappeared. The reaction mixture was then hydrolyzed by adding 30 ml of water and subsequently diluted with ether. The organic phase was separated and washed with 1M $NaHCO_3$, followed by 3 X 20 ml washings with 1N of NaOH. The combined NaOH washings were extracted into ether; the organic phase was separated and dried with $MgSO_4$, and the ether was removed via vacuum. The identity and purity of p'-hydroxy-p-methyl-trans-stilbene was assessed by 300mhz ^1H NMR and gas chromatography.

P-hydroxy-trans-stilbene was obtained from Lancaster Chemical and p-methoxy-trans-stilbene was obtained from Sigma Chemical and both were used without further purification.

CHAPTER FOUR

EXPERIMENTAL RESULTS AND ASSIGNMENTS

A considerable amount of published work on trans-stilbene has focused on its photoisomerization dynamics. Several reviews cover the current understanding of stilbene properties, mechanism of cis-trans isomerization, and influence of substitution on excited states of stilbenes in solution[52-54]. The extensive chemical work already performed on trans-stilbene will help in the understanding of the chemical relevance of our physical observations. For example, substituted stilbenes show fluorescence emission in the range from 340-400nm in solution and the fluorescence maximum is sensitive to the particular substituent[55]. Obviously, studies in the condensed phase prevent the resolution of low frequency modes such as methyl internal rotation, but they help provide an approximate location for absorption.

Supersonic jet spectroscopy has allowed the study of collision-free, isolated trans-stilbene[56,57]. Jet studies were crucial in the assignment of the low frequency vibronic structure in determining the geometry for trans-stilbene. Although trans-stilbene has 72 normal modes, only a few appear in the first 300 cm^{-1}, so that complete assignment of the low frequency region can be

achieved[52]. A description of the low frequency modes investigated and assigned in trans-stilbene is shown in Figure 8.

Since all vibronic transitions in the cold jet are from the totally symmetric zero-point energy vibrational state, the fluorescence excitation and emission of a "planar" stilbene are expected to exhibit mainly A_g (in-plane) bands. According to the Franck-Condon principle, the similar C_{2h} point group symmetry for the ground and excited states of trans-stilbene allow nontotally symmetric vibrations to be seen only as totally-symmetric double quantum jumps[58]. The two lowest frequency, out-of-plane modes, ν_{36} and ν_{37}, are of A_u (or A" in C_s) symmetry and require two quanta ($A_u \otimes A_u = A_g$) to be allowed. The absence of certain symmetry forbidden bands, such as 37^1_0, has led to a general acceptance of a planar C_{2h} structure in both the S_0 and S_1 states for trans-stilbene[59].

Since ν_{37} is the C_e-phenyl torsion, it measures the rigidity of the stilbene molecule. The observance of the low frequency, anharmonic, out of plane ν_{37} mode and the dramatic frequency change in the S_0-S_1 excitation from 9 cm^{-1} to 45 cm^{-1} has given considerable insight into the extent of conjugation in trans-stilbene[35]. The increased frequency is supported by the decreased C_e-phenyl bond length from 1.48 angstroms in S_0 to 1.42 angstroms in S_1[59]. The increased delocalization of the π electron density in the excited state, exemplified by the five-fold increase in the ν_{37} frequency, can be a reason behind the observed increase in the barrier of the methyl rotor in the excited state.

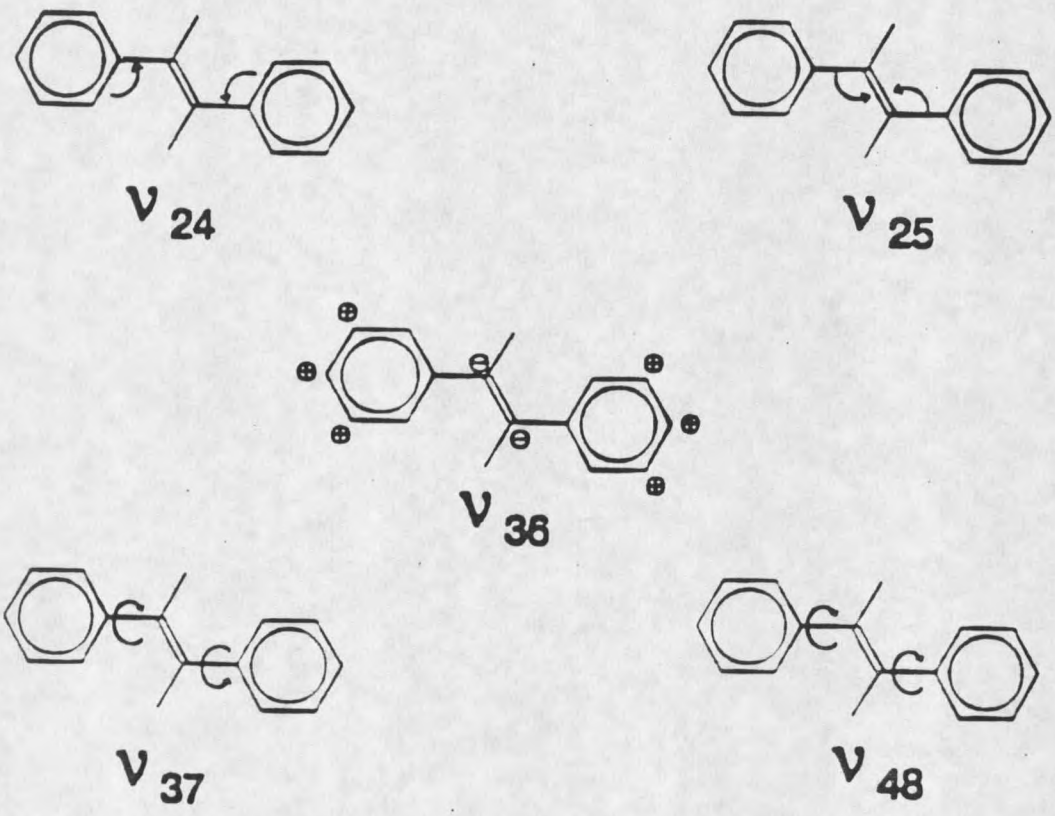

Figure 8. A description of the low frequency modes of trans-stilbene.

This section presents the spectra of ten compounds, four of which do not contain a ring methyl group. The substituents were chosen for either their electron donating or withdrawing properties. The influence of the electronic effects of substituents and their mode of transmission through the aromatic system can be measured by the changes in the barrier to internal rotation relative to p-methyl-trans-stilbene as described in the introduction.

In previous work by others, both the amino and methoxy functional groups were found to lower the barrier to internal rotation of the methyl group relative to p-methyl-trans-stilbene[21,22]. Additionally, two methoxy conformers were observable in the p'-methoxy-p-methyl-trans-stilbene excitation spectrum and the methyl barrier was found to be dependent on the methoxy conformation. The methyl torsional levels built off the red-shifted methoxy conformer electronic origin can be fit to a 10% lower barrier relative to the second conformer. Following the relationship between donating strength and barrier height of the amino and methoxy functional groups, the red-shifted conformer was determined to be a stronger donor. The red-shifted origin was assigned to the syn (with respect to the ethylenic linkage in stilbene) conformer from rotational coherence spectroscopy discussed in Chapter Five.

Experimental Results

p-hydroxy-trans-stilbene

The hydroxy group is a strong electron donor similar to the methoxy, and amino functional groups. Additionally, the hydroxy substituent has been previously shown to hydrogen-bond with various solvent molecules having proton-accepting ability in the supersonic jet[60]. The electronic excitation changes the acid-base properties of the molecule making the transfer process possible. Thus, p'-hydroxy-p-methyl-trans-stilbene is an attractive candidate for investigation of hydrogen bonding influences on methyl behavior in conjugated systems

But given the complications caused by the anharmonic methyl torsion, the possible hydroxy conformations, and the possible presence of water complexes, the experimental work on the simpler p-hydroxy-trans-stilbene will be presented first. Figure 9 shows the one-photon fluorescence excitation spectrum of p-hydroxy-trans-stilbene. The frequencies are given in cm^{-1} units relative to the electronic origin. The dye laser was scanned at a rate of 0.2 cm^{-1}/sec, with points digitized and stored every 0.15 cm^{-1}. The vibronic structure is consistent with the normal mode vibrations of the stilbene molecule, and nearly identical to p-methoxy-trans-stilbene[21]. Figure 10 aligns the previously published, excitation spectrum of p-methoxy-trans-stilbene above the p-hydroxy-trans-stilbene

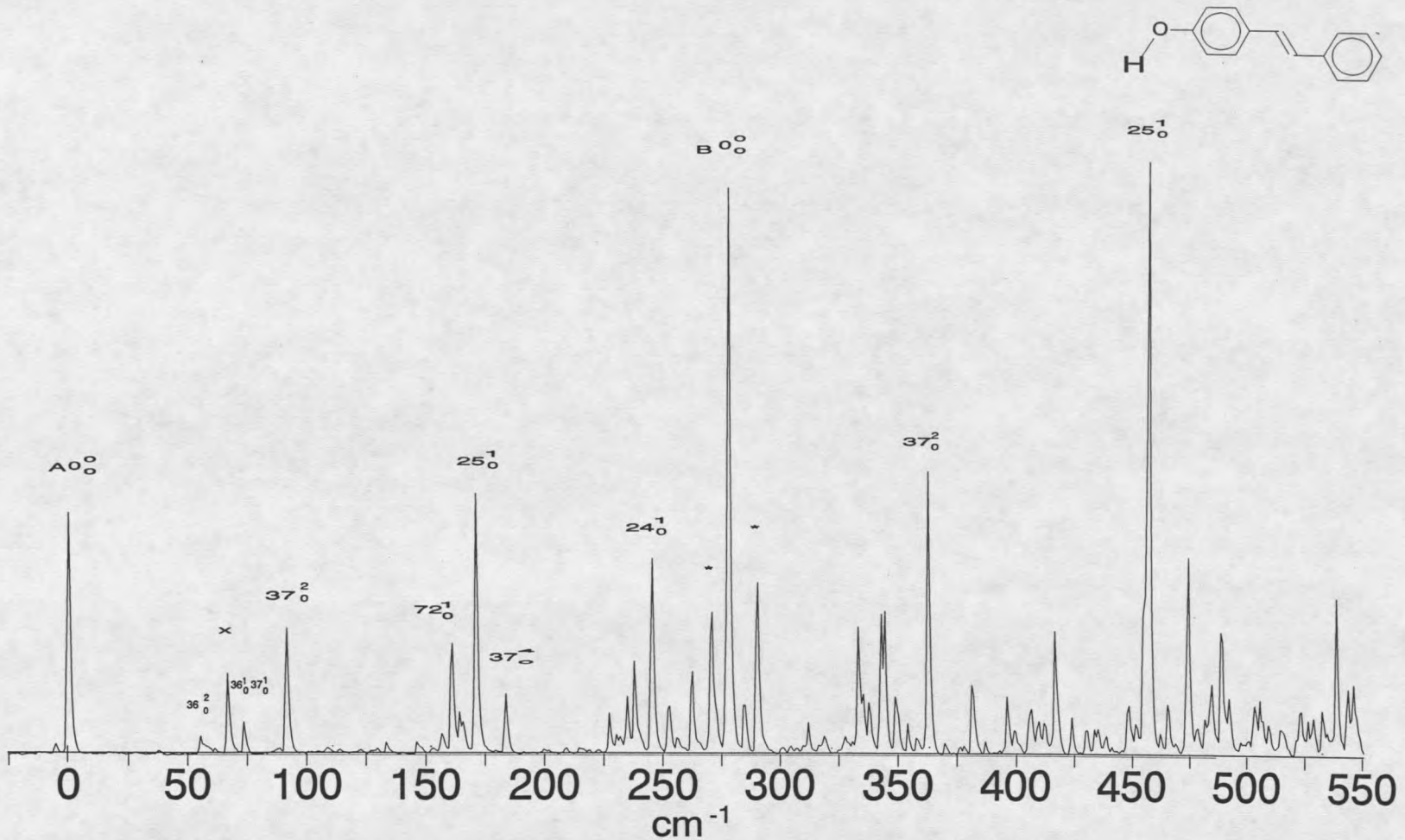

Figure 9. The fluorescence excitation spectrum of p-hydroxy-trans-stilbene. The conformer origins are identified with labels A and B.

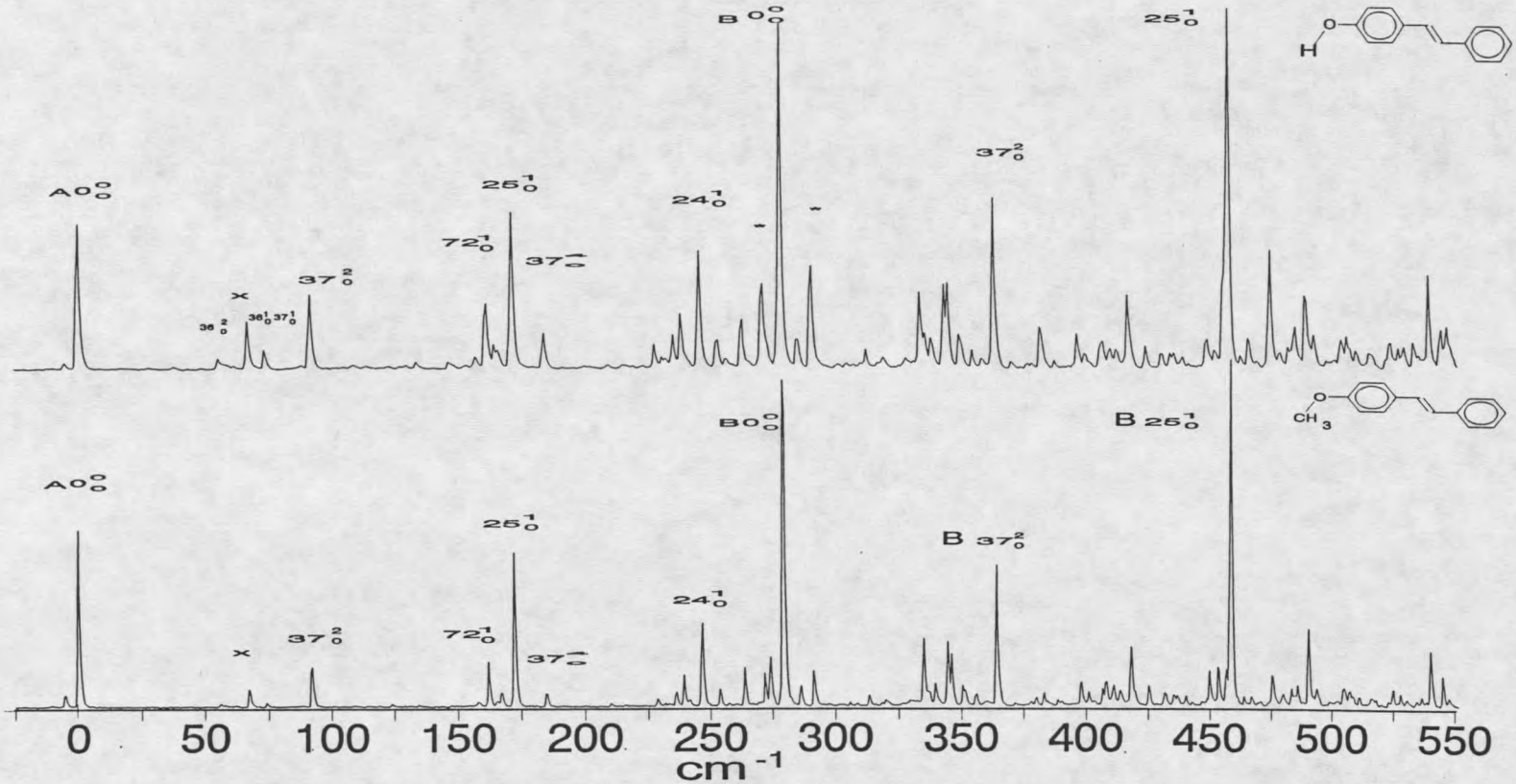

Figure 10. Comparison of the fluorescence excitation spectra of p-hydroxy-trans-stilbene and p-methoxy-trans-stilbene.

spectrum to illustrate the similarity between the two molecules. This similarity yields an important piece of information since by analogy to p-methoxy-trans-stilbene, two electronic origins can be identified and are labeled A and B 0^0_0, respectively. The same arguments made for the two origins in p-methoxy-trans-stilbene can be made for p-hydroxy-trans-stilbene. The increased congestion in the spectrum of p-hydroxy-trans-stilbene compared to p-methyl-trans-stilbene suggests more than one electronic origin, since replacing the methyl group with a hydroxy group should not greatly increase vibrational structure. The lowest energy feature and intense band at 30,744 cm^{-1} is readily identified as an electronic origin since it is not temperature dependent and no features appear further to the red. The strong transition 278 cm^{-1} above the first origin has no analog to a skeletal vibration in trans-stilbene and has a ν_{25} frequency much different than that of the first origin built on it. The absence of a strong transition at 2 x 278 cm^{-1}, expected for a vibronic mode built off the A origin, is additional support for a second origin. As in p-methoxy-trans-stilbene, the two origins are due to the conformation of the functional group. The preferred conformation of the methoxy or hydroxy functional group is found to be planar with respect to the aromatic ring. The stabilizing conjugation between the lone pair electrons in the p-type oxygen orbital and the π system of the aromatic ring dominates over repulsive steric forces[61].

The low frequency transitions built off the A origin can readily be assigned by analogy to p-methoxy-trans-stilbene as 36^2_0 at 55.4 cm^{-1}, 37^2_0 at 91.5 cm^{-1},

and 25^1_0 at 171.4 cm^{-1}. The frequencies for these vibrations built off the B origin shift to 60.0 cm^{-1} , 85.2 cm^{-1}, and 179.5 cm^{-1}, respectively. The frequencies are summarized in Table 4. All transitions listed in the tables are reported relative in frequency to the electronic origin.

Transitions appearing at A+67 cm^{-1} and B+67.2 cm^{-1}, which have no analogs in trans-stilbene, appear at the same frequency in both the methoxy- and the hydroxy-trans-stilbenes. The substantial mass differences between OH and OCH_3 and the identical frequencies rule out vibrations and torsions involving these functional groups.

Table 4. Normal mode transition frequencies for the S_1 state of p-hydroxy-trans-stilbene.

assignment	A conformer	B conformer
36^2_0	55.5 cm^{-1}	60 cm^{-1}
37^2_0	91.5	85
$36^1_0 37^1_0$	73.5	72
x	67	67
25^1_0	171	179.5
37^4_0	183.8	171.0
24^1_0	245.3	211
25^2_0	342.5	358
$25^1_0 24^1_0$	416.5	390
25^3_0	516.4	537.5

Dispersed fluorescence can be very helpful in identifying features due to the two conformers. The dispersed emission from the two origins are shown in Figure 11. The dispersed emission from the A origin is an average of 7 six

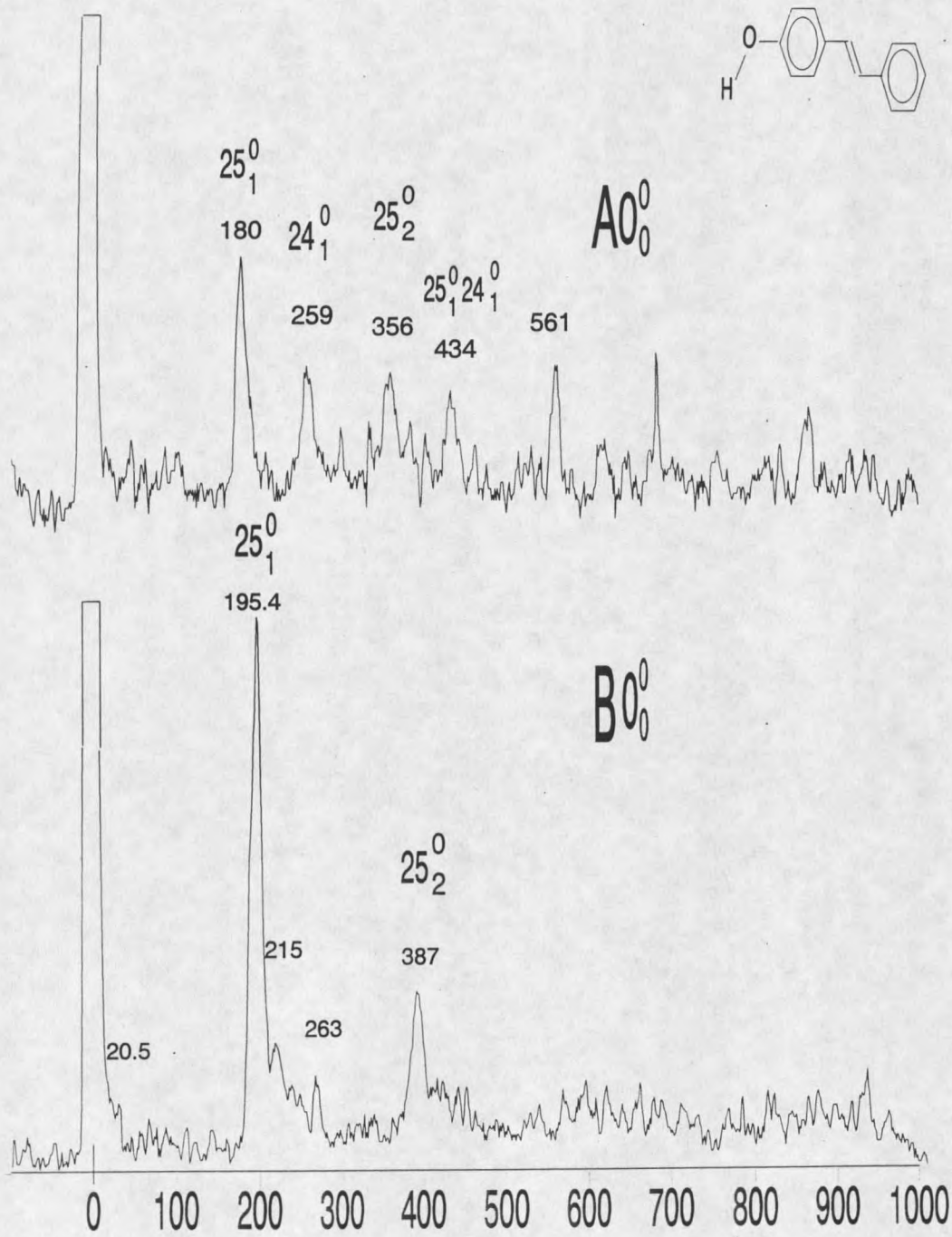

Figure 11. The dispersed emission from the origins of the A and B conformers of p-hydroxy-trans-stilbene.

minute exposures at 210μm slits. The B origin emission is an average of 9 six minute exposures at 210μm slits. With an entrance slit of 200 microns, the overall resolution will be approximately 11 cm^{-1}. In the dispersed emission spectra presented in this thesis, the bands at 0 cm^{-1} are coincident with the laser frequency and the intensity of the peaks has not been corrected for some contribution from scattered light.

The most intense feature in the dispersed fluorescence of the A conformer is 25^0_1 at 180.2 cm^{-1}. The dispersed fluorescence spectrum of the B origin band at 31,015 cm^{-1} shows the intense 25^0_1 at 195 cm^{-1}. Another distinct characteristic identical to that of the two conformer origins in p-methoxy-trans-stilbene is the large Franck-Condon activity in ν_{24} seen in the emission from the A conformer origin and missing from the B origin emission[22]. This is additional evidence to the striking similarities between the two molecules.

The dispersed emission intensity is much lower for p-hydroxy-trans-stilbene than p-methoxy-trans-stilbene because of less sample in the gas phase. The dispersed emission proved futile for transitions belonging to the A conformer other than the electronic origin. The combination of weaker transitions in the excitation spectra for the A conformer relative to the B conformer and a higher Franck-Condon activity (evident from the A-0^0_0 emission) produces emission spectra with poor S/N. On the other hand, dispersed emission of certain transitions belonging to the B conformer could be obtained and are shown in Figure 12. The ν_{25} vibration is the most prominent feature in trans-stilbene

spectra and forms a long progression in both excitation and emission. The dispersed emission spectrum of 25^1 is an average of 10 ten minute exposures with 200μm slits. The absence of the 25^1_1 band in the 25^1 level emission spectrum is noteworthy since it would be the strongest for a small geometry change from S_0 to S_1. Franck-Condon analysis of the intensity distribution in trans-stilbene confirms a calculated geometry change of 1.3° in the bend angle between S_0 and S_1[62]. Thus, the absence of 25^1_1 can be used in general to support the assignment of ν_{25} in the excited state spectrum of the stilbenes studied in this thesis.

Table 5. The major vibrational frequencies for the S_0 state of p-hydroxy-trans-stilbene.

assignment	A conformer	B conformer
37^0_2		20.5 cm^{-1}
37^0_4		52.8
25^0_1	180.2 cm^{-1}	195.4
24^0_1	259	224
25^0_2	362	387
25^0_3		577

The dispersed emission from B 37^2_0 shows a nice progression in the ground state at 20.5, 52.5, and 82 cm^{-1} for 37^0_2, 37^0_4, and 37^0_6, respectively. Although several ground state vibrational frequencies remain unassigned for the A conformer of p-hydroxy-trans-stilbene due to inadequate S/N, the nearly identical frequencies that have been observed in the excited state and ground

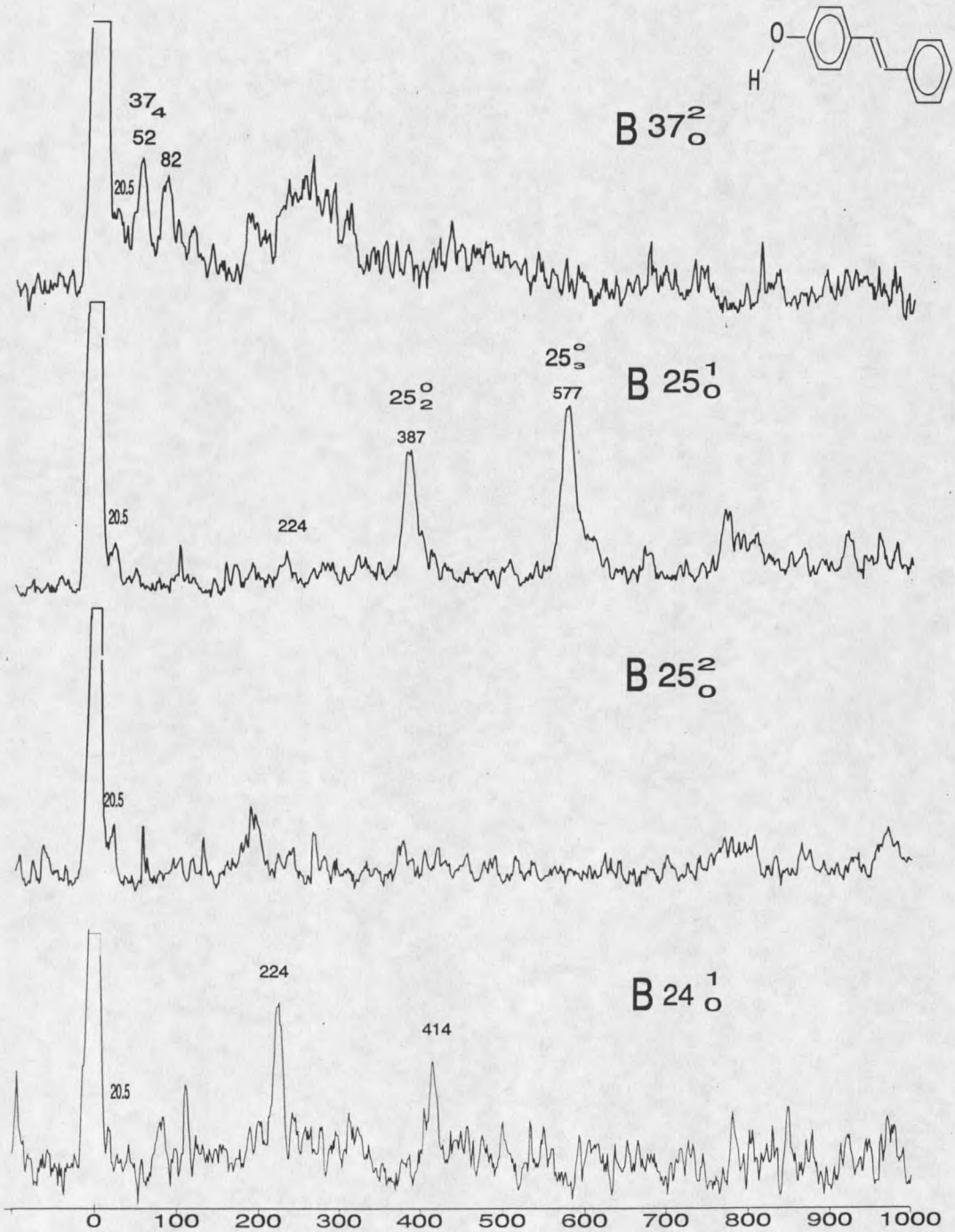

Figure 12. The dispersed emission spectra of the low frequency vibrations for the B conformer of p-hydroxy-trans-stilbene.

state of p-hydroxy-trans-stilbene and p-methoxy-trans-stilbene suggests that both molecules act the same under supersonic expansion.

p-hydroxy-trans-stilbene·$(H_2O)_n$

Water complexes of p-hydroxy-trans-stilbene were investigated as a function of water concentration in the carrier gas. Since the supersonic expansion is a nonequilibrium process where only a limited number of effective collisions occur, the formation of large clusters is inhibited[63]. Also, cluster formation is sensitive to expansion conditions, so the partial pressure of the water was kept as low as possible in order to see the first step of the complexation. This was performed using a fine metering valve on a second solvent flow line to introduce small amounts of water vapor into the carrier gas as described in the experimental section. The spectral grade water was contained in a liquid reservoir placed upstream from the hot sample/nozzle system. The ability to control water concentration is crucial in determining cluster size, especially in a molecule such as p-hydroxy-trans-stilbene which has several binding sites for complex formation.

Figure 13 shows the growth of the p-hydroxy-trans-stilbene∗$(H_2O)_1$ complex under increasing water conditions. The water molecule changes the electronic energy and produces a spectral shift relative to the bare species. Since the growth of new peaks separated by 20 cm^{-1} and centered around the B origin seems to correlate with an increase in water concentration, they are

assigned to the hydrogen-bonded complex formed between p-hydroxy-trans-stilbene and water. Another important feature seen in the spectra at increasing concentrations of water is that the intensity ratio of the A_{H2O} and B_{H2O} bands is nearly equal to the ratio of the A band to the B band. With only a small amount of water added, the new blue-shifted water complex peaks are more intense than the bare molecule. The similar intensity ratio of the new peaks (labeled A_{H2O} and B_{H2O}) under the various water concentrations in combination with the bare molecule behavior indicate the new peaks are the cis and trans conformers of the one water complex. The blue shift induced for the hydrogen bonding is 270.5 cm^{-1} and 13 cm^{-1} for the A_{H2O} and B_{H2O}, respectively. The almost-complete solvation of the bare molecule, evident from the very low intensity of the bare molecule origins, is seen in the spectrum taken with a water concentration obtained by opening the fine metering valve to 50 units (second from bottom trace in Figure 14). The fluorescence spectrum arising from the water complex displays similar vibrational structure as the bare p-hydroxy-trans-stilbene indicating that solvation with a single molecule of water does not strongly modify the structure of the molecule. Eventually, two more peaks separated from each other by 45 cm^{-1} begin to appear with the continued increase of water. The second set of new peaks are red shifted 130 cm^{-1} and 86 cm^{-1} from the bare origin, respectively. Given the depletion of the initial water complex peaks as a result of these new peaks, the red-shifted peaks are tentatively assigned as the A and B conformer for p-hydroxy-trans-stilbene·$(H_2O)_2$.

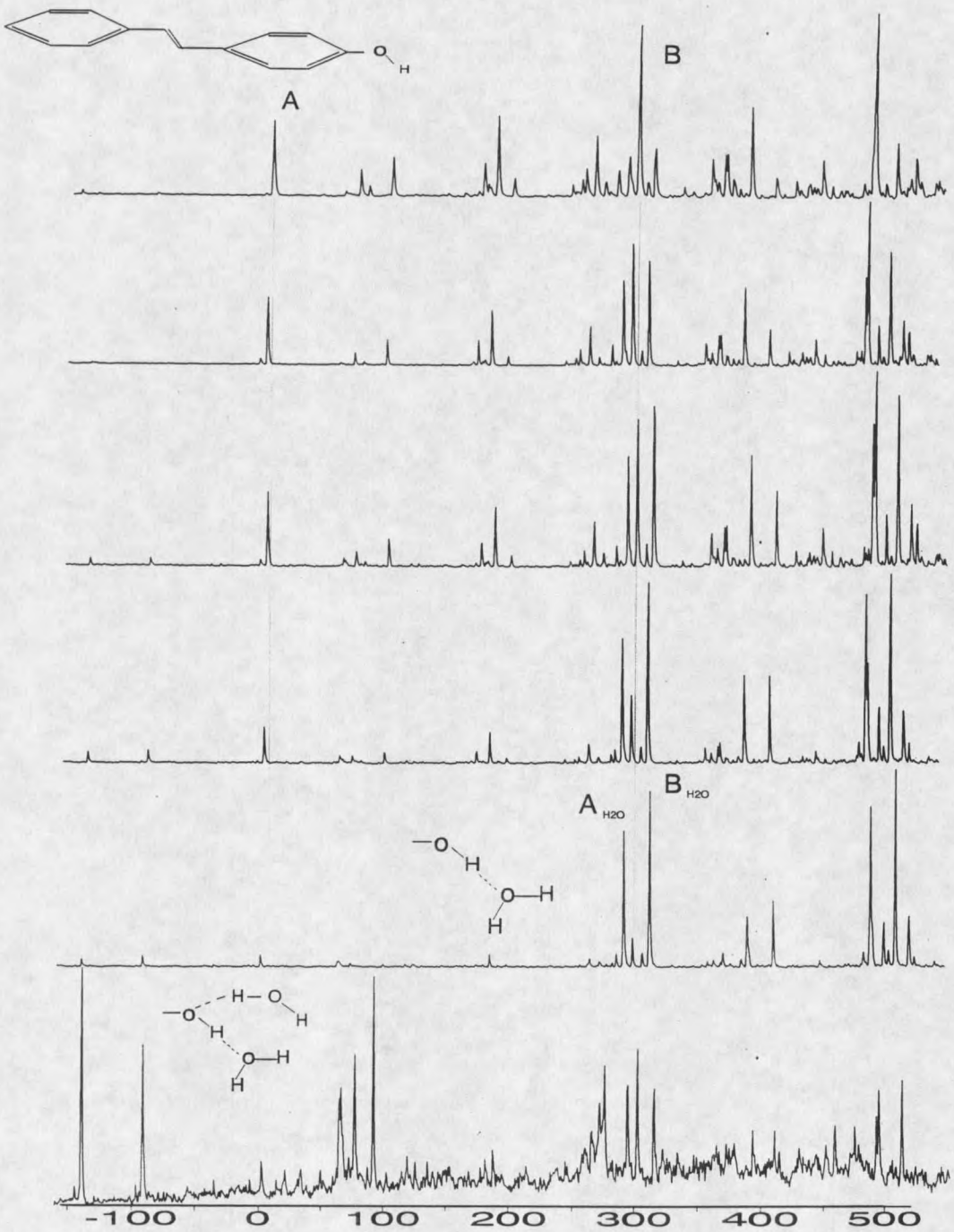

Figure 13. Dependence of p-hydroxy-trans-stilbene/H_2O cluster fluorescence intensity from H_2O concentration.

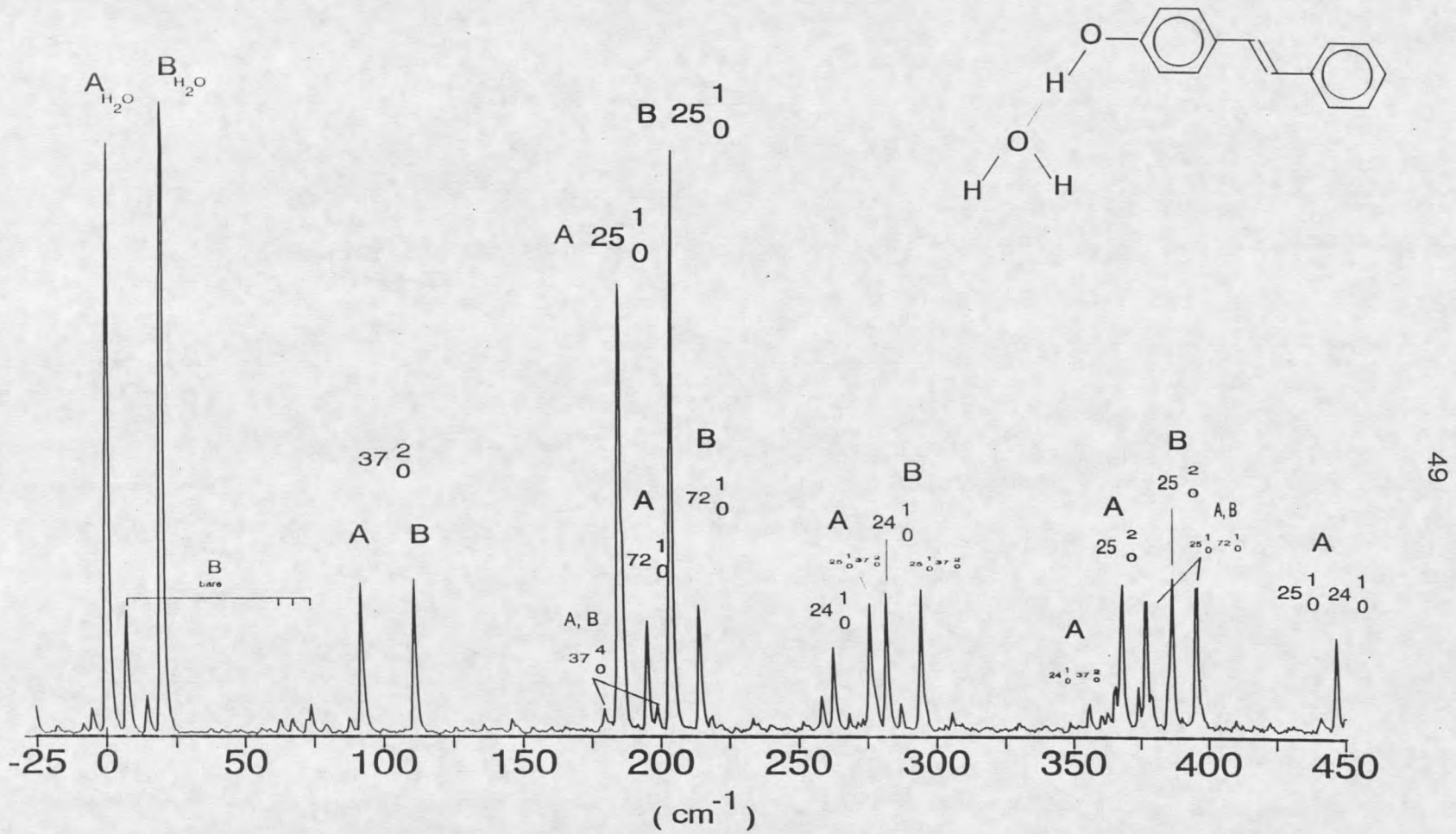

Figure 14. The fluorescence excitation spectrum of p-hydroxy-trans-stilbene$*(H_2O)_1$. The conformer origins are identified with labels A and B.

Figure 14 shows the one-photon fluorescence excitation spectrum of p-hydroxy-trans-stilbene$*(H_2O)_1$. The frequencies are summarized in Table 6. One feature of this spectrum that is worth mentioning is the absence of a strong transition near 67 cm^{-1}. To understand the importance of the missing 67 cm^{-1} transition in the water complex species, it is useful to briefly present the ideas first discussed with p-methoxy-trans-stilbene[22]. Since the transition appears at 67 cm^{-1} in both p-hydroxy-trans-stilbene and p-methoxy-trans-stilbene, the differences in the reduced mass between OCH_3 and OH rule out an assignment as a functional group vibration of the remote substituent. This transition could then be a stilbene vibration that is modified by the presence of the hydroxy group. The low frequency of the peak suggests either ν_{36}, ν_{37} or ν_{48} as the perturbed vibrational mode. Noting the fact that this transition only appears in substituents that lack para axis symmetry, the torsional modes of the phenyl rings may be involved because the hydroxy group can spoil the twofold symmetry of the phenyl rotor.

Table 6. Normal mode transition frequencies for the S_1 state of p-hydroxy-trans-stilbene$*(H_20)_1$.

assignment	A conformer	B conformer
37^2_0	92	91
x	?	?
25^1_0	185	184
37^4_0	180	179
72^1_0	195	194
24^1_0	263	262
25^2_0	368	367
$25^1_0 24^1_0$	447	446

The four planar ring conformations in trans-stilbene are fourfold degenerate in energy and separated by high energy barriers. The horizontal axis in the ring torsion surface potential is the torsional coordinate for a single ring (ϕ_1); the vertical axis is the torsional coordinate of the other ring (ϕ_2). The diagonals of the potential surface correspond to moving both rings with one being ν_{37} (ϕ_1-ϕ_2) and the other ν_{48} (ϕ_1+ϕ_2). The ν_{37} and ν_{48} vibrational description is appropriate for the phenyl torsions in trans-stilbene. In the limiting case, substitution of one phenyl with several very large groups would localize the ring torsion in the less hindered ring and could be expressed as a linear combination of ν_{37} and ν_{48}. Flipping the phenol ring in p-hydroxy-trans-stilbene by 180° converts between the two hydroxy conformers, which differ by ~270 cm^{-1} on the S_1 potential surface. This energy difference between the pairs of minima requires more local torsional character for an accurate description and is probably sufficient to cause noticeable ν_{37} and ν_{48} mixing.

Since the energy difference between the two hydroxy conformers in the van der Waals complex of p-hydroxy-trans-stilbene with water is 20 cm^{-1}, the possible mechanism that allows for ν_{37} and ν_{48} mixing is removed. While the exact assignment of the observed peak at 67 cm^{-1} remains uncertain, we strongly suspect that this mechanism described above is responsible for the transition in both p-hydroxy-trans-stilbene and p-methoxy-trans-stilbene.

p-methoxy-trans-stilbene·$(H_2O)_n$

p-methoxy-trans-stilbene was also examined under similar expansion conditions and the water complexing behavior is completely different. Comparison of p-methoxy-trans-stilbene and p-hydroxy-trans-stilbene under the same expansion conditions and water concentration is shown in Figure 13. New methoxy*H_2O transitions are seen only at much higher water concentration and at different frequencies than for p-hydroxy-trans-stilbene. These transitions are likely due to a water molecule attached to the methoxy group, but may be due to a π complex. Otherwise, the p-methoxy-trans-stilbene spectra look the same under increasing water conditions. These differences in hydrogen bonding behavior will be further addressed in the discussion.

p-hydroxy-p'-methyl-trans-stilbene

The expansion cooled, fluorescence excitation spectrum of p'-hydroxy-p-methyl-trans-stilbene is presented in Figure 16. Readily apparent are two origins separated by 266 cm^{-1}, similar to the p-hydroxy-trans-stilbene spectrum. With the addition of the methyl group, the spectrum is nearly identical to p'-methoxy-p-methyl-trans-stilbene. This similarity in the spectra between the two methylated species compliments the result found for p-methoxy- and p-hydroxy-trans-stilbene. The absolute frequency of the A-0^0_0-$0a_1$ in p'-hydroxy-p-methyl-trans-stilbene has decreased to 30,536 cm^{-1} upon methyl substitution. The

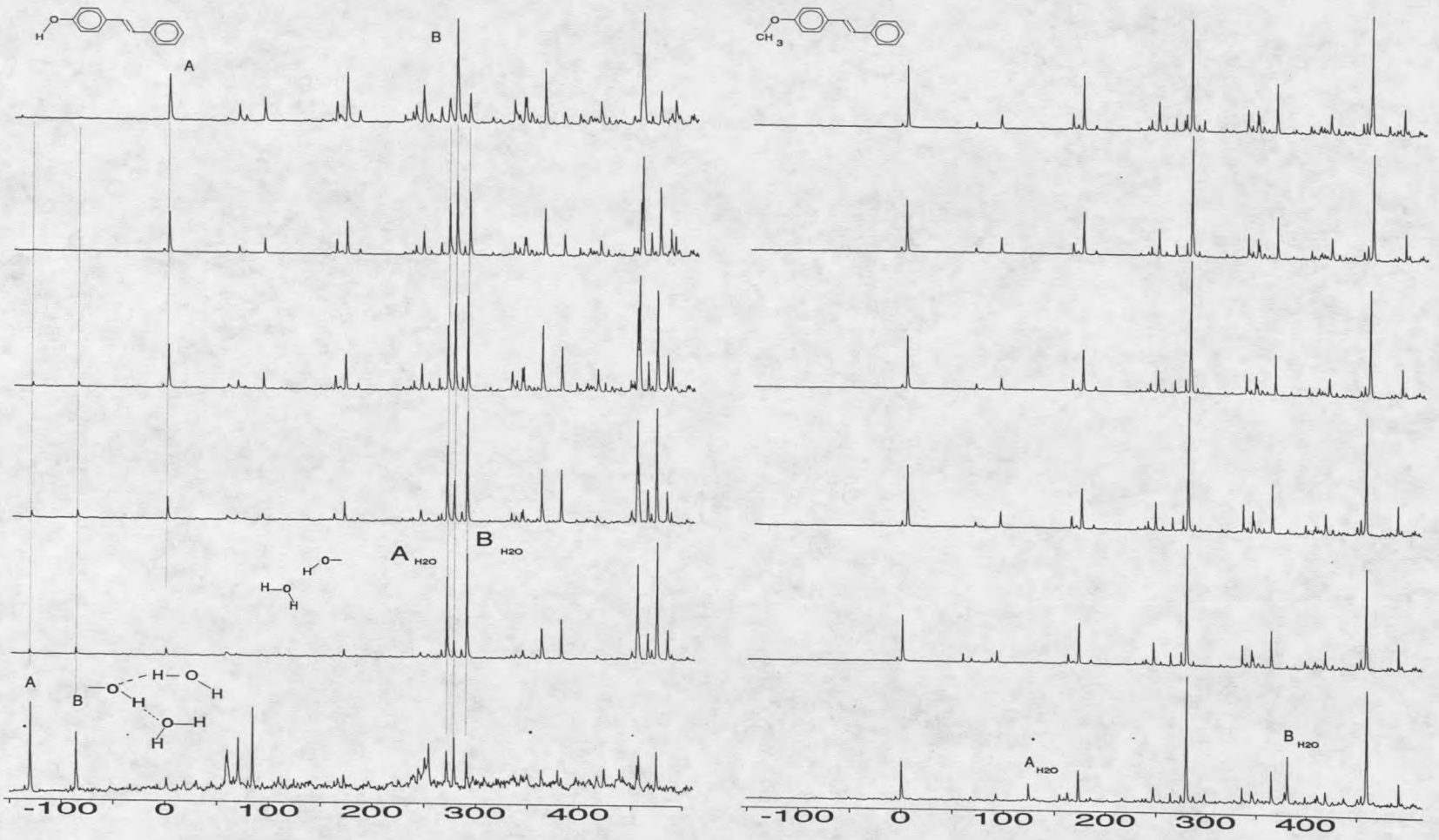

Figure 15. Fluorescence excitation spectra of p-hydroxy-trans-stilbene and p-methoxy-trans-stilbene under the same water concentration.

assignments for the B conformer are complicated by the presence of many transitions assigned to the A conformer. We were unable to completely dry the p'-hydroxy-p-methyl-trans-stilbene, so water complex peaks are visible near the B conformer. The conformer origins and several other normal mode transitions appear as a doublet and are accompanied by low frequency transitions. By analogy with p-methyl-trans-stilbene, p'-amino-p-methyl-trans-stilbene, and p'-methoxy-p-methyl trans-stilbene, the low frequency transitions are ascribed to the very anharmonic, hindered internal methyl rotor. Methyl torsional levels will not display the doublet splitting, so most unsplit transitions can be assigned to the methyl rotor.

As discussed in Chapter Two, the anharmonic internal rotor levels require a different symmetry treatment than C_s point group symmetry used for the stilbene skeletal modes because the three-fold symmetrical methyl group may tunnel between the triple minimum potential well. The appropriate symmetry group in this case is G_6 which has three irreducible representations (shown in Table 1) labeled A_1, A_2 and E. The levels of the methyl rotor are labeled with an internal rotation angular quantum number and the symmetry of the level increasing in energy as $0a_1$, 1e, 2e, $3a_1$, 4e, 5e, etc... . The tunneling of the internal rotor wave functions, however, splits the triply degenerate levels into singly and doubly degenerate levels A and E, respectively. Transitions between levels of A and E symmetries are forbidden. If the barrier to rotation remains

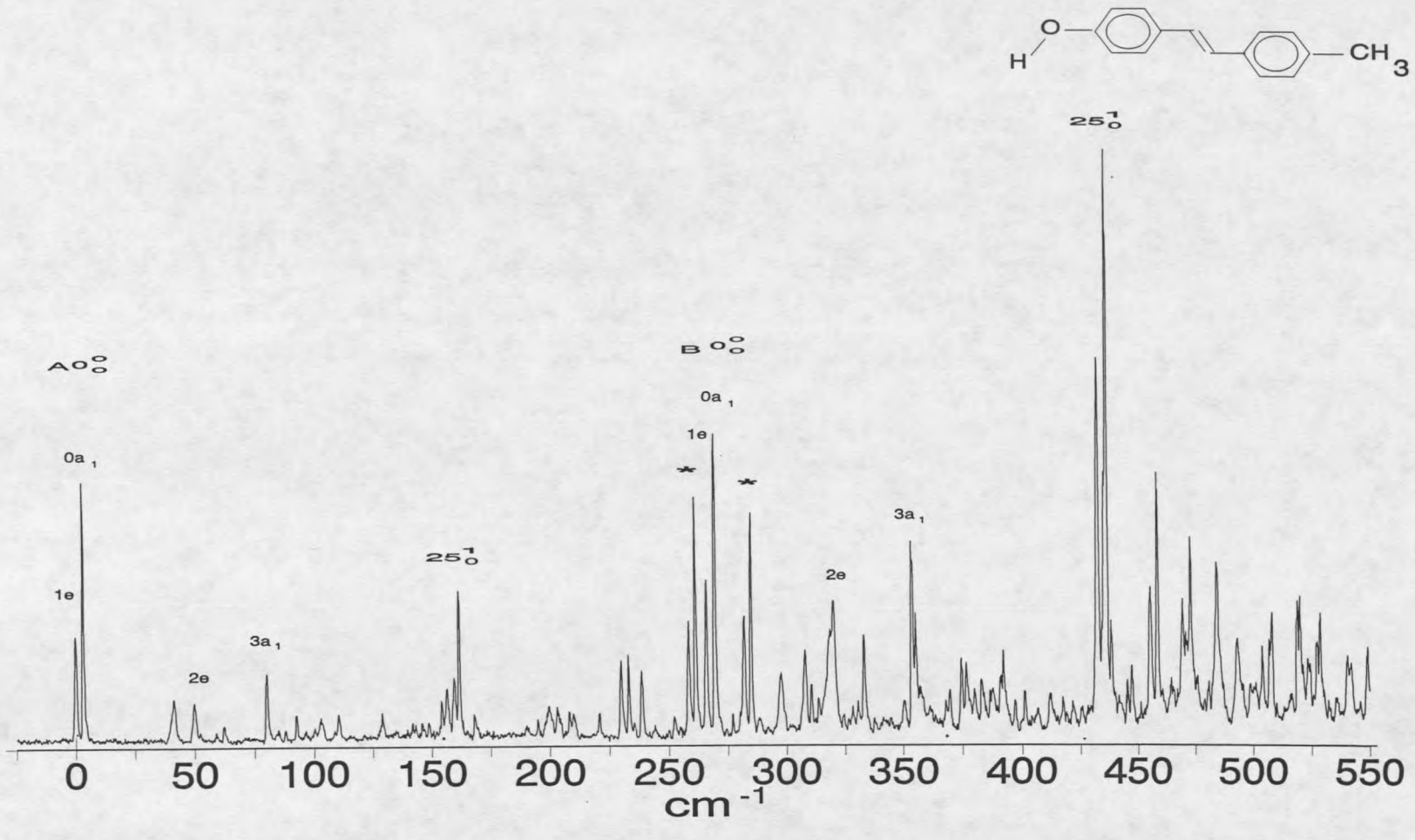

Figure 16. The fluorescence excitation spectrum of p'-hydroxy-p-methyl-trans-stilbene. The conformer origins are identified with labels A and B.

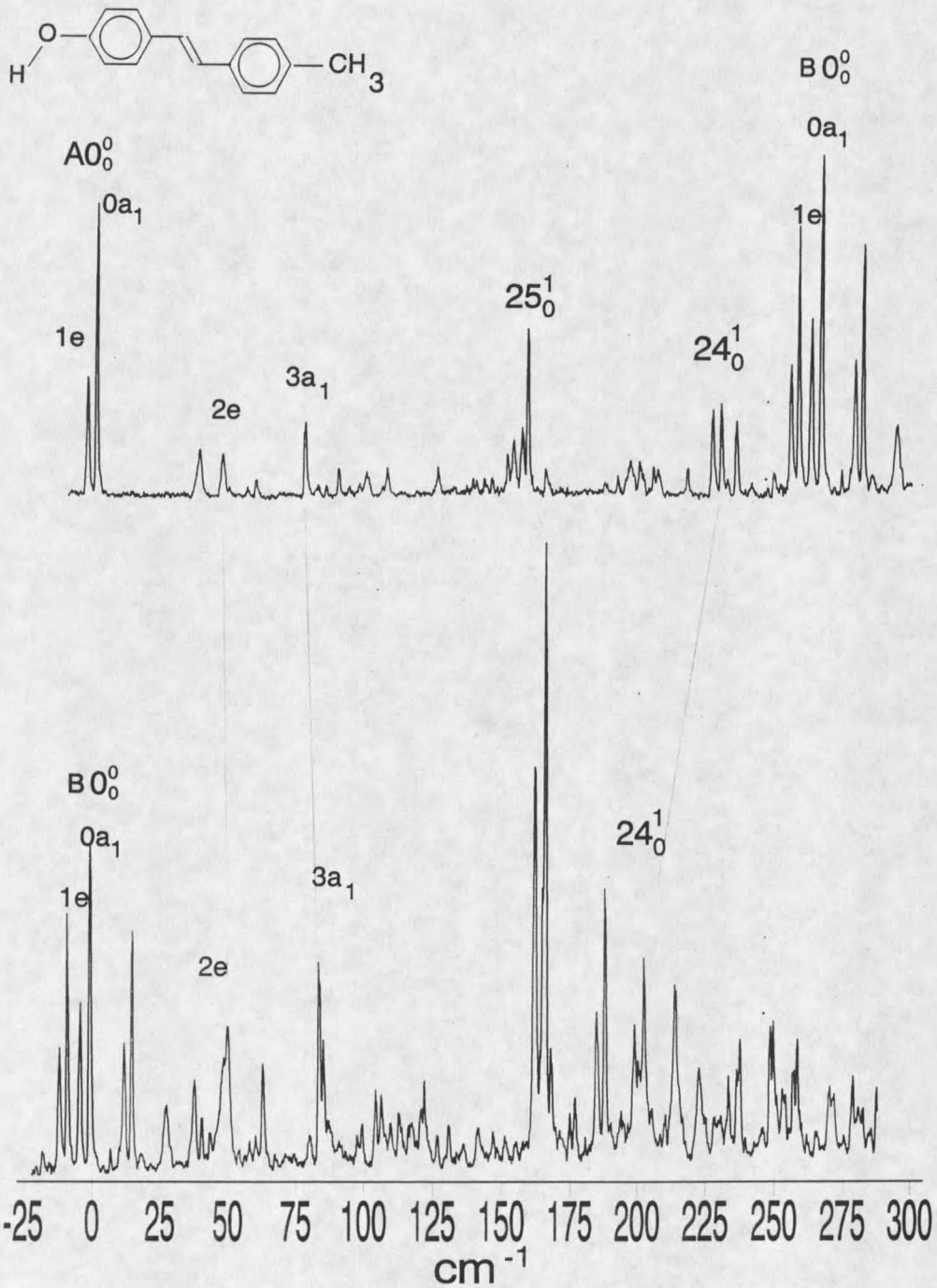

Figure 17. The first 300 cm^{-1} of each conformer in the fluorescence excitation spectrum of p'-hydroxy-p-methyl-trans-stilbene. The B conformer origin has been placed directly under the A origin for comparison purposes.

unchanged between S_0 and S_1 energy states, the $0a_1$"-$0a_1$' and 1e"-1e' transitions will be the same frequency and the origin will be only one peak, containing both transitions. If the barrier to rotation changes, however, the origin will appear as a doublet due to the slightly different energies for the $0a_1$-$0a_1$ and e-e transitions.

The origin doublet for the bare A conformer at 0 and -3.0 cm^{-1} relative frequency is assigned to the $0a_1$-1e transitions and the singlet bands at 47 cm^{-1}, and 77.3 cm^{-1} are assigned to the 2e and $3a_1$ methyl torsional bands, respectively. Likewise, the methyl torsional bands $0a_1$,1e, 2e, and $3a_1$ for the bare B conformer are assigned at 0, -3.3, 51, and 84.5 cm^{-1}. For comparison purposes, the B origin is aligned underneath the A origin in Figure 17. The difference in the torsional level energies between the A and B conformers is indicative of a change in the methyl rotational barrier and points to the sensitivity of the methyl rotor to the conformation of the hydroxy group. Since the fluorescence excitation and dispersed emission spectra for the p-methoxy- and p-hydroxy-trans-stilbenes are nearly identical, and the excitation spectra for the methylated species are also nearly identical, dispersed emission experiments on p'-hydroxy-p-methyl-trans-stilbene were deemed unnecessary. The striking similarity between the p'-hydroxy-p-methyl-trans-stilbene spectrum and the p'-methoxy-p-methyl-trans-stilbene spectrum helped in the assignment of transitions.

The most prominent vibration is ν_{25} and 25^1_0 for the A conformer is at 159 cm^{-1} and 25^1_0 for the B conformer is located at 167 cm^{-1}. The individual vibrations A-25^2_0, B-36^2_0, B-2e, and B*(H_2O)-2e are nearly degenerate in energy and create the very broad peak 50 cm^{-1} above the B bare origin in the spectrum.

Table 7. Normal mode transition frequencies for p'-hydroxy-p-methyl-trans-stilbene.

assignment	A-S_1	B-S_1
$0a_1$	0 cm^{-1}	0 cm^{-1}
1e	-3.0	-3.3
2e	47	51
$3a_1$	77.3	84.5
X	38	38.6
36^2_0	59.4	52
72^1_0	154	169
25^1_0	159	167
24^1_0	230	203
25^2_0	318	334
$25^1_0 24^1_0$	389	636
25^3_0	476	767

<u>p'-hydroxy-p-methyl-trans-stilbene*(H_2O)$_n$</u>

The p'-hydroxy-p-methyl-trans-stilbene spectrum undergoes a dramatic change with the addition of small amounts of water vapor. Figure 14 shows the one-photon fluorescence excitation spectrum of p'-hydroxy-p-methyl-trans-stilbene*(H_2O)$_1$. As with p-hydroxy-trans-stilbene, the behavior of the new

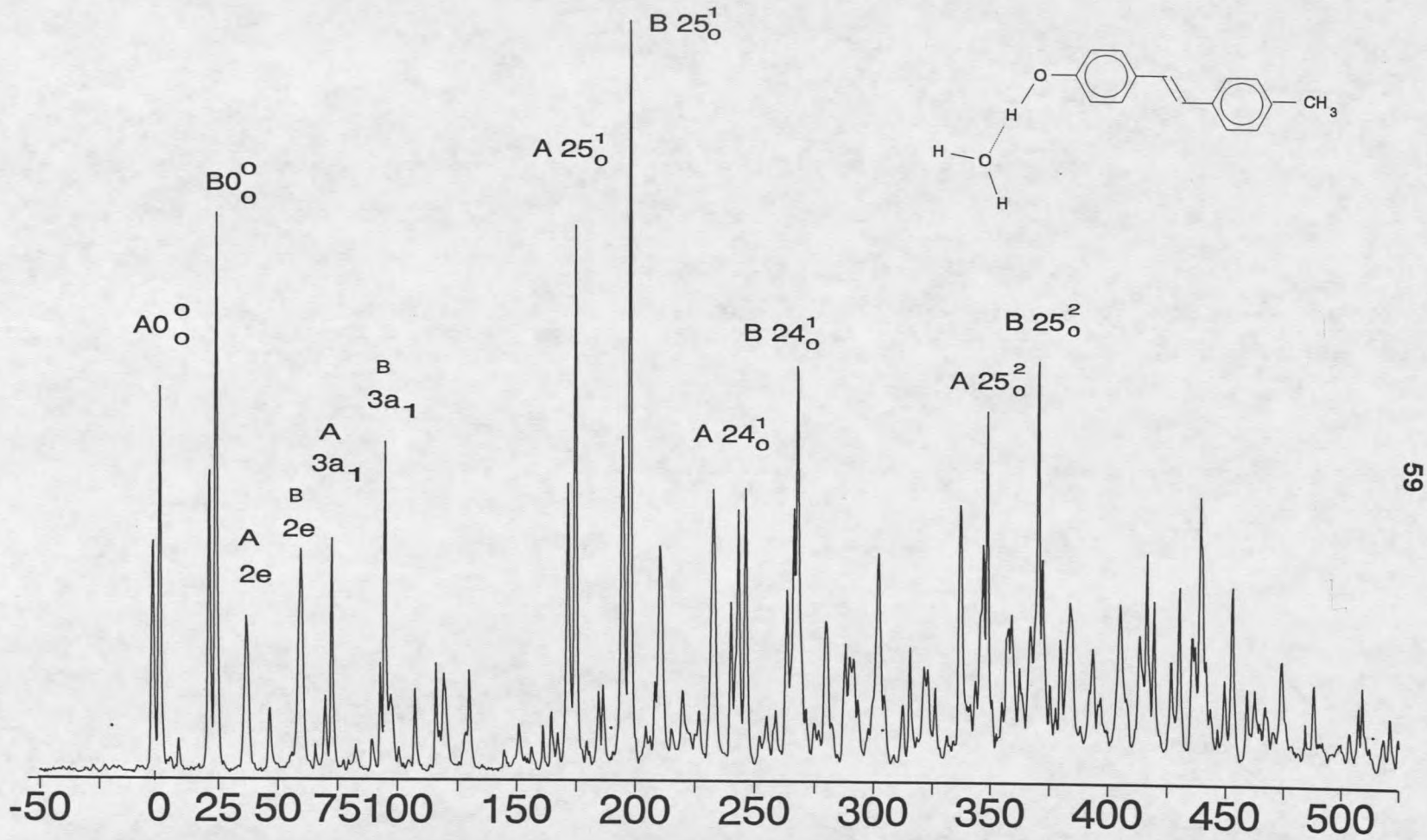

Figure 18. The fluorescence excitation spectrum of p'-hydroxy-p-methyl-trans-stilbene$*(H_2O)_1$. The conformer origins are identified with labels A and B.

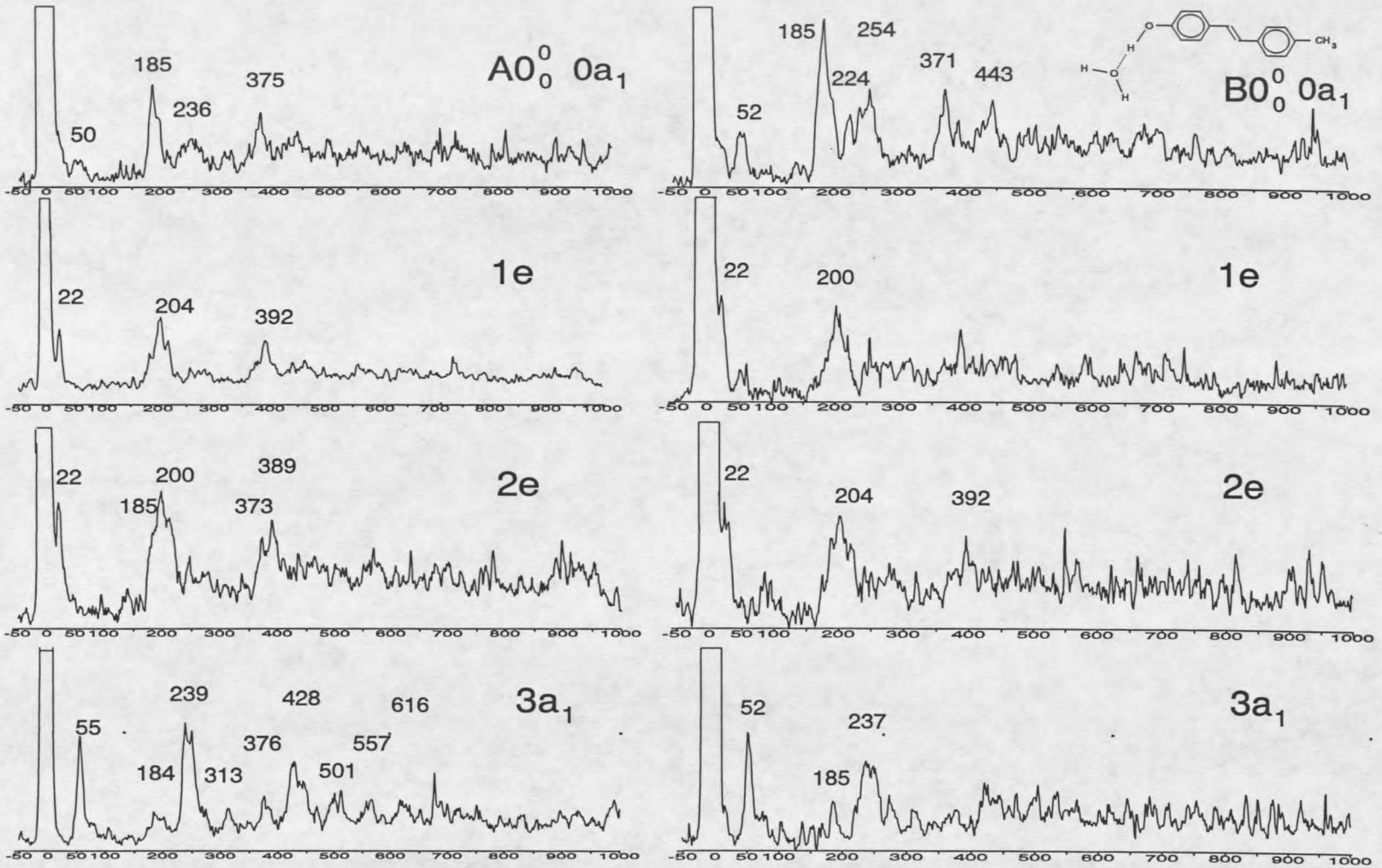

Figure 19. The dispersed emission spectra of the methyl torsional levels for the A and B conformers of p'-hydroxy-p-methyl-trans-stilbene$*(H_2O)_1$.

transitions centered around the B origin confirm them as the A_{H2O} and B_{H2O} conformers of the one water complex. In comparison with the bare p'-hydroxy-p-methyl-trans-stilbene spectrum, the A conformer in the water complex has blue shifted 258 cm^{-1} to within close proximity of the B origin. The B origin has slightly blue-shifted 16.5 cm^{-1}. The water complex peaks also exhibit the torsional splitting seen in other methylated species and gives a great opportunity to investigate remote hydrogen bonding effects on the methyl barrier.

The splitting between the 1e-0a_1 transition for the A_{H2O} conformer is 2.8 cm^{-1} and increases just slightly to 2.9 cm^{-1} for the B_{H2O} conformer. Both of these a-e splittings have decreased relative to the A and B conformers for the bare p'-hydroxy-p-methyl-trans-stilbene. For the A_{H2O} conformer, the 2e is assigned at 36.4 cm^{-1}, and the 3a_1 is assigned at 72.4 cm^{-1}. The B_{H2O} conformer torsional frequencies are very similar with the 2e assigned at 35.2 cm^{-1}, and the 3a_1 at 70.8 cm^{-1}. There are several higher frequency transitions that can be possible candidates for internal rotor levels. A careful examination of the excitation spectrum reveals two broad peaks near the calculated frequencies (100 cm^{-1}) for the 4e level for each conformer. It is generally accepted that the *e* transitions are significantly broader than *a* transitions, so the peaks at 96.8 cm^{-1} above the A_{H2O} and 95.6 cm^{-1} above the B_{H2O} have been assigned as the 4e level for each conformer. The "e" only transitions can be identified at 46.5 cm^{-1} and 46.1 cm^{-1} for the A_{H2O} and B_{H2O} levels, respectively. Worth mentioning is the two narrow transitions appearing 4.5 cm^{-1} and 3.4 cm^{-1} to lower frequency of the A_{H2O} and

B_{H2O} 4e levels, respectively. A similar transition accompanying the 4e level in p-methyl-trans-stilbene was identified as $37^1_0 3a_2$ based on dispersed emission[35]. This transition is also seen in the p'-p-dimethyl-trans-stilbene spectrum presented later in this chapter and is further discussed in that section. Thus, we speculate that $37^1 3a_2$ is also present in the spectrum here.

Table 8. The torsional and vibrational frequencies for S_0 and S_1 of the A and B conformers of p'-hydroxy-p-methyl-trans-stilbene $(H_2O)_1$.

assignment	A-S_0	A-S_1	B-S_0	B-S_1
$0a_1$	0 cm^{-1}	0 cm^{-1}	0 cm^{-1}	0 cm^{-1}
1e		-2.8		-2.9
2e	21.60	36.4	23.25	35.2
$3a_1$	56.16	72.4	52.06	70.8
4e		96.8		95.6
X		46.5		46.1
ν_{25}, v=1	183.93	174.4	185.4	173
ν_{24}, v=1	256.96	243	259	242.7
ν_{25}, v=2	374.29	348.4	371.24	347
$\nu_{25}+\nu_{24}$		416.4	443.9	414.7
ν_{24}, v=2		487.4		486
ν_{25}, v=3	556.77		557	

The ν_{25} in-plane vibration for the A conformer has increased with the addition of the water molecule from 159 to 175 cm^{-1}. The B conformer ν_{25} frequency has also increased from 167 to 173 cm^{-1}. The overlap of the spectra of the two water complexed conformers, now separated by only 23.7 cm^{-1},

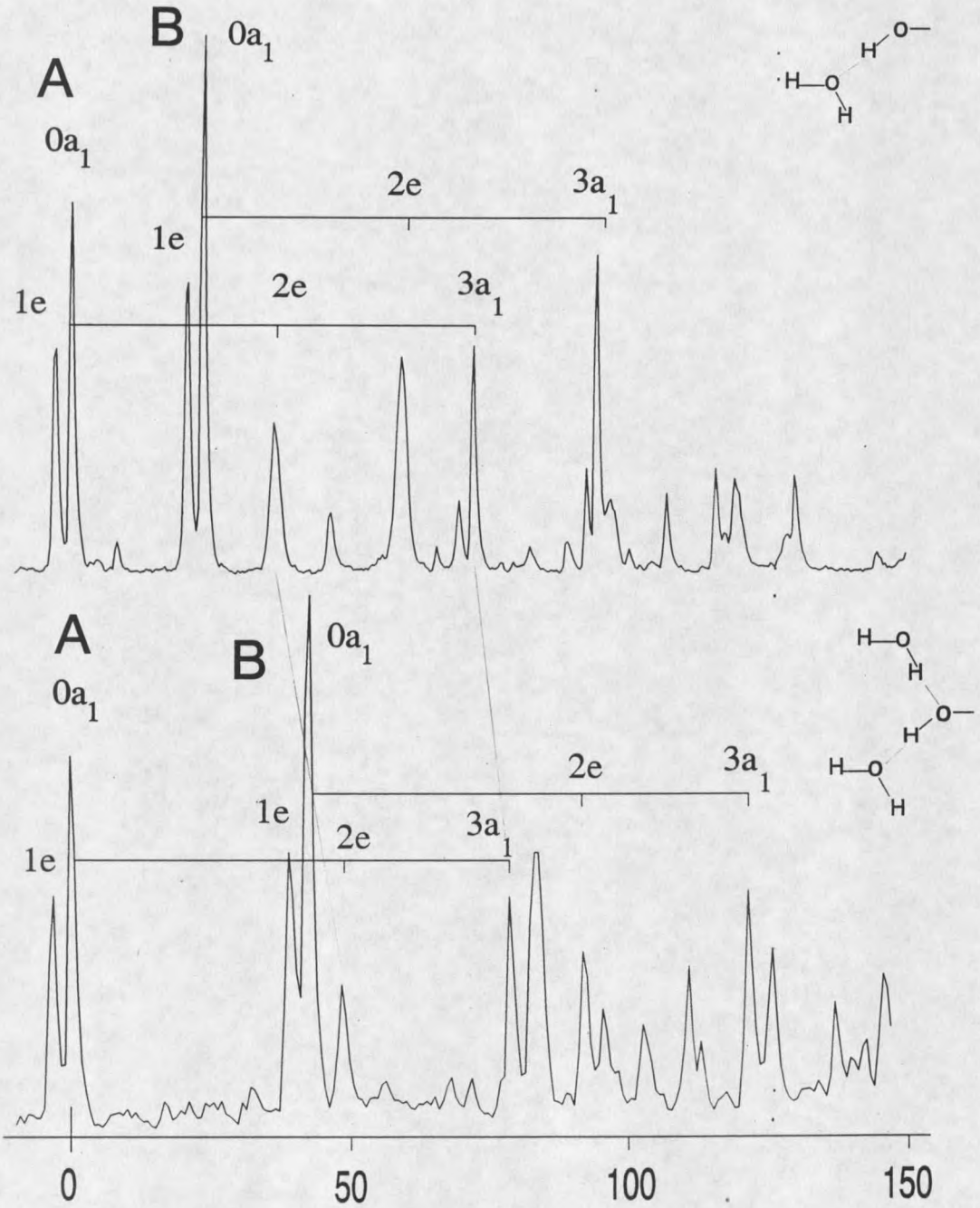

Figure 20. The methyl torsional progressions for p'-hydroxy-p-methyl stilbene clustered with one and two water molecules, respectively.

makes the methyl rotor assignments difficult. For this reason, the assignments are largely based on information obtained from dispersed emission.

Each dispersed emission spectrum shown in Figure 19 was an average of ten 300 second exposures taken with slit widths between 250-300 μm. Symmetry based selection rules state that the emission from an a_1 level must go to another a_1 levels, and e to e levels. Since the ground state frequencies are extracted from combination differences, selection rules prevent the $0a_1$-1e splitting from being found experimentally. Exciting the complexed A-$0a_1$ transition gives a transition at 56 cm^{-1}, which is assigned to the $3a_1$ level in the ground state. The 56 cm^{-1} band is also seen in emission from the $3a_1$ level in S_1. The methyl torsional frequencies of the one water complex can be fit with a barrier resulting in $V_3' = 77.8$ cm^{-1} for the A conformer and $V_3' = 74.5$ cm^{-1} for the B conformer.

With the increasing H_2O, a new pair of complex origins red shifted by 118 cm^{-1} with respect to the bare molecule is obtained. These transitions are at a similar relative frequency to the red complex transition observed in p-hydroxy-trans-stilbene+H_2O. Thus, the pair of red shifted complex origins, shown in Figure 20, are tentatively assigned as p'-hydroxy-p-methyl-trans-stilbene*$(H_2O)_2$. The complex still retains sharp features and the methyl torsional frequencies built off these red shifted origins can be fit to a barrier resulting in a $V_3' = 96.42$ cm^{-1} and $V_6' = 15.13$ cm^{-1} for the A-$(H_2O)_2$ conformer and $V_3' = 97.79$ cm^{-1} and $V_6' = 21.32$ cm^{-1} for the B-$(H_2O)_2$ conformer. The

conformer barrier difference between the cis and trans species is again significantly reduced for this complex, and the addition of a second water increases the methyl torsional barrier back to an average of the torsional barriers found for the bare molecule.

Table 9. Methyl torsional levels for p'-hydroxy-p-methyl-trans-stilbene and water complexes in the S_1 excited state.

	hydroxy-methyl		hydroxy-methyl·$(H_2O)_1$		hydroxy-methyl·$(H_2O)_2$	
Transition	A	B	A	B	A	B
$0a_1$	0 cm^{-1}	0 cm^{-1}	0 cm^{-1}	0 cm^{-1}	0 cm^{-1}	0 cm^{-1}
1e	-3.0	-3.3	-2.8	-2.9	-3.0	-3.1
2e	47.0	51.0	39.2	38.1	49.55	50.2
$3a_1$	77.3	84.5	72.4	70.8	80.25	80.2
4e			99.6	98.5		
V_3'	91.26	103.9	77.8	74.5	96.4	97.8
V_6'	16.10	10.49	-9.9	-9.0	15.1	21.3

p'-cyano-p-methyl-trans-stilbene

In para'-substituted-p-methyl-trans-stilbenes, it was quickly recognized that electron-donating functional groups exert a characteristic "substituent effect" on the torsional barrier of the methyl group ten carbons away. Inspection of the data revealed a pattern in the lower torsional barriers that was consistent with the electron-donating ability of the substituents. Lower torsional barriers were also found for the remote chlorine and fluorine halogen substituents[64]. Halogens

are strongly electronegative, withdrawing electron density from the carbon atom through the sigma bond, yet donate electron density from the nonbonding electrons through π bonding[65]. In light of this dual nature of the halogens, remote electron-withdrawing functional groups "substituent effect" on the methyl torsional barrier are inconclusive. Thus we include in this study several electron-withdrawing groups to cover a wider range of substituent inductive and resonance properties. The cyano functional group has strong electron-withdrawing behavior and should pull electron density from the stilbene π system. The electron density throughout the conjugated system, including the area near the methyl group, should be affected by the CN substitution.

Figure 21 shows the fluorescence excitation of p'-cyano-p-methyl-trans-stilbene. The electronic origin and several other strong skeletal modes appear as doublets, which is a characteristic of the methyl rotor splitting seen in every other methylated stilbene investigated thus far. The absolute frequency of the $0a_1$ transition of the origin is 30,682 cm^{-1}. The spectrum shown was recorded at a speed of 0.2 cm^{-1}/s with a backing pressure of 2.6 bar He. The spectrum is very similar to the spectrum of p'-fluoro-p-methyl-trans-stilbene, except for two transitions near 140 cm^{-1} above the origin. This is intuitively reasonable since the cyano group and the fluorine atom are comparable in their electronegativity properties and their molecular weight[65]. The $1e\text{-}0a_1$ splitting is 3 cm^{-1}, 2e is assigned at 43.85 cm^{-1}, and $3a_1$ is identified at 75.55 cm^{-1}. As with other stilbene analogues, there are two transitions near the expected frequency for 2e which

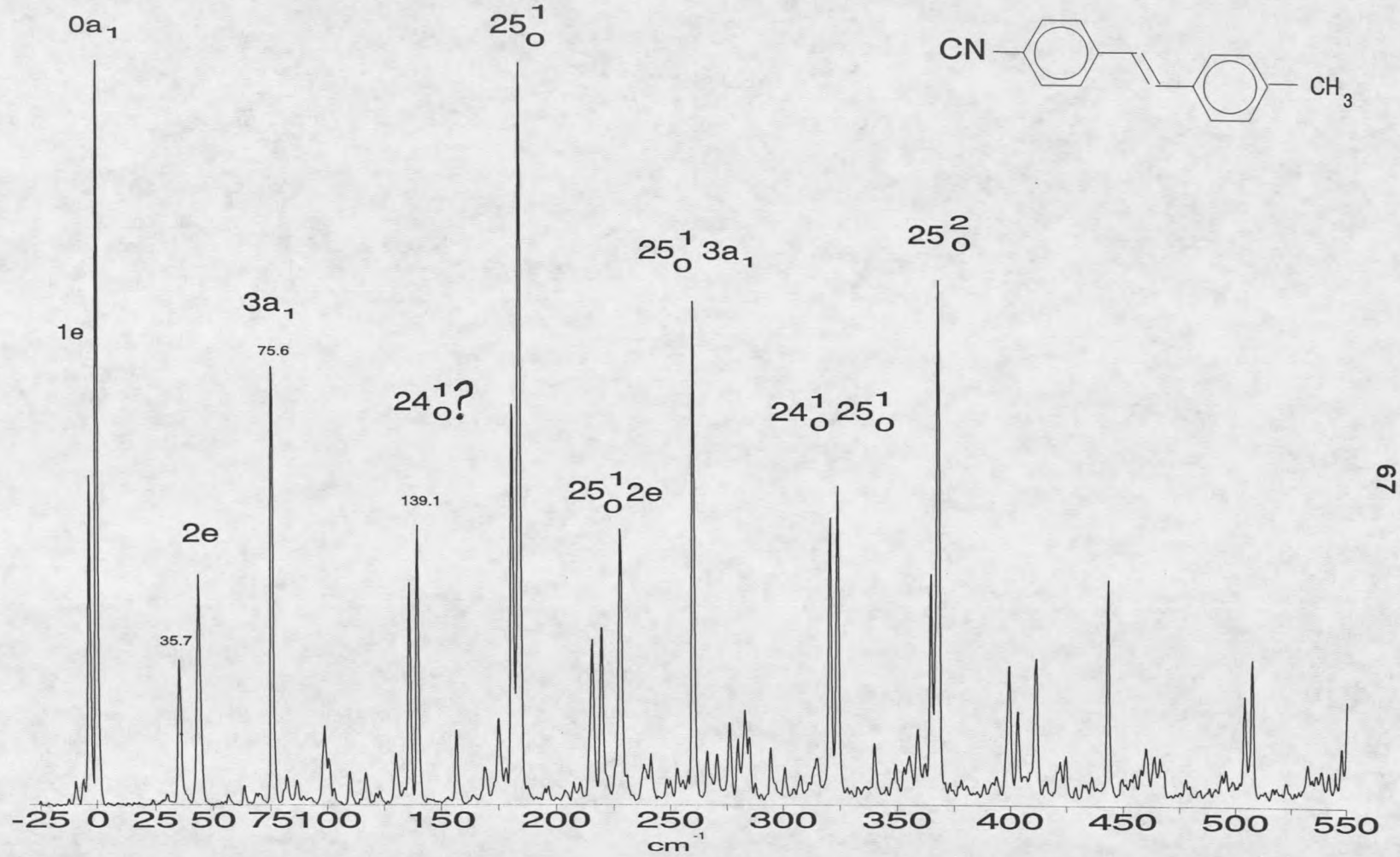

Figure 21. The fluorescence excitation spectrum of p'-cyano-p-methyl-trans-stilbene.

have characteristics of e levels (see Figure 22). This low frequency transition appearing at 35.7 cm^{-1} will be explained in the discussion. Higher members of the torsional progression can not be identified due to lack of intensity and spectral congestion.

The most prominent normal mode vibrational progression is ν_{25} at 183 cm^{-1}; 367.9 cm^{-1}, and 552 cm^{-1} above the origin for 25^1_0, 25^2_0, and 25^3_0, respectively. A new transition relative to p-methyl-trans-stilbene is observed at 139.1 cm^{-1} above the origin and displays the $0a_1$-1e splitting. Since the CN functional group bend appears at 527 and 494 cm^{-1} for p-aminobenzonitrile and dimethylaminobenzonitrile, respectively, it can be ruled out as a possible candidate for any of the low frequency structure in p'-cyano-p-methyl-trans-stilbene[66]. A comparison between the p'-fluoro-p-methyl-trans-stilbene and p'-cyano-p-methyl-trans-stilbene shows the transition appearing at 241 cm^{-1} in the fluoro compound is absent in the cyano compound. Conversely, the 140 cm^{-1} transition in p'-cyano-p-methyl-trans-stilbene is absent in the fluoro compound. Since the dispersed emission spectra between these corresponding transitions show very similar characteristics, it seems likely that they are the same transition.

The in-plane C_e-C-C bending mode, ν_{24}, is calculated by Warshell[67] to have a frequency of 309 cm^{-1}, but has generally been assigned to a transition appearing between 200-300 cm^{-1} above the origin in the stilbene spectra, including p'-fluoro-p-methyl-trans-stilbene[58]. Previous work on p'-fluoro-p-

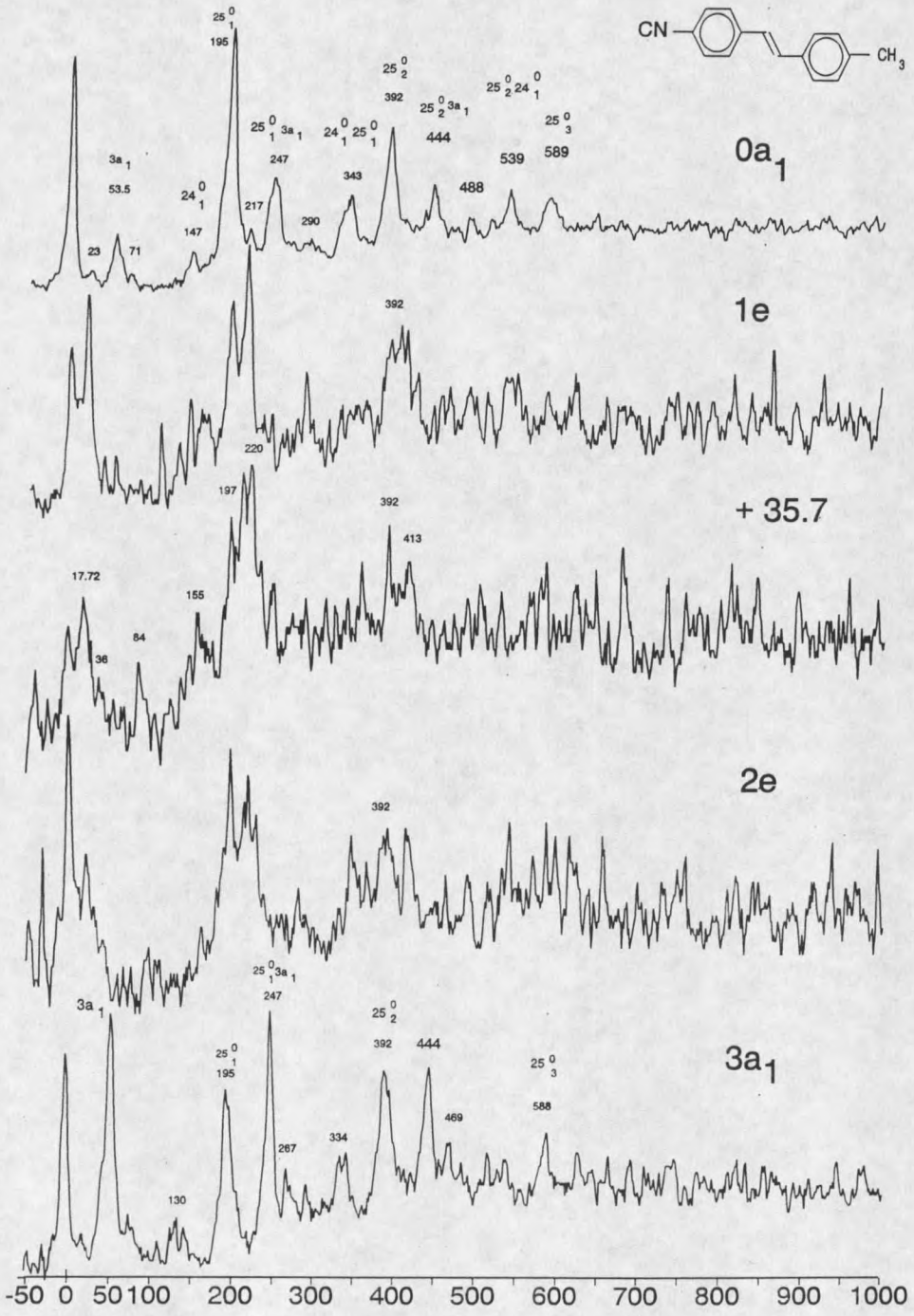

Figure 22. Dispersed emission spectra of methyl torsional transitions for p'-cyano-p-methyl-trans-stilbene. Note the similarity of the 35.7 cm^{-1} band with the e torsional levels.

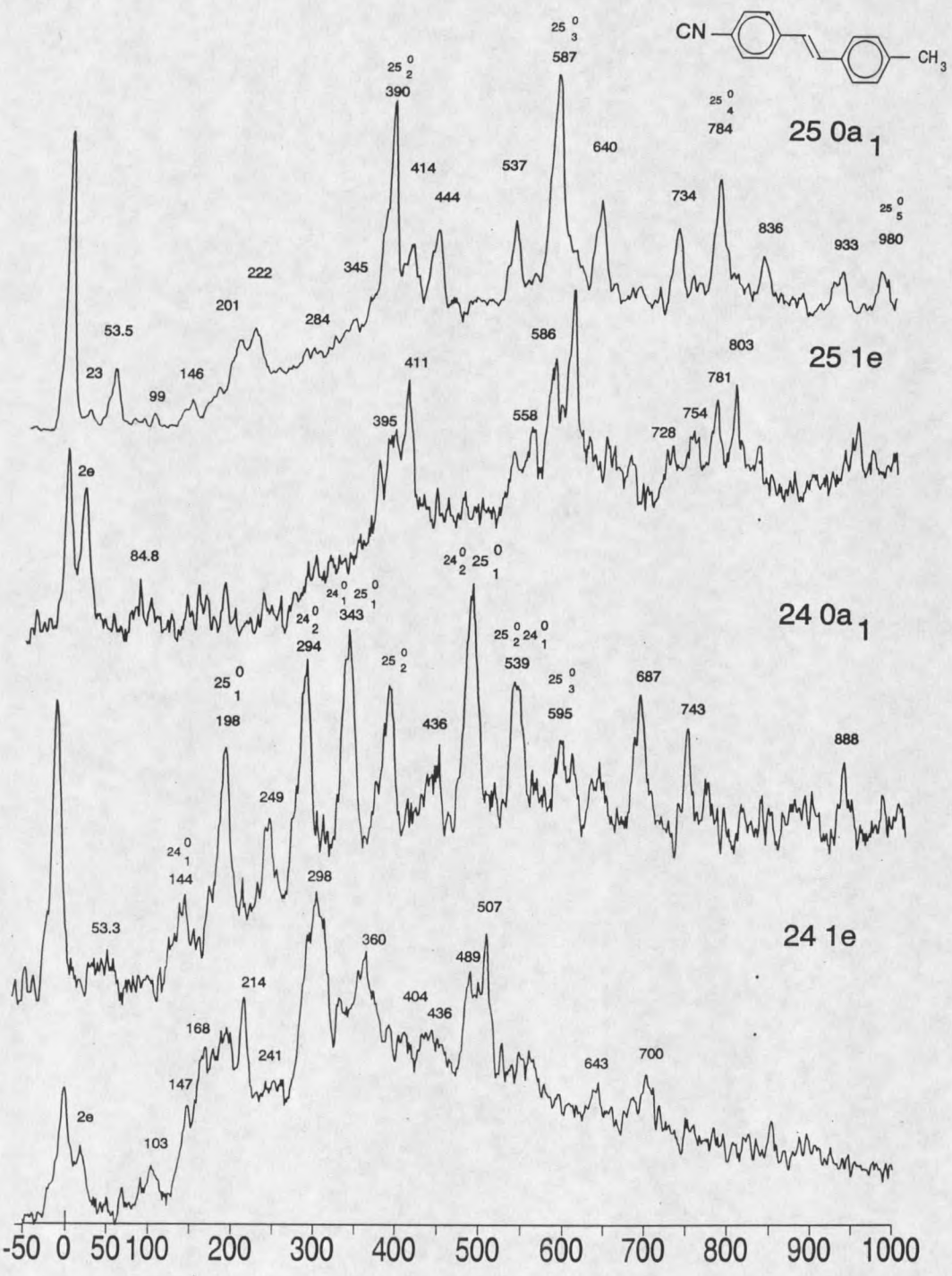

Figure 23. The dispersed emission spectra of the low frequency vibrations of p'-cyano-p-methyl-trans-stilbene.

methyl-trans-stilbene identifies 24^1_0 at 241.6 cm^{-1} and 24_1 at 256 cm^{-1} [64]. The 140 cm^{-1} transition is tentatively assigned as 24^1_0 since (i) no transition appears in the expected range of 240 cm^{-1}, and (ii) the dispersed emission is similar to the +241 cm^{-1} transition in p'-fluoro-p-methyl-trans-stilbene. Note that for p'-hydroxy-p-methyl-trans-stilbene (see Figure 17), 24^1_0 red shifts 30 cm^{-1} for only a cis (A) to trans (B) conformer change, so a significant shift in ν_{24} is not uncommon. Although there are several other low frequency transitions that remain unassigned, most of the transitions seen in the spectrum can be identified as methyl torsional levels, ν_{24}, ν_{25}, and combinations thereof.

Table 10. The torsional and vibrational frequencies for the ground and excited states of p'-cyano-p-methyl-trans-stilbene.

Assignment	S_0	S_1
$0a_1$	0 cm^{-1}	0 cm^{-1}
1e		-3.0
2e	19.5	43.85
$3a_1$	53.5	75.55
24, v = 1	147	139.1
25, v = 1	195	183
24 + 25	343	323.9
25, v = 2	390	367.9
25, v = 3	585	552

Dispersed emission from the ν_{24} and ν_{25} transitions in p'-cyano-p-methyl-trans-stilbene are shown in Figure 23. The dispersed emission spectrum from the $0a_1$ transition of ν_{24} shows a progression of peaks at 147, 298, and 436 cm^{-1}.

assigned to the first three quanta of ν_{24} in the ground state. The 198, 392, and 590 cm^{-1} bands are assigned to the first three quanta of ν_{25}; these peaks can also be seen in the dispersed emission from 25^1_0. The strong ν_{25} progression produces numerous combinations with ν_{24} which can be identified at 344, 489, 687, and 743 cm^{-1} completing the rest of the assignments of the observed peaks for this spectrum.

The assignments of the methyl torsional progression are supported by dispersed emission (see Figure 22). Excitation of the $0a_1$ and $3a_1$ transitions gives the frequency for $3a_1$ of 54 cm^{-1} in the ground state. Excitation of 1e and 2e levels yielded the expected frequency for 2e of 20 cm^{-1} in the ground state.

Table 11. The calculated and experimental torsional frequencies for p'-cyano-p-methyl-trans-stilbene.

assignment	S_0		S_1	
	experimental	calculated	experimental	calculated
$0a_1$	0 cm^{-1}	0 cm^{-1}	0 cm^{-1}	0 cm^{-1}
1e			-3.1	-2.75
2e	19.5	19.49	43.8	43.78
$3a_1$	53.5	53.50	75.6	75.55
4e		89.11	101.5	101.8
V_3		32.67		87.36
V_6		-6.09		9.12

The barrier to internal rotation for the methyl group has been fit for both S_0 and S_1. The barrier for S_0 is V_3"= 32.7 cm^{-1} with a small contribution from V_6 of

-6.09 cm^{-1}. The first excited state fit is V_3'= 87.36 cm^{-1} with a small contribution from V_6 of 9.12 cm^{-1}. It was assumed that a 60° conformational change occurs as analogous to other stilbenes and B'= 5.4 cm^{-1}. Experimentally, the methyl torsional barrier in p'-cyano-p-methyl-trans-stilbene is lower than p-methyl-trans-stilbene (150 cm^{-1}) and p'-fluoro-p-methyl-trans-stilbene (100.5 cm^{-1}).

p'-nitro-p-methyl-trans-stilbene

A brief mention will be made of a stilbene containing a stronger electron withdrawing group, p'-nitro-p-methyl-trans-stilbene. A sample was prepared and the analyzed by NMR, UV-VIS, FTIR, and GC for purity and quality. The melting point of 150°c was also compared to literature results[68]. Multiple attempts to find signal at various times were unsuccessful. There are several possibilities for this lack of fluorescence intensity in a $S_1 \leftarrow S_0$ electronic transition. It has been suggested that nitroaromatic molecules undergo an initial dissociation of the nitro group followed by photon absorption from the secondary structure[69]. There is general acceptance of this photodissociation owing to the readiness with which nitro-type compounds lose their nitro groups when irradiated with ultraviolet light[70]. Other researchers have found the nitro functional group capable of enhancing the intersystem crossing efficiency to triplet formation and photoisomerization[71,72]. Finally, p-nitro-trans-stilbene is weakly fluorescent even

at low temperatures and this may be the case for p'-nitro-p-methyl-trans-stilbene as well[73].

p-trifluoromethyl-trans-stilbene

Our interest in this molecule comes from the need for an additional electron-withdrawing group to validate the behavior found for the CN electron-withdrawing functional group. The electron-withdrawing nature of CF_3 is caused by the great electronegativity of the fluorine atoms[74]. Given the complexities of the low frequency torsional structure of the CF_3 group, an investigation of a species containing a lone CF_3 group will allow for a better understanding of the electronic spectra.

The fluorescence excitation spectrum of p-trifluoromethyl-trans-stilbene is shown in Figure 24. The glaring feature of p-trifluoromethyl-trans-stilbene which makes it so distinctive is the length and strength of a regular series of bands extending over 120 cm^{-1} built off the origin and other skeletal transitions. As explained in the experimental section, a 100μ pinhole diameter was used in the pulsed nozzle to further cool the molecule to reduce the number of hot bands observed. The progression is similar to the behavior found in 2-aminobenzotrifluoride and attributed to the substituent, CF_3[75]. Significant differences are expected between the torsional levels in the spectra of p-methyl-trans-stilbene and p-trifluoromethyl-trans-stilbene because of the greater mass of the CF_3, as compared to the CH_3 rotor. The internal rotational constant (*F*) of the

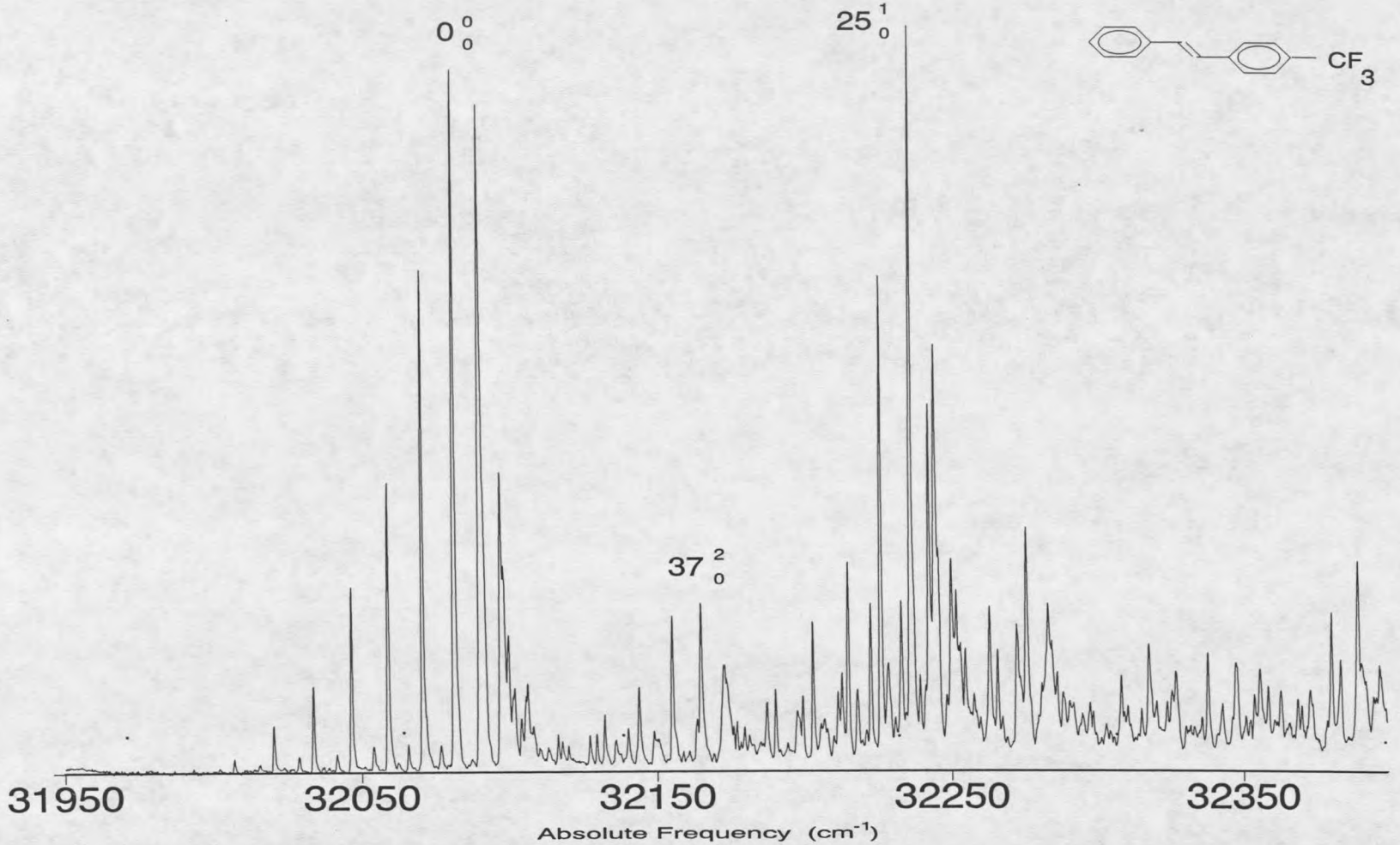

Figure 24. The fluorescence excitation spectrum of p-trifluoromethyl-trans-stilbene.

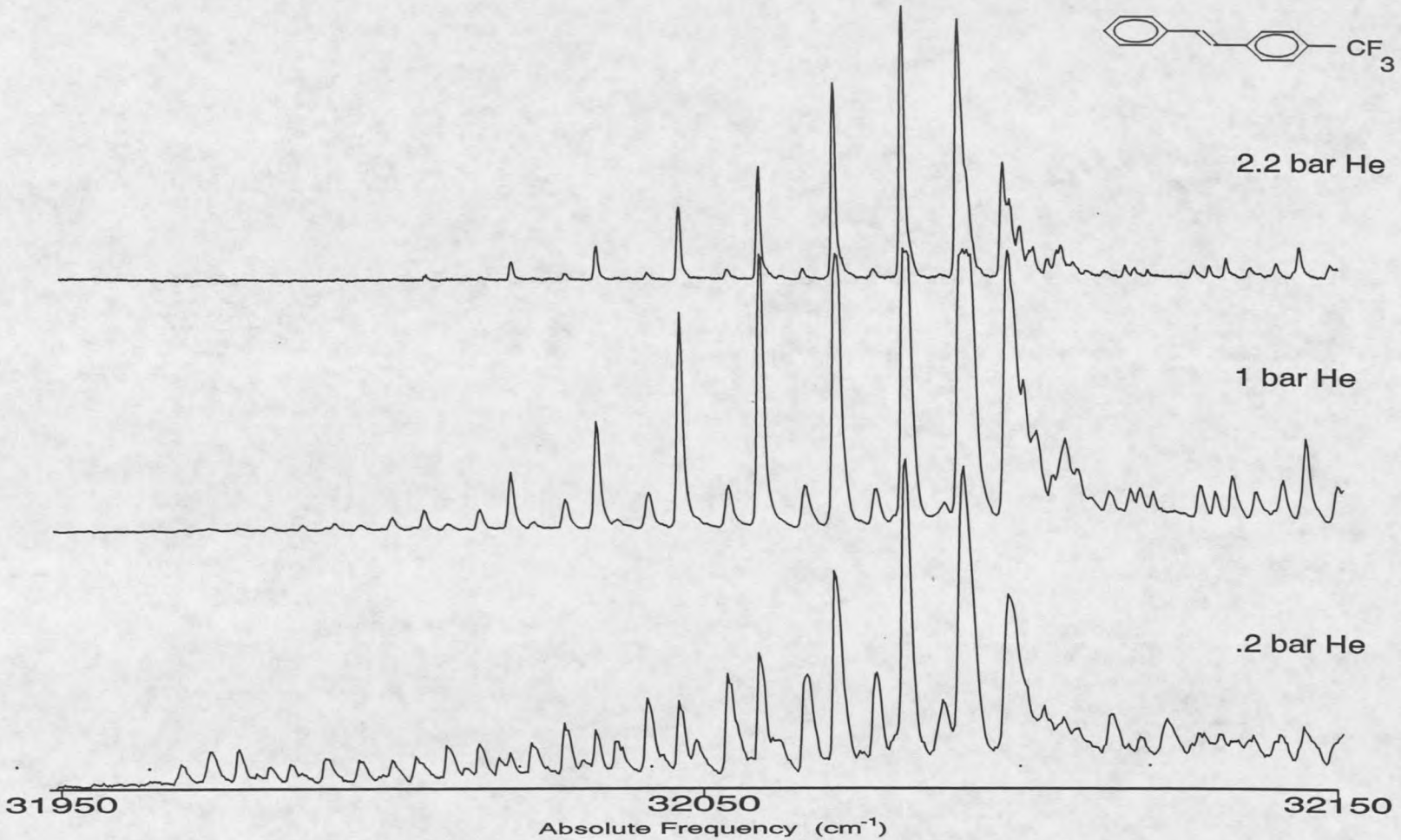

Figure 25. Torsional progressions for the trifluoromethyl group in p-trifluoromethyl-trans-stilbene. Prominent hot bands are observed at low pressures due to the small rotational constant of the trifluoromethyl group.

CF_3 group is much lower than CH_3 owing to the higher mass of the fluorine atoms off the rotational axis.

The combination of a smaller rotational constant, and the heavier fluorine atom being poor at tunneling results in (i) most of the torsional states lying well below the barrier and (ii) no splitting into the "a" and "e" components will be observed. The loss of tunneling behavior will make the CF_3 torsional levels appear more harmonic. The regularity of the observed series and absence of splitting signify that at least eleven torsional vibrational levels lie below the S_1 torsional barrier, which must be higher than 110 cm^{-1}, and the motion can be described as a torsional vibration versus internal rotation.

The lower value for *F* in CF_3 drastically reduces the spacing between the torsional levels and a greater number of S_0 levels will have population even at the low temperature of the supersonic jet. Figure 25 highlights the origin under different expansion conditions. As the helium backing pressure is decreased from 2 bar to 0.2 bar, new transitions grow in with different intensities characteristic of hot bands. The hot bands are CF_3 torsional transitions originating from higher levels. The presence of these hot band progressions gives us several ground state torsional level energies that may not have been resolved using dispersed emission. The first three levels have a frequency separation of only 5 cm^{-1}, which fits a ground state barrier for the trifluoromethyl group in the ground state of V_3"=15 cm^{-1}. Such a low barrier indicates that the third torsional level is at the top of the barrier and may explain the congestion.

that occurs at the low frequency end of the spectrum under warm expansion conditions.

The CF_3 torsional progressions clearly present a congested and complicated spectrum. The complex spectrum prevents a confident assignment of all members of each progression, hence the experimental frequencies are found by measuring the frequency difference between the correlating members of each identifiable progression. The most intense band progression at 144 cm^{-1} above the origin progression in the spectrum is assigned as 25^1_0. V_{25} is likewise split by the trifluoromethyl torsional splitting similar to the origin. Another progression can be identified at 75 cm^{-1}, and is assigned tentatively as 37^2_0.

The CF_3 torsion can be treated similar to a methyl functional group. Even under the cold conditions of the supersonic jet, the pattern of bands appears to march continuously out to the red end of the spectrum and a major problem has been to find the first member of the progression. The calculations presented here appear to solve this problem in that they are able to reproduce to a good approximation the overall profile of the band spectrum.

The CF_3 torsional vibration progression can be fit to a barrier using an estimated value for F' =0.24 cm^{-1}. The length of the band series suggests the S_1 torsional conformation differs substantially from that in S_0. See Table 12 for a comparison of the experimental and calculated frequencies and intensities. The rotational barrier for CF_3 in the excited state is V_3'= 125.8 cm^{-1}. It is observed in

the spectrum that the CF_3 torsional level intensities drop off rapidly with a peculiar 2 cm^{-1} splitting at the high frequency end of the progression.

Table 12. The frequencies and potential term constants of CF_3 torsion for p-trifluoromethyl-trans-stilbene. (V_3'= 125.8 cm^{-1}, V_6'= -7.0 cm^{-1}, 60° conformation change).

Transition	Frequency (cm^{-1})		Intensity	
	Experimental	Calculated	Experimental	Calculated
T_1	0 [a]	0.0	?	7.1e-4
T_2	14.5 [a]	14.39	?	1.3e-3
T_3	28.5	28.59	0.00413	0.006
T_4	41.5	42.45	0.0124	0.0078
T_5	55.5	56.06	0.0210	0.0256
T_6	68.5	69.16	0.0438	0.0279
T_7	80.5	81.79	0.0738	0.0811
T_8	92.5	93.5	0.1381	0.0831
T_9	103	104.1	0.1990	0.233
T_{10}	112.5	113.3	0.2966	0.200
T_{11}	119.5	119.7	0.2108	0.207
T_{12}	121.5	123.3	0.1104	0.0685
T_{13}	127.5	129.8	0.037	0.0338

[a] observed under saturated conditions

Additionally, the members of the progression have become broader with increasing energy. It is intuitively reasonable that as the torsional levels reach the top of the barrier, the degeneracy of the levels breaks down and the torsional levels begin to conform to that of a free rotor. The model calculations support this splitting activity near the top of the barrier, although the quantitative fit begins

60° conformation change for CF_3 upon excitation, similar to conformation changes seen for the CH_3 rotor in methylated stilbenes.

p'-trifluoromethyl-p-methyl-trans-stilbene

The combination of low frequency torsional modes coming from the trifluoromethyl group and the methyl group create a much more complex spectrum than any other para'-para-substituted stilbene molecule investigated thus far. The fluorescence excitation spectrum for p'-trifluoromethyl-p-methyl-trans-stilbene is shown in Figure 26. A similar progression of CF_3 torsional levels observed for p-trifluoromethyl-trans-stilbene (see Figure 24) can also be seen in this spectrum. It follows from Franck-Condon arguments that this activity can only occur if the trifluoromethyl group adopts a conformation in the upper S_1 state which is different than the lower S_0 ground state. Thus, it would be anticipated that the trifluoromethyl group here undergoes a 60° rotational displacement similar to that found for p-trifluoromethyl-trans-stilbene. One key difference between the two molecules, however, is the characteristic $0a_1$-1e methyl rotor splitting built off each member of the CF_3 progression coming from the addition of the methyl group. The methyl rotor splitting has significantly complicated the excitation spectrum here relative to the unmethylated species since the number of the prevalent CF_3 bands has basically doubled.

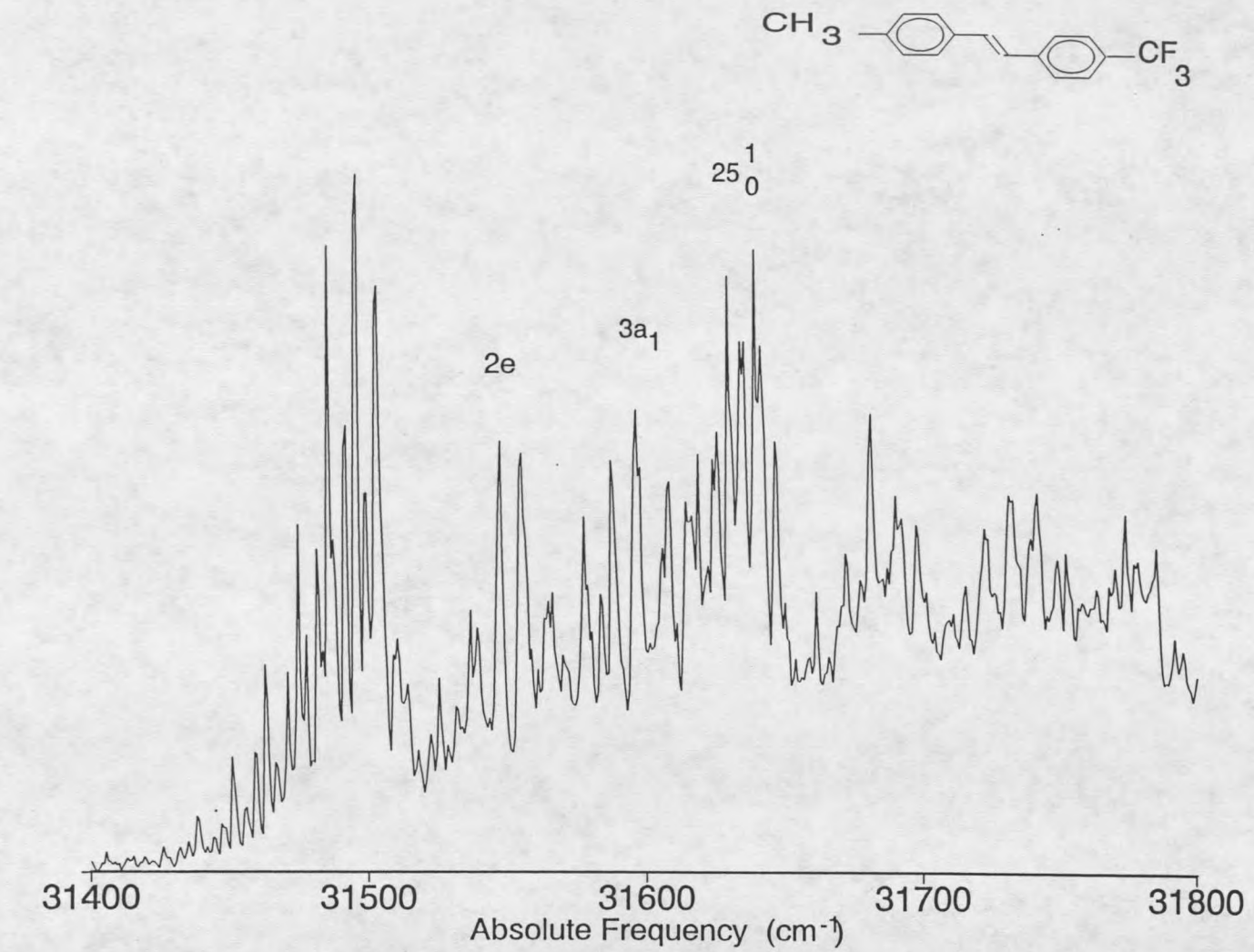

Figure 26. The fluorescence excitation spectrum of p'-trifluoromethyl-p-methyl-trans-stilbene.

Although the interest in p'-trifluoromethyl-p-methyl-trans-stilbene is how the remote CF_3 electron-withdrawing functional group affects the methyl torsional barrier, the task of identifying torsional structure belonging to the methyl group is difficult in the heavily congested spectrum. As mentioned in the beginning of this chapter, methyl torsional levels will not display the $0a_1$-1e splitting, so most unsplit transitions can be assigned to the methyl rotor. On the other hand, the methyl torsional levels in this molecule will display CF_3 torsional structure. Since the 2e, $3a_1$, and 4e are the only methyl torsional levels having significant intensity in the methylated stilbenes investigated thus far, the presence of CF_3 progressions between the origin and ν_{25} that do not display the $0a_1$-1e splitting would be characteristic of these methyl torsional levels.

Table 13. The calculated and experimental frequencies of CH_3 torsion for p'-trifluoromethyl-p-methyl-trans-stilbene.

assignment	experimental frequency	calculated frequency
$0a_1$	0 cm^{-1}	0 cm^{-1}
1e	-3.5	-3.45
2e	52.00	52.16
$3a_1$	101.0	101.00
4e		118.19
v'_3		134.6
v'_6		-24.4

Under close examination, there are two recognizable progressions that seem to fit the description. The complex spectrum prevents a confident

assignment of all members of each progression, hence the experimental frequencies are found by measuring the frequency difference between a correlating member of each identifiable progression. The tentative assignment of the frequencies of the methyl transitions (see Table 13) translates to an estimated barrier of 138 cm^{-1} in the excited state.

While our interest is in the effects of remote substituents on the methyl group, a comparison of the effect a CH_3 group has on the CF_3 torsional barrier does speak to the electronic effects between functional groups. Since our observations suggest that the CH_3 group is sensitive to the presence of remote functional groups at the far end of the molecule, it would be anticipated that the CF_3 group would also be sensitive to the presence of a remote substituent, the CH_3 group in this case, located ten carbons away. Furthermore, the CH_3 is a weak electron donor, so the barrier should decrease by a smaller percentage than that found for the methoxy group; A 33% reduction in the methyl torsional barrier was observed for p'-methoxy-p-methyl-trans-stilbene relative to p-methyl-trans-stilbene[22].

It is observed in the spectrum that the CF_3 torsional level intensities drop off rapidly with a peculiar 2 cm^{-1} splitting at the high frequency end of the progression similar to that found for p-trifluoromethyl-trans-stilbene. Additionally, the members of the progression have become broader with increasing energy. As stated previously, when the torsional levels reach the top of the barrier, the degeneracy of the levels breaks down and the torsional levels begin to conform

to that of a free rotor. The model calculations (see Table 14) support this splitting activity near the top of the barrier, although the quantitative fit breaks down near and above the barrier for p'-trifluoromethyl-p-methyl-trans-stilbene as well. The broadening observed at the high end of the progression is due to unresolvable splitting of the torsional levels.

Table 14. The experimental and calculated frequencies/intensities of CF_3 torsion for p'-trifluoromethyl-p-methyl-trans-stilbene (V_3'= 98.1 cm^{-1}, V_6'= -8 cm^{-1}, 60° conformation change, B' = 0.24 cm^{-1}).

Transition	Frequency		Intensity	
	experimental	calculated	experimental	calculated
T_1	0.0[a]	0.0	?	0.001
T_2	12.0	12.06	0.00752	0.002
T_3	24.0	24.11	0.0258	0.0097
T_4	36.0	36.03	0.0345	0.0127
T_5	48.0	47.67	0.0566	0.0420
T_6	58.0	58.92	0.0792	0.0464
T_7	68.0	69.56	0.1852	0.137
T_8	80.0	79.33	0.2214	0.144
T_9	87.0	87.08	0.2573	0.351
T_{10}	94.0	94.53	0.0833	0.139
T_{11}	99.0	100.3	0.0491	0.0953

a. estimated

The barrier to internal rotation has been fit for the trifluoromethyl group in S_1 and the rotational barrier for CF_3 in the excited state is V_3'= 98 cm^{-1}, a 22% reduction in the CF_3 barrier relative to p-trifluoromethyl-trans-stilbene. The

increasing intensity in the higher transitions correspond to a dramatic conformation change between the ground and excited states. The model calculations fit the intensity distribution best with a 60° conformation change for CF_3 upon excitation, similar to conformation change seen for the CF_3 rotor in p-trifluoromethyl-trans-stilbene.

p-dimethylamino-trans-stilbene

The dimethylamino functional group is one of the strongest electron donating groups known and is widely used as the donating species in "push-pull" stilbene experiments[76]. As mentioned in the introduction, previous studies have found that the strong donating character of remote functional groups, such as the amino and methoxy functional groups, reduce the barrier of the methyl group ten atoms away on the stilbene skeletal frame relative to p-methyl-trans-stilbene. Furthermore, there is a pattern in the reduction of the barrier suggesting that the stronger the electron-donating group, the lower the barrier. Since the dimethylamino functional group is a stronger donor than the amino group, p'-dimethylamino-p-methyl-trans-stilbene should possess a lower barrier than the 55 cm^{-1} barrier found for p'-amino-p-methyl-trans-stilbene. Thus, p'-dimethylamino-p-methyl trans-stilbene is a logical candidate in testing the applicability of remote electron donating substituent effects on the methyl barrier.

As a first step in this direction, the fluorescence excitation and dispersed emission spectra of p-dimethylamino-trans-stilbene will be presented. Since the

dimethylamino functional group consists of three rotors and could possibly be non-planar, the precise nature of the vibronic structure is unclear and a study of p-dimethylamino-trans-stilbene should allow for a fuller assignment. The dimethylamino functional group is widely known to become non-planar in the excited states of several molecules, including 4-dimethylaminobenzonitrile[77]. The ability of the dimethylamino functional group to twist during excitation results in a "twisted internal charge transfer" (TICT) state, which creates unusual emission properties like dual fluorescence. The spectral simplicity of p-dimethylamino-trans-stilbene should facilitate analysis of the torsional and inversion modes of the dimethylamino group, hence making analysis of the methyl torsional progression expected for the p'-dimethylamino-p-methyl-trans-stilbene possible.

A recent publication reporting the fluorescence excitation of p'-dimethylamino-p-cyano-trans-stilbene (DCS) will be used as a guide for the proposed assignments[78]. The low frequency transitions in DCS and p-dimethylamino-trans-stilbene should be comparable for the following reasons. Previous research found the electron-withdrawing para cyano substituent to have little contribution to the fluorescence excitation spectrum of 4-dimethylamino-benzonitrile[79]. Consequently, the spectrum of 4-dimethylaminobenzonitrile is virtually identical to N,N-dimethylaniline instead of benzonitrile; the low frequency modes are clearly associated with the dimethylamino group. It is reasonable to

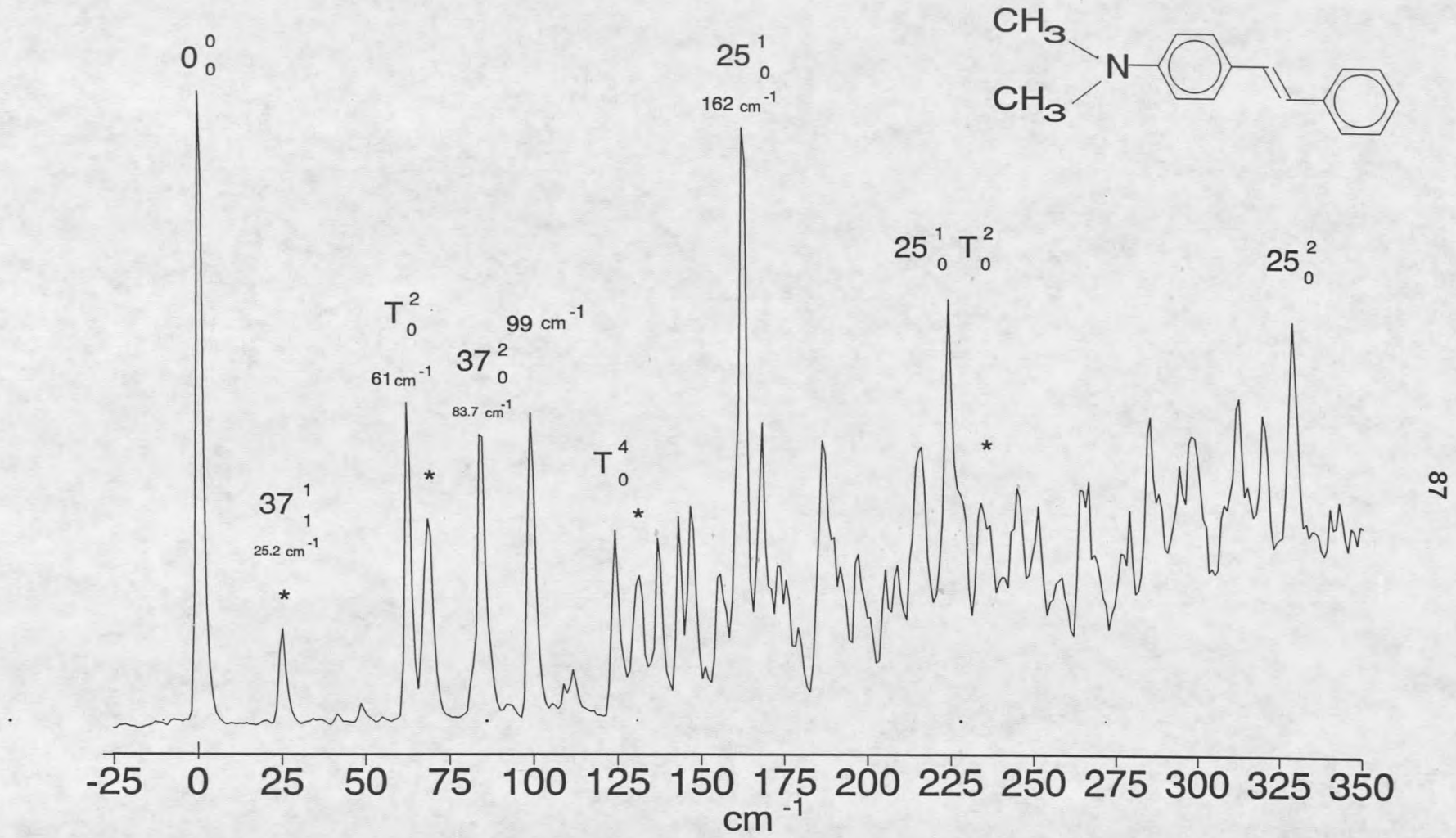

Figure 27. The fluorescence excitation spectrum of p-dimethylamino-trans-stilbene.

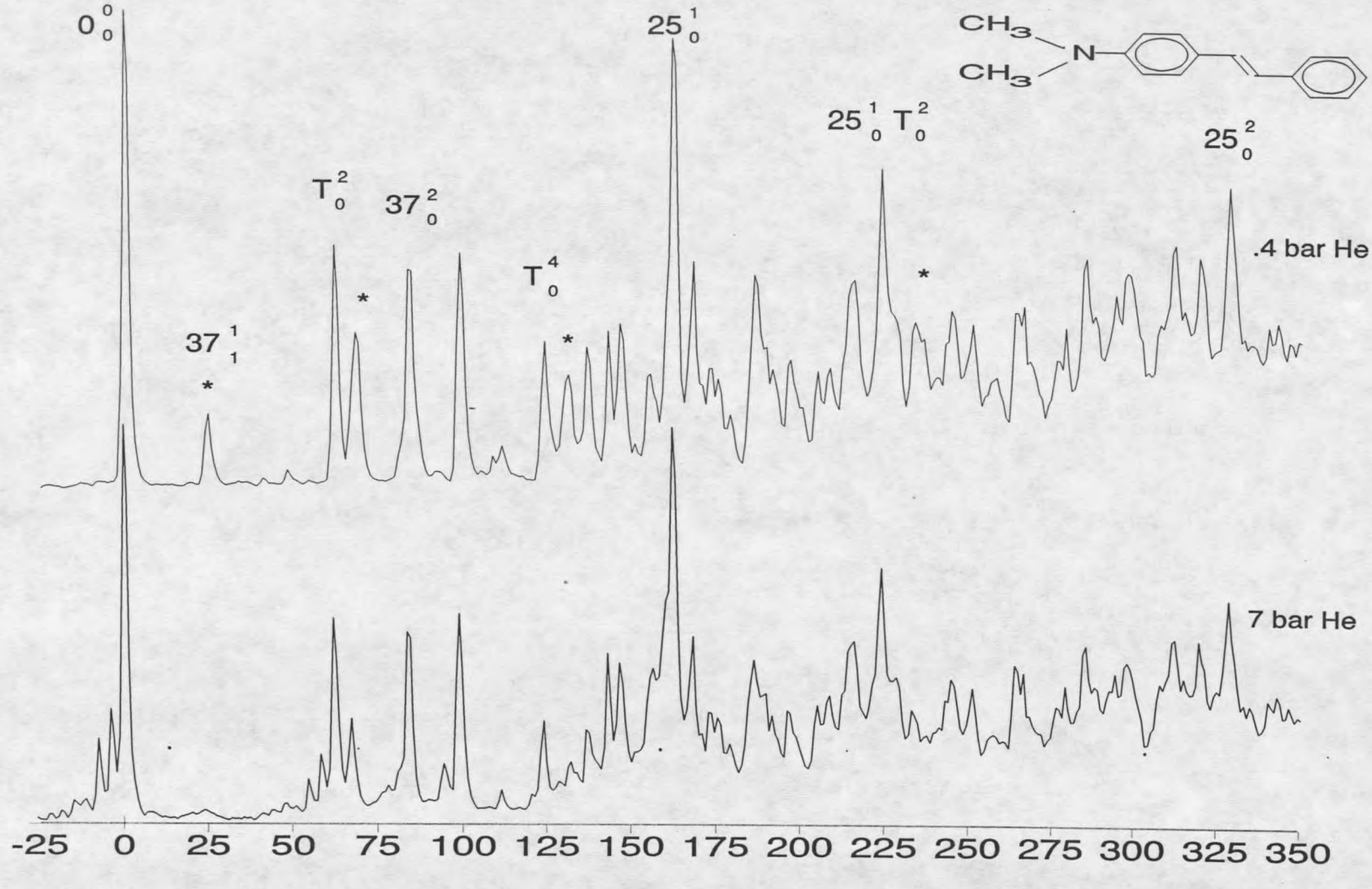

Figure 28. Comparison of the fluorescence excitation spectra of p-dimethylamino-trans-stilbene under different expansion conditions.

expect the low frequency transitions of DCS to resemble that of p-dimethylamino-trans-stilbene.

The fluorescence excitation of p-dimethylamino-trans-stilbene is shown in Figure 27. The origin is assigned at 28,591 cm^{-1} and is a singlet which indicates that the methyl rotors of the functional group have similar barriers in both electronic states and do not change conformation upon excitation. Furthermore, the absence of higher frequency torsional structure indicates that there is no change in conformation. The strong transition at 162 cm^{-1} to the blue of the origin can be identified as the ν_{25} vibration owing to similarities in previous stilbene molecules. The ν_{25} vibration in DCS was assigned at 131 cm^{-1}, which is even lower than for p-dimethylamino-trans-stilbene. While the authors attribute the low frequency to a mass effect, experiments on p-methoxy-trans-stilbene and p-hydroxy-trans-stilbene reported here provide evidence that ν_{25} is affected more by electron density in the conjugated system.

There are several bands in the p-dimethylamino-trans-stilbene spectrum below 100 cm^{-1} that may be the torsional and inversion modes of the dimethylamino functional group. Figure 28 shows a close up view of the low frequency modes in p-dimethylamino-trans-stilbene under different expansion conditions. At a backing pressure of 7 bar, the discrete helium peaks seen for the origin and the 62.1 cm^{-1} transition are missing for the 83.7 cm^{-1} transition. In both the trans-stilbene van der Waals helium complex and the p-methyl-trans-stilbene van der Waals helium complex, the strong coupling of the out-of-plane

phenyl torsion 37^2_0 with the van der Waals modes leads to a broadening of the transitions to several times their breadth in in-plane vibrations[80,81]. The helium atom is generally accepted to be above the stilbene frame moving in a pseudotranslational motion, thus phenyl bending or torsional motion will involve motion directly against the van der Waals-bound species. The dramatic broadening is only observed for the 83.7 cm^{-1} supports the assignment as the out-of-plane-torsion (37^2_0).

Under different expansion conditions shown in Figure 28, hot bands appear at 25.2, 69, and 131.5 cm^{-1} above the origin. An assignment of the 25.2 cm^{-1} hot band as a dimethylamino functional group torsion (T^1_1) seems unlikely since dispersed emission spectra indicates that the dimethylamino group torsion has a similar frequency in both states. 37^1_1 has been observed in this frequency range under warm expansion conditions at 32.7 cm^{-1}, 35.9 cm^{-1}, and 37.8 cm^{-1} in p'-amino-p-methyl-trans-stilbene, p-methyl-trans-stilbene, and p-methoxy-trans-stilbene, respectively[23,15,22]. The fact that ν_{37} in p'-amino-p-methyl-trans-stilbene increases in frequency for S_0 and decreases in frequency for S_1 relative to the parent trans-stilbene molecule also supports the assignment here since both the amino and dimethylamino functional groups have similar character[23]. Moreover, the increased electron donating ability of the dimethylamino functional group could mean a higher 37^0_1 frequency relative to p'-amino-p-methyl-trans-stilbene. If 37^0_1 is assumed to be approximately 14 cm^{-1} in the ground state based on similar frequency in all other stilbenes, then an assignment of the 25.2 cm^{-1} hot

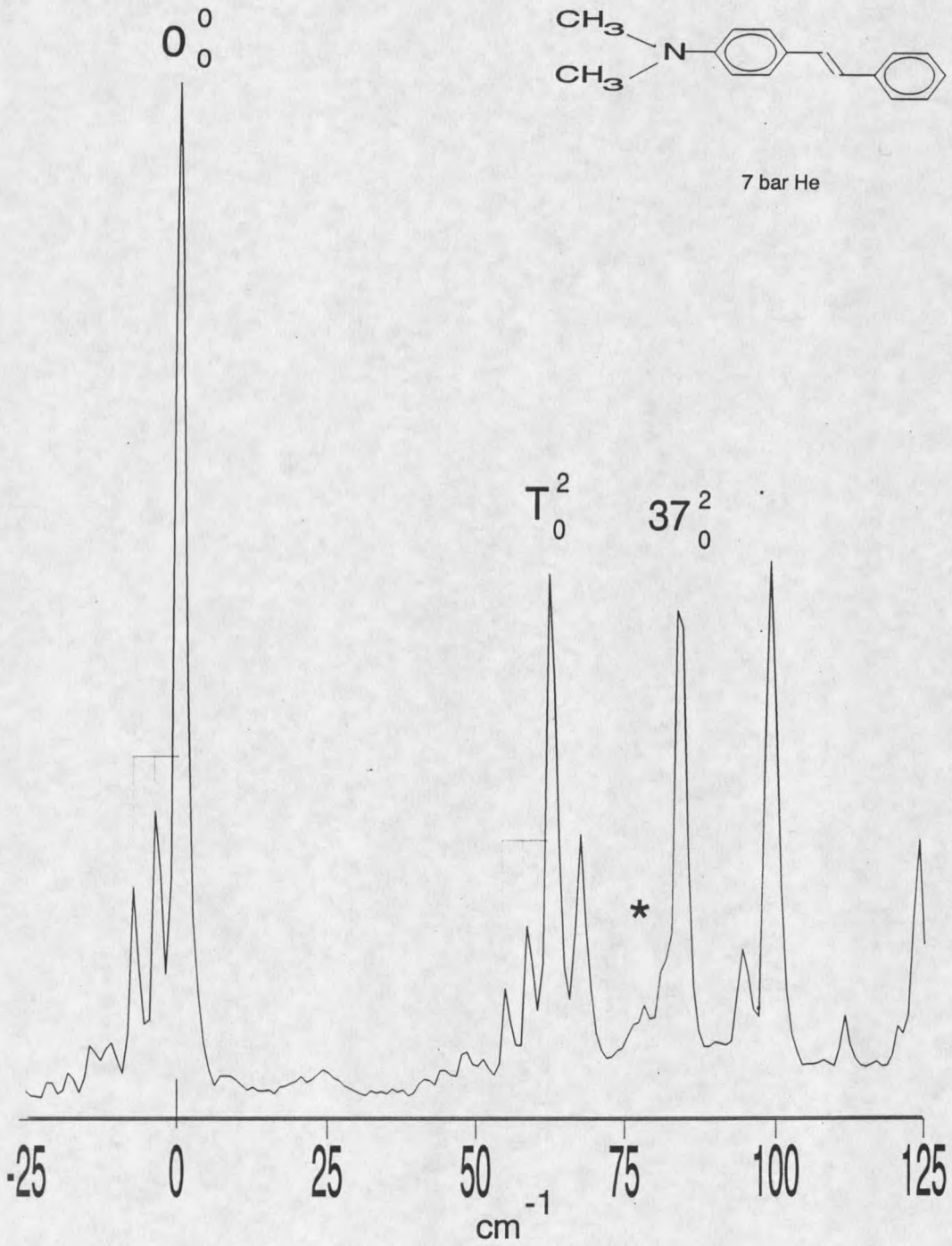

Figure 29. Close-up fluorescence excitation spectrum of p-dimethylamino-trans-stilbene under cold expansion conditions. Note that only the 37^2_0-He transitions are broadened.

band as 37^1_1 indicates a lower frequency for 37^2_0 relative to other stilbenes in the excited state. The transition observed at 83.7 cm^{-1} is near the correct frequency and is thus assigned as 37^2_0 and 37^1_1 is assigned at 25.2 cm^{-1}.

By contrast to the broadened van der Waals transitions on 37^2_0, the helium peaks near the 62.1 cm^{-1} peak are narrow and virtually indistinguishable from the peaks near the origin. This behavior would be expected for either in-plane vibrations or localized motion of the dimethylamino functional group. Furthermore, It is generally accepted that the dimethylamino torsion mode is largely unaffected by the remainder of the intramolecular environment and appears at a frequency near 65 cm^{-1} in the excited state in molecules containing a dimethylamino group[79,82-84]. Therefore, the 62.1 cm^{-1} peak is assigned to the dimethylamino group torsion about the C_{aryl}-N bond. Two quanta of the dimethylamino torsion is assigned to the transition 124.2 cm^{-1} above the origin. The transition at 99 cm^{-1} still remains unassigned.

Table 15. The major vibrational frequencies for the ground and excited state of p-dimethylamino-trans-stilbene.

Assignment	S_0	S_1
$N(CH_3)_2$ torsion, v=2	63 cm^{-1}	62.1 cm^{-1}
$N(CH_3)_2$ torsion, v=4	123	124.2
ν_{37}, v=2		83.7
?	98	
ν_{25}, v=1	180	162
ν_{25}, v=2	358	328.5

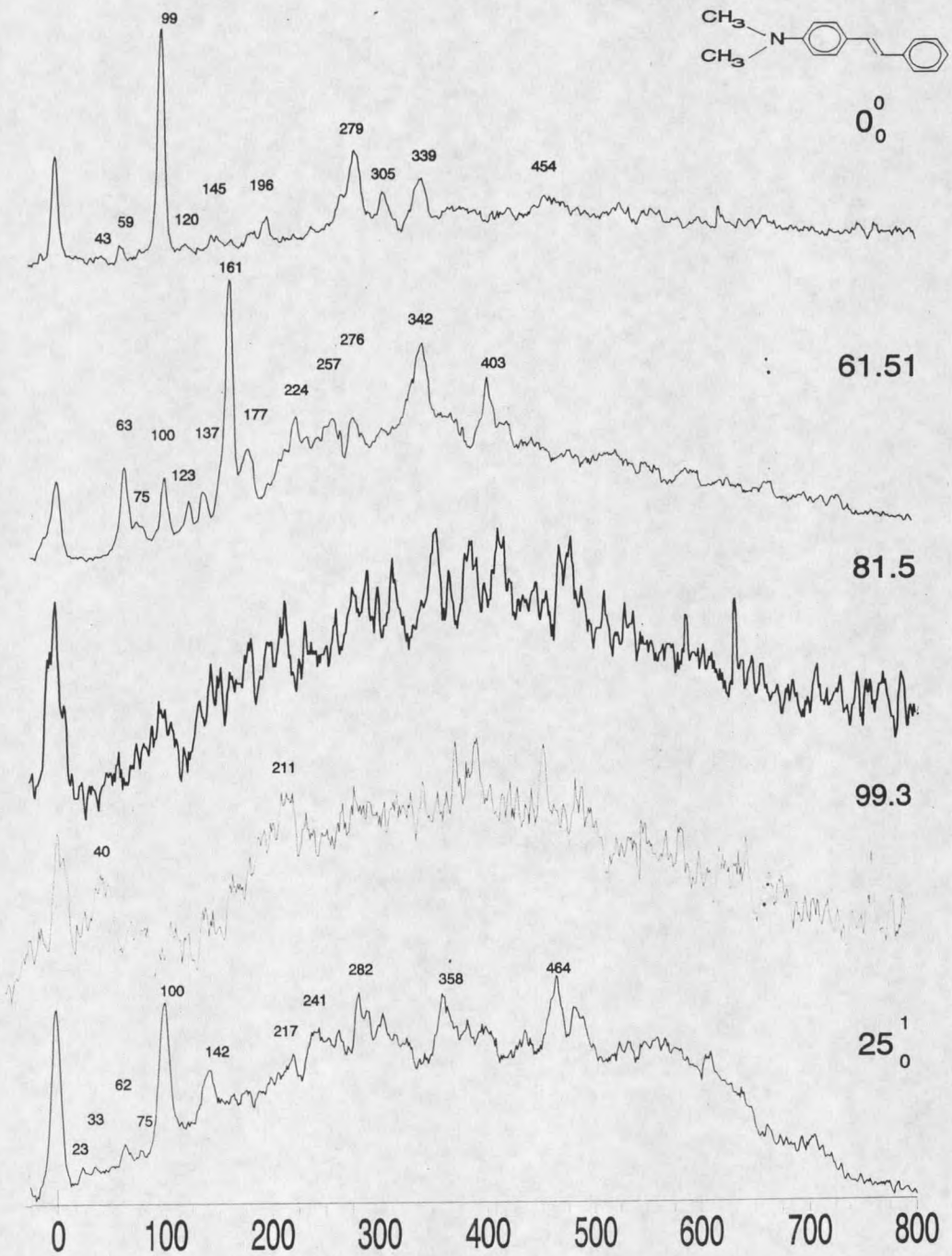

Figure 30. Dispersed emission from the low frequency transitions in p-dimethylamino-trans-stilbene.

The dispersed emission for p-dimethylamino-trans-stilbene are shown in Figure 30. Each spectrum is an average of ten 5 minute exposures taken with slit widths varying between 200-300μ except for a slit width of 500μ for emission from the 83.7 cm^{-1} transition. The assignment of the ground state energy levels has proven to be difficult in p-dimethylamino-trans-stilbene because the dispersed emission does not show the familiar characteristics seen in the emission spectra of other stilbenes. The dispersed emission spectra show a clear combination of discrete vibronic transitions superimposed on a rising congested background.

The dispersed emission spectrum produced by exciting the 0^0_0 transition does not bear a symmetric relationship with the excitation spectrum; there is a strong additional feature at 100 cm^{-1} above the origin, the assignment of which is not immediately obvious. Dispersed emission from both the origin and 25^1 show this intense peak at 100 cm^{-1}. In contrast, this same peak is weak in the emission from the 61.5 cm^{-1} peak, yet is present in combination. The transitions at 82 cm^{-1} and at 96 cm^{-1} have unresolvable dispersed emission. This could be due to IVR or spectral congestion caused by the very low frequency vibrations in the ground state.

The clear absence of a strong ν_{25} presence in any of the emission spectra can not be clearly explained. A reason for this may be due to a nonplanar geometry coming from a twisted dimethylamino functional group. The different geometry could change the symmetry and selection rules of certain transitions.

The rotational constants found for DCS suggest that both the S_0 and S_1 states are non-planar, hence p-dimethylamino-trans-stilbene might be nonplanar as well[78].

More compelling evidence can be found in the excitation spectrum taken under super cold conditions (bottom trace in Figure 28). The transitions are still very broad even at a high carrier gas backing pressure; the f.w.h.m. is typically 1 cm^{-1} at 7 bar of helium, but for this molecule the f.w.h.m. is 2.7 cm^{-1}. Since the sharpness of vibronic structure decreases with non-planarity, the broadness in the p-dimethylamino-trans-stilbene spectrum supports a non-planar geometry[85]. A nonplanar geometry could have major implications on the donating ability of dimethylamino functional group to the methyl rotor on the opposite para position in the p'-dimethylamino-p-methyl-trans-stilbene.

p'-dimethylamino-p-methyl-trans-stilbene

Previous results in this group have shown how the electron donating capabilities of a substituent can dramatically reduce the barrier to internal rotation of the methyl group. The barrier to methyl internal rotation in p'-amino-p-methyl-trans-stilbene was found to be 55 cm^{-1}, the lowest barrier observed so far. The electron donating capabilities of the dimethylamino functional group exceeds the amino group and should affect the barrier to internal rotation of the ring methyl group separated by the extended conjugated π system accordingly.

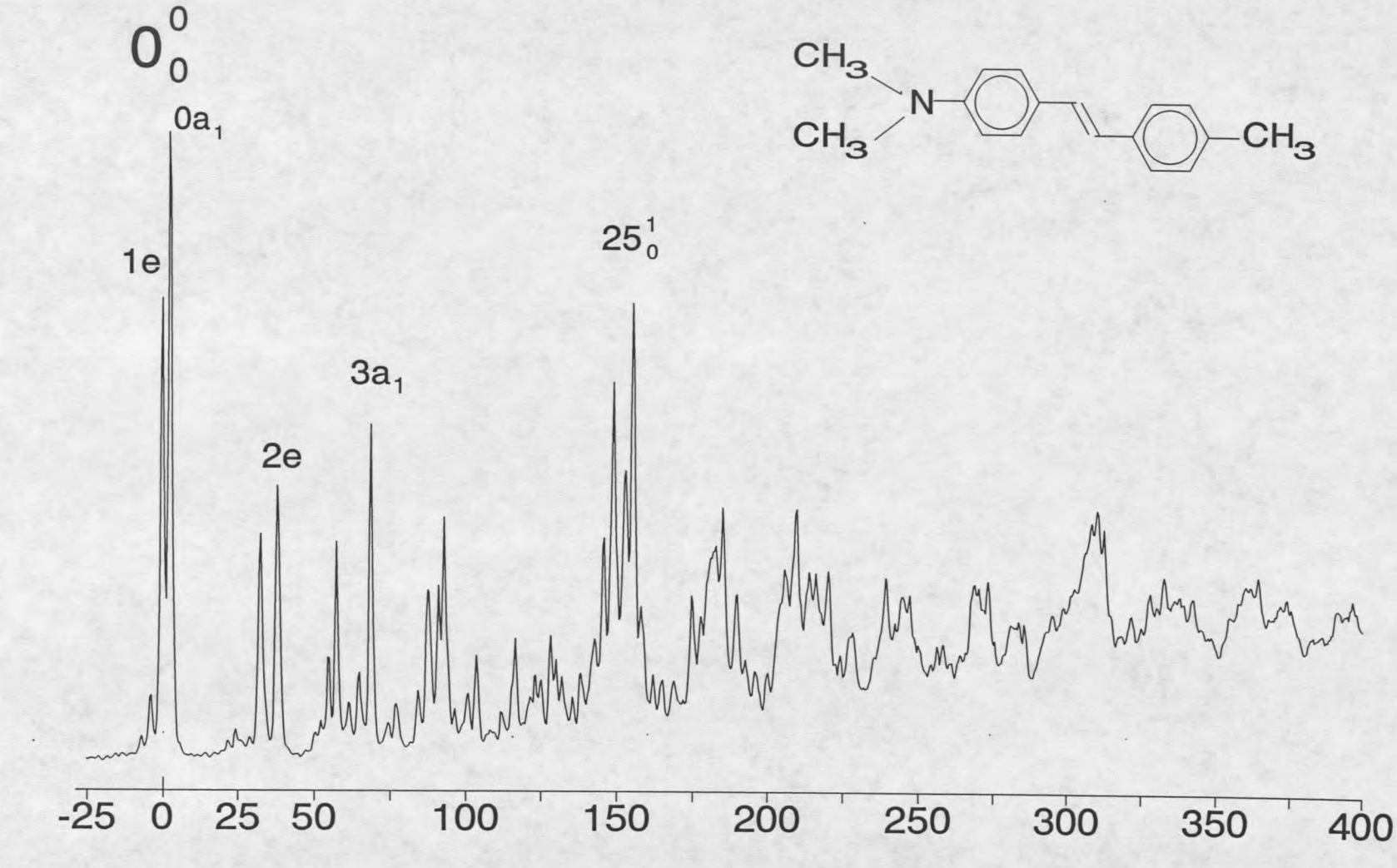

Figure 31. The fluorescence excitation spectrum of p'-dimethylamino-p-methyl-trans-stilbene.

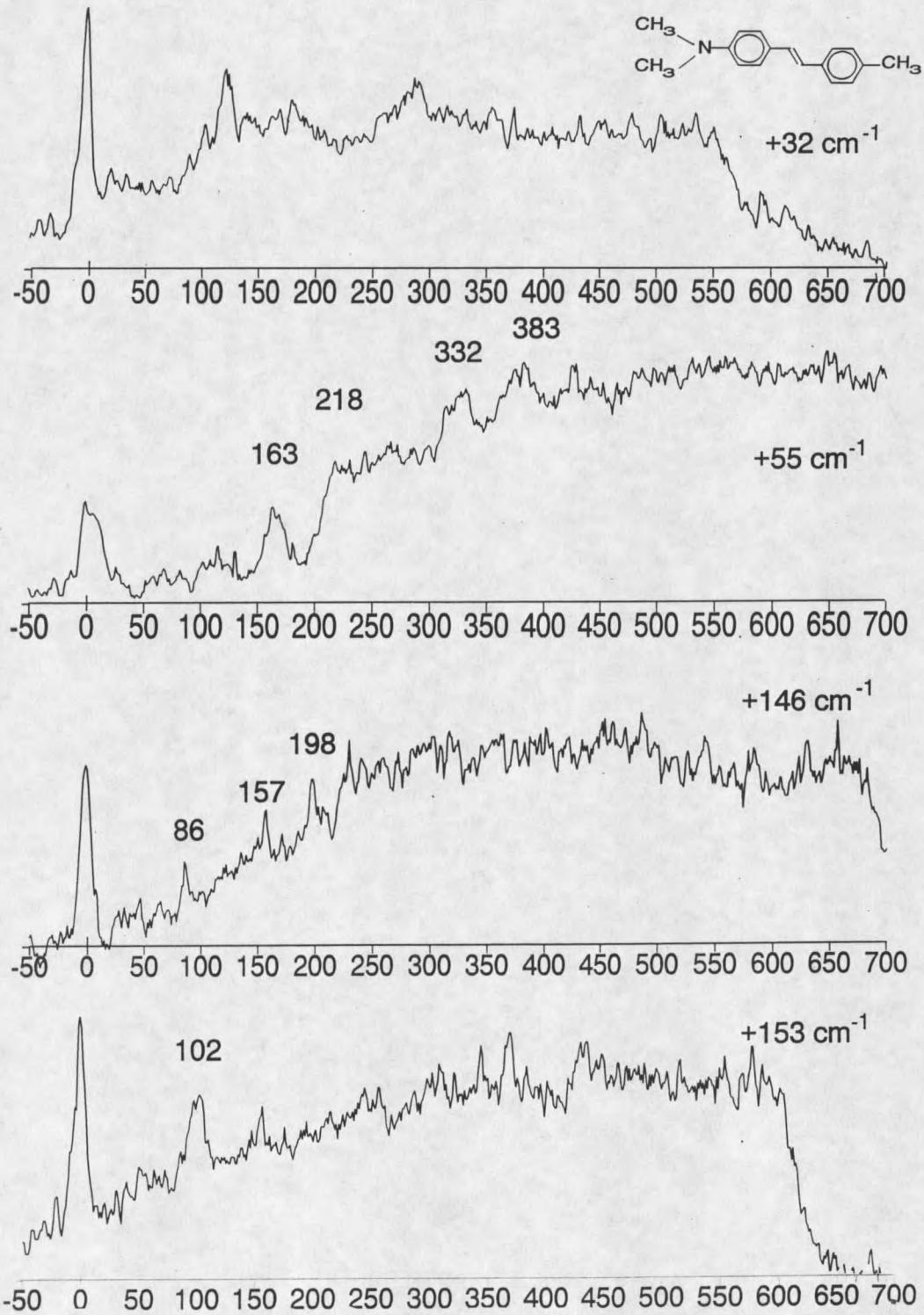

Figure 32. The dispersed emission from the low frequency vibrations of p'-dimethylamino-p-methyl-trans-stilbene.

Table 16. The major vibrational frequencies for the ground and excited state of p'-dimethylamino-p-methyl-trans-stilbene.

Assignment	S_0	S_1
$0a_1$	0 cm^{-1}	0 cm^{-1}
1e		-2.3
2e	22.0	35.5
$3a_1$	51.0	66.1
T, v=2		54.8
ν_{37}, v=2	27	74.4
?	101	
ν_{25}, v=1	178	152.9
ν_{25}, v=2	360	307.8

The jet-cooled fluorescence excitation spectrum of p'-dimethylamino-p-methyl-trans-stilbene is presented in Figure 31. The spectrum shown had a backing pressure of 3 bar He and was ran at 0.3cm^{-1}/s. Weak helium complexes can be observed at this pressure. Readily apparent is the methyl torsional splitting of the origin and other normal modes similar to other methylated stilbenes. The absolute frequency of the origin has decreased to 28,533.7 cm^{-1} upon methyl substitution. Since the energies of the π-π^* electronic transitions decrease with growing charge transfer character, the stronger electron-donating capability of the dimethylamino functional group should lower the absolute frequency of p'-dimethylamino-p-methyl-trans-stilbene below that of p'-amino-p-methyl-trans-stilbene[85]. The 1000 cm^{-1} absolute frequency difference for the dimethylamino group does imply significant charge transfer. Such charge transfer is further supported by the absolute frequency of DCS, discussed in the

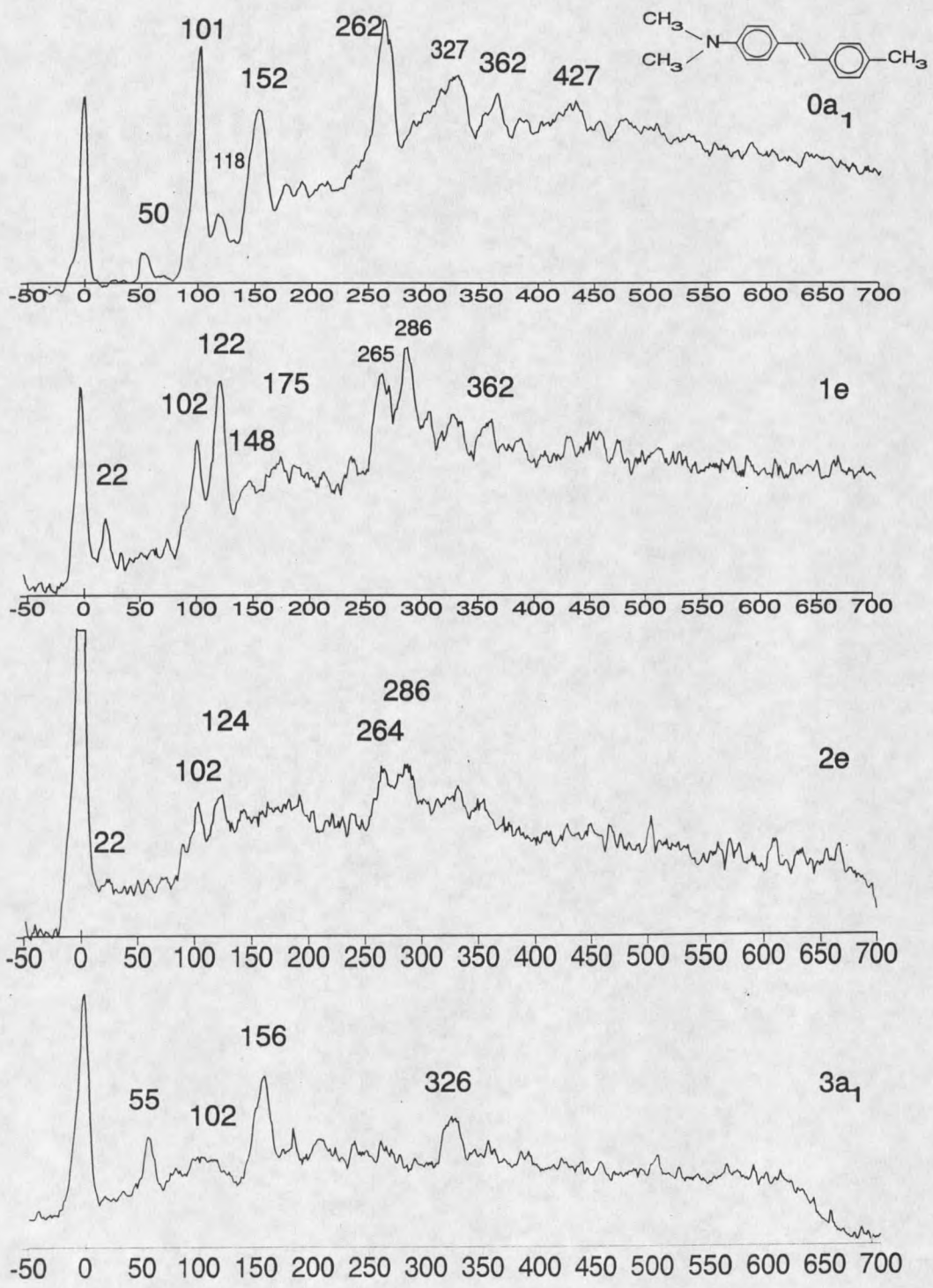

Figure 33. Dispersed emission from the methyl torsional levels in p'-dimethylamino-p-methyl-trans-stilbene.

last section. The replacement of a methyl group with the cyano electron-withdrawing group has lowered the absolute frequency to 27,038 cm^{-1} [78].

The presence of hot bands were confirmed with pressure studies at 22.1, 62.6, and 74.9 cm^{-1} above the origin and are also split by the methyl rotor. While the spectrum is heavily congested with low frequency transitions from both para functional groups, 25^1 can be identified at 153.4 cm^{-1}. The splitting between the 1e-$0a_1$ transitions is 2.3 cm^{-1}, the 2e is assigned at 35.5 cm^{-1}, and the $3a_1$ is assigned at 65.1 cm^{-1} above the origin.

The peaks near 54.9 cm^{-1} displaying the $0a_1$-1e splitting is comparable to the intense peak at 62.1 cm^{-1} in p-dimethylamino-trans-stilbene and is assigned as the dimethylamino torsion. The lower frequency for the torsion stems from the interaction the methyl group has with the electron density of the π system. A comparison of the hot band at 22.7 cm^{-1} to the 25.2 cm^{-1} hot band seen in p-dimethylamino-trans-stilbene indicates 37^2_0 is the small peak at 74.4 cm^{-1}. The weakness of ν_{37} is not surprising and has been hard to identify for other methylated species. Besides the expected combination of the mentioned transitions with ν_{25}, the other transitions in the spectrum are weak and unidentifiable.

Due to the appearance of low frequency modes of the dimethylamino functional group, the assignments of the methyl torsional levels were confirmed by dispersed emission.

The dispersed emission spectra shown in Figures 32 and 33 were obtained with the CCD acquisition system with an average entrance slit width of 250μm and exposure time of six minutes. The presence of a strong transition in combination with methyl torsional levels in the dispersed emission, shown in Figure 33, is similar to the transition seen in p-dimethylamino-trans-stilbene at the same frequency of 100 cm^{-1}. The presence of the e-only transition at 30.1 cm^{-1} is consistent with other methylated stilbenes and the intensity of the peak and the separation from the 2e transition is important in the understanding of a possible Fermi resonance. The 4e and higher torsional levels are not readily identified due to low intensity and spectral congestion. The barrier to internal rotation has been fit for the S_0 and S_1 with V_3" = 28.62 cm^{-1} and V_3' = 68.08 cm^{-1}.

Table 17. The experimental and calculated torsional frequencies for p'-dimethylamino-p-methyl-trans-stilbene in S_1 (V_3'= 68.08 cm^{-1}, V'_6= 4.36 cm^{-1}).

Assignment	experimental frequency	calculated frequency
$0a_1$	0 cm^{-1}	0 cm^{-1}
1e	-2.3	-2.17
2e	35.5	35.62
$3a_1$	65.1	65.09
4e		94.66

p'-p-dimethyl-trans-stilbene

We now extend these studies to p-p'-dimethyl-trans-stilbene. This work seeks to investigate the interaction between the two methyl rotors separated by an extended conjugated system. Since this molecule contains two methyl groups, simultaneous rotations can and do occur. The molecule's rotating groups may show coupled motion illustrating the significant electronic interaction of the two rotors. Additionally, the methyl group has been shown to display coupling with the torsional motions of the phenyl rings. Recent theoretical and experimental work has suggested that the phenyl torsions are involved in the multidimensional potential energy surface used to describe the cis-trans isomerization of stilbene. Photoisomerization will be discussed in detail in Chapter Five.

It is well known for a single methyl group attached to an asymmetric frame that the torsional potential well is made up of non degenerate A states and degenerate E states following the proper symmetry labeling of G_6. In p'-,p-dimethyl-trans-stilbene, there are two methyl groups attached to the stilbene frame, so the molecular symmetry group required is the form of a direct product of the two simple molecular symmetry groups, specifically $G_6 \otimes G_6$. Hence, there are nine torsional states associated with the lowest level for the methyl rotor. To determine the electronic spectrum emerging from these energy states, the wavefunctions must be classified according to the symmetry species of the G_{36} molecular symmetry group. The nuclear spin statistical weights and symmetries

of the torsional levels in p'-p-dimethyl-trans-stilbene are identical to other G_{36} molecules, such as acetone and biacetyl, and are given in Table 18[32,34]. The nuclear spin weights average to a 1:2:1 ratio for the A_1, G, and E_i levels, respectively.

The $0a_10a_1$, $0a_11e$, and 1e1e have A_1, G, and E_1+E_3 torsional symmetry in G_{36}, respectively. The correlation between G_{36} and C_{2h} is as follows: $A_1 \rightarrow a_g$, $A_2 \rightarrow b_g$, $A_3 \rightarrow a_u$, and $A_4 \rightarrow b_u$[86]. The complete internal wave function for a molecule of G_{36} symmetry can only be of either A_4 or A_2 species. Thus, the different nuclear spin symmetries associated with each torsional species prevents the three different types of molecules from interconverting.

Table 18. The symmetry species and statistical weights for the internal rotation quantum numbers of the two rotors in G_{36} symmetry.

m_1	m_2	Torsional Symmetry	Statistical weight
0	0	A_1	8
0	+1		
0	-1	G	16
+1	0		
-1	0		
+1	-1	E_1	4
-1	+1		
+1	+1	E_3	4
-1	-1		

Pierce first investigated the torsional barrier's effect upon the vibrational spectra of molecules with two equivalent tops where the top axes lie in the symmetry plane of the molecular frame[87]. The two-top model is heavily based on the internal isometric group introduced by Günthard et al. which proves the potential energies are symmetric with respect to the operations of the full isometric group[88]. The potential function for internal rotation of the methyl groups in p'-p-dimethyl-trans-stilbene would be expected to contain at least six different kinds of terms $\cos 3f_1$, $\cos 3f_2$, $\cos 6f_1$, $\cos 6f_2$, $\cos 3(f_1+f_2)$, and $\sin 3(f_1+f_2)$ where *f* represents the torsional angle and may be written in the form

$$V(f_1, f_2) = \tfrac{1}{2}[V_{30}(1-\cos 3f_1) + V_{03}(1-\cos 3f_2) + V_{60}(1-\cos 6f_1) + V_{06}(1-\cos 6f_2) + V_{33}(\cos 3f_1 \cos 3f_2 - 1) + V_{33'}(\sin 3f_1 \sin 3f_2 - 1)] .$$

The first four terms represent barriers of independent methyl groups, and the last two are coupling terms describing the torsional-torsional interaction, and cogwheel (gearing/antigearing) effect between the two groups, respectively[89]. Symmetry restrictions for a potential function involving equivalent tops require V_{n0} and V_{0n} to be equal in magnitude[90]. In analogy to biacetyl, the coupling terms V_{33} and $V_{33'}$ are expected to be small due to the rigidity of the stilbene frame and the distance between the two methyl groups[91].

The fluorescence excitation of p'-p-dimethyl-trans-stilbene is shown in Figure 34. Upon initial examination of the spectrum, it appears highly congested

with many low frequency transitions within the first 400 cm^{-1}. In contrast to the other compounds presented thus far, p'-p-dimethyl-trans-stilbene displays an intense triplet feature at the origin with components at 31,391 cm^{-1}, 31,395 cm^{-1}, and 31,399 cm^{-1}. A number of additional features, several of which appear to be doublets are seen above the origin.

The simplest method for the symmetry labeling of energy levels for a two rotor system is to consider the internal rotor states of each rotor separately. For a double rotor with different barriers in the ground and excited state, the origin will appear as a triplet representing three different types of molecules ($0a_10a_1$, $0a_11e$, and 1e1e). The $0a_11e$ form of symmetry is adopted here because of the clarity it reveals in each individual methyl rotor level and the particular transition taking place. The $0a_10a_1$, $0a_11e$, and 1e1e molecules have A_1, G, and E_1+E_3 symmetry in G_{36}. Transitions between levels of A, G, and E symmetries are forbidden, as are transitions between $A(E)_n \leftrightarrow A(E)_{m,\ m\neq n}$. The energy splitting between the A_1 and G states equal the energy splitting between the G and the two E states as would be expected from the simple addition of the energy levels of two independent rotors.

The starting point for the assignment of transitions in the fluorescence excitation spectrum of p'-p-dimethyl-trans-stilbene is the recognition that the spectrum will appear very similar to p-methyl-trans-stilbene, except for the additional torsional levels from the second methyl group. P'-p-dimethyl trans-stilbene has higher symmetry than p-methyl-trans-stilbene due to the two methyl

groups in the para position. The overall symmetry of the molecule increases to C_{2h} point group symmetry, similar to trans-stilbene itself. The low frequency modes of p-methyl-stilbene, however, are expected to be very similar to those of trans-stilbene and the selection rules regarding allowed transitions will hardly be effected. Thus, the forbidden bands for p'-p-dimethyl-trans-stilbene should still show little if any intensity for p-methyl-stilbene. Figure 35 shows the comparison between the fluorescence excitation spectra of p-methyl-trans-stilbene and p'-p-dimethyl-trans-stilbene.

The most prominent vibronic band built off the origin in trans-stilbenes, ν_{25}, is not easily recognized in this molecule. The expected region for ν_{25} is congested with many transitions indicating more than one normal mode present. Identifying and assigning ν_{25} is tricky since dispersed emission from transitions in this region is broad and unresolved. A tentative assignment for 25^1_0 comes from a comparison with ν_{25} in p-methyl-trans-stilbene in which it has the strongest intensity. The slightly stronger transition at 177 cm^{-1} is thus assigned as 25^1_0. A second peak next to ν_{25} in p-methyl-trans-stilbene was assigned as ν_{72} based primarily upon the dispersed emission and it's absence in the higher symmetrical trans-stilbene. Vibrations of b_u symmetry in C_{2h} will be allowed for molecules of C_s point group symmetry[15]. The appearance of the second peak near ν_{25} in (C_{2h}) p'-p-dimethyl-trans-stilbene suggests the peak is a totally symmetric vibration of A_g (A' in C_s) symmetry and tentatively assigned as ν_{24}. 36^2_0 and 37^2_0 are assigned at 65 cm^{-1} and 90 cm^{-1}, respectively. The strength of the ν_{37}

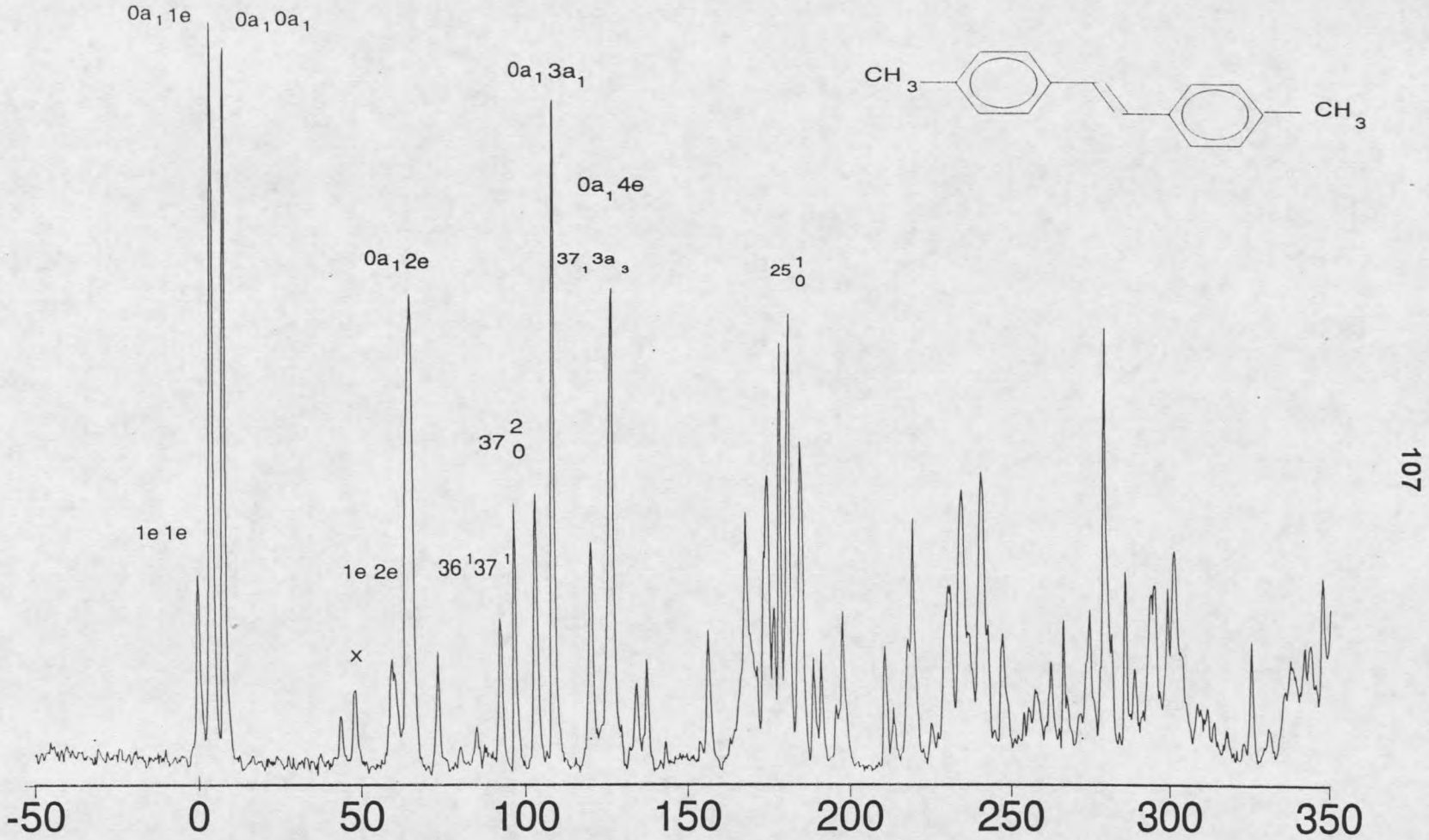

Figure 34. The fluorescence excitation spectrum of p'-p-dimethyl-trans-stilbene.

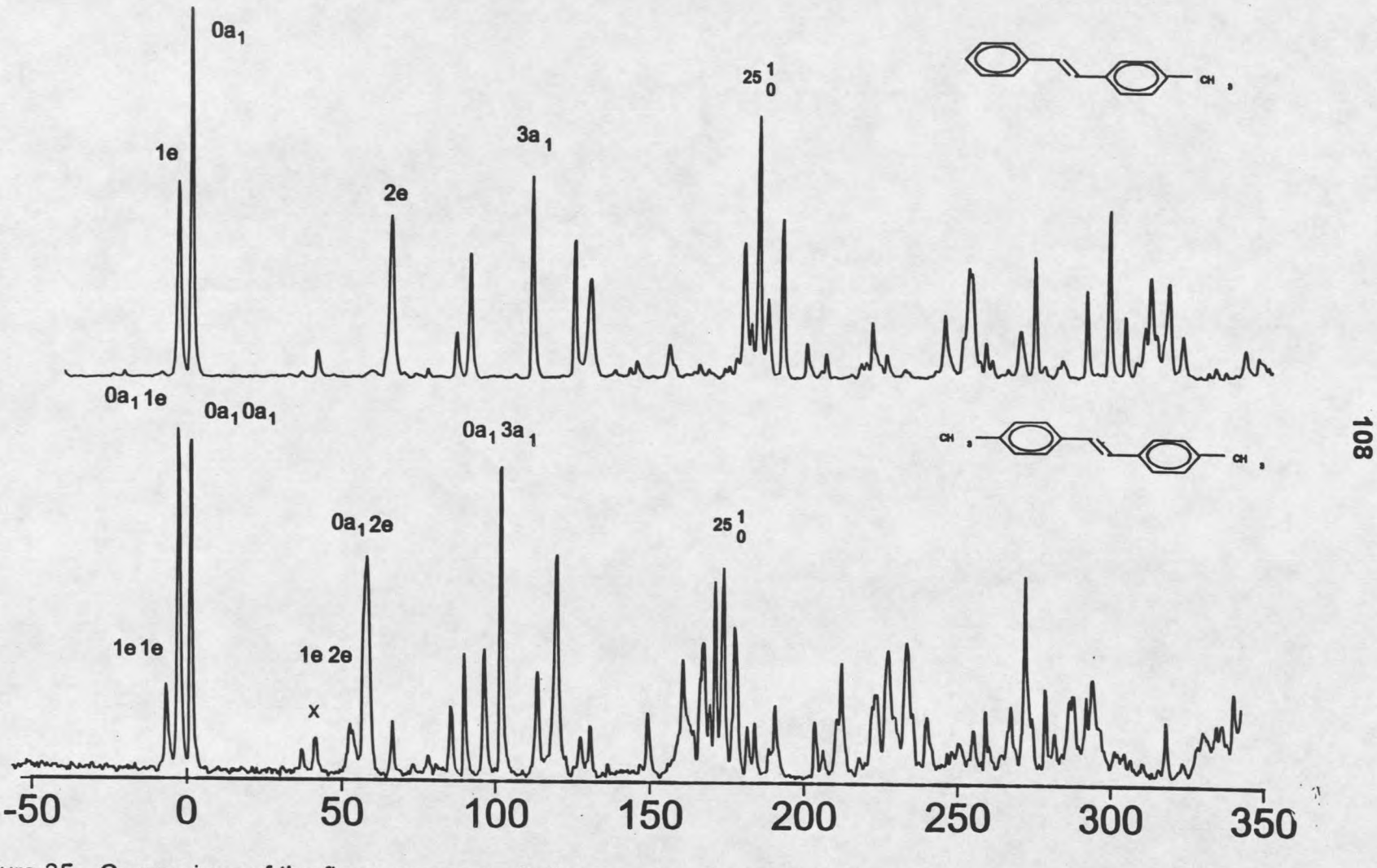

Figure 35. Comparison of the fluorescence excitation spectra of p-methyl-trans-stilbene and p'-p-dimethyl-trans-stilbene.

transition is surprising since we usually have troubles finding ν_{37} in most para-para- substituted species. These peaks carry the methyl triple splitting expected of normal modes and are summarized in Table 20. The 2e is assigned as 57 cm^{-1} and appears as a doublet characteristic of the double rotor. The "x" transition at 40 cm^{-1} also appears as a doublet lending support to its' assignment as an e-only combination. The $3a_1$ is assigned at 101 cm^{-1} and the 4e is assigned as 119 cm^{-1}.

Table 19. Torsion frequencies belonging to main vibronic bands in the fluorescence excitation spectrum of p'-p-dimethyl-trans-stilbene.

Transition	0^0_0 (cm^{-1})	37^2_0 (cm^{-1})	24^1_0 (cm^{-1})	25^1_0 (cm^{-1})
relative frequency	0	89	171	177
$0a_10a_1$"- $0a_10a_1$'	0	0	0	0
$0a_11e$"-$0a_11e$'	-4	-5	-4	-4
1e1e"-1e1e'	-8	-9	-8	-8
1e1e"- 1e2e'	52	?	52	52
$0a_11e$"-$0a_12e$'	57	60	56	56
$0a_11e$"- $3a_11e$'	95	94	96	97
$0a_10a_1$"- $0a_13a_1$'	101	101	100	101
$0a_11e$"-$0a_14e$'	119			

The assignments of the torsional levels can be supported by dispersed fluorescence. The torsional data for p'-p-dimethyl-trans-stilbene provides an excellent example of the way in which complementary data for the dispersed emission must be utilized in the assignment of transitions. The assignment of 25^1_0 is tricky since dispersed emission from this region is highly congested.

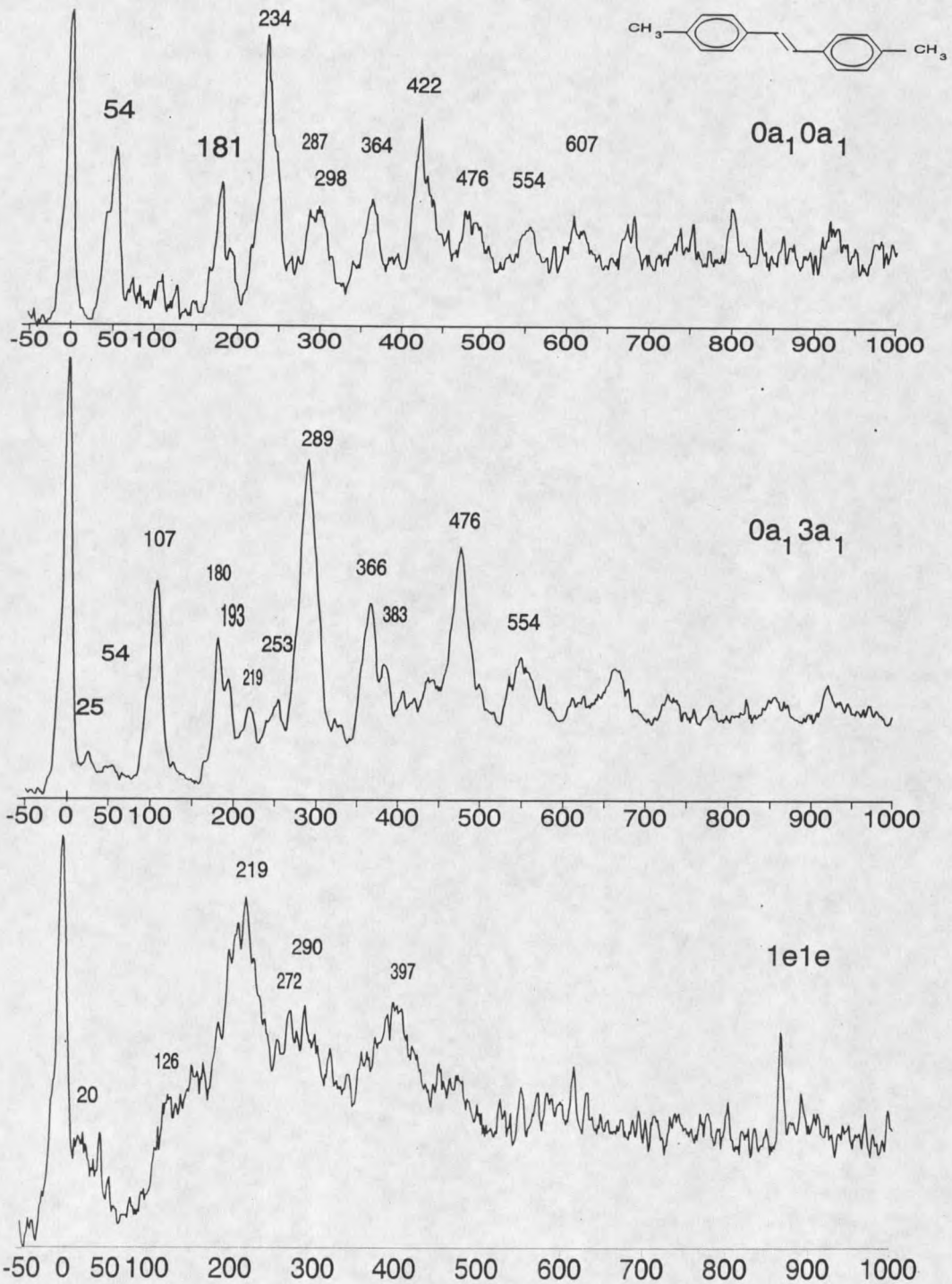

Figure 36. Dispersed fluorescence from the $0a_10a_1$, $0a_13a_1$, and 1e1e torsional levels of p'-p-dimethyl-trans-stilbene.

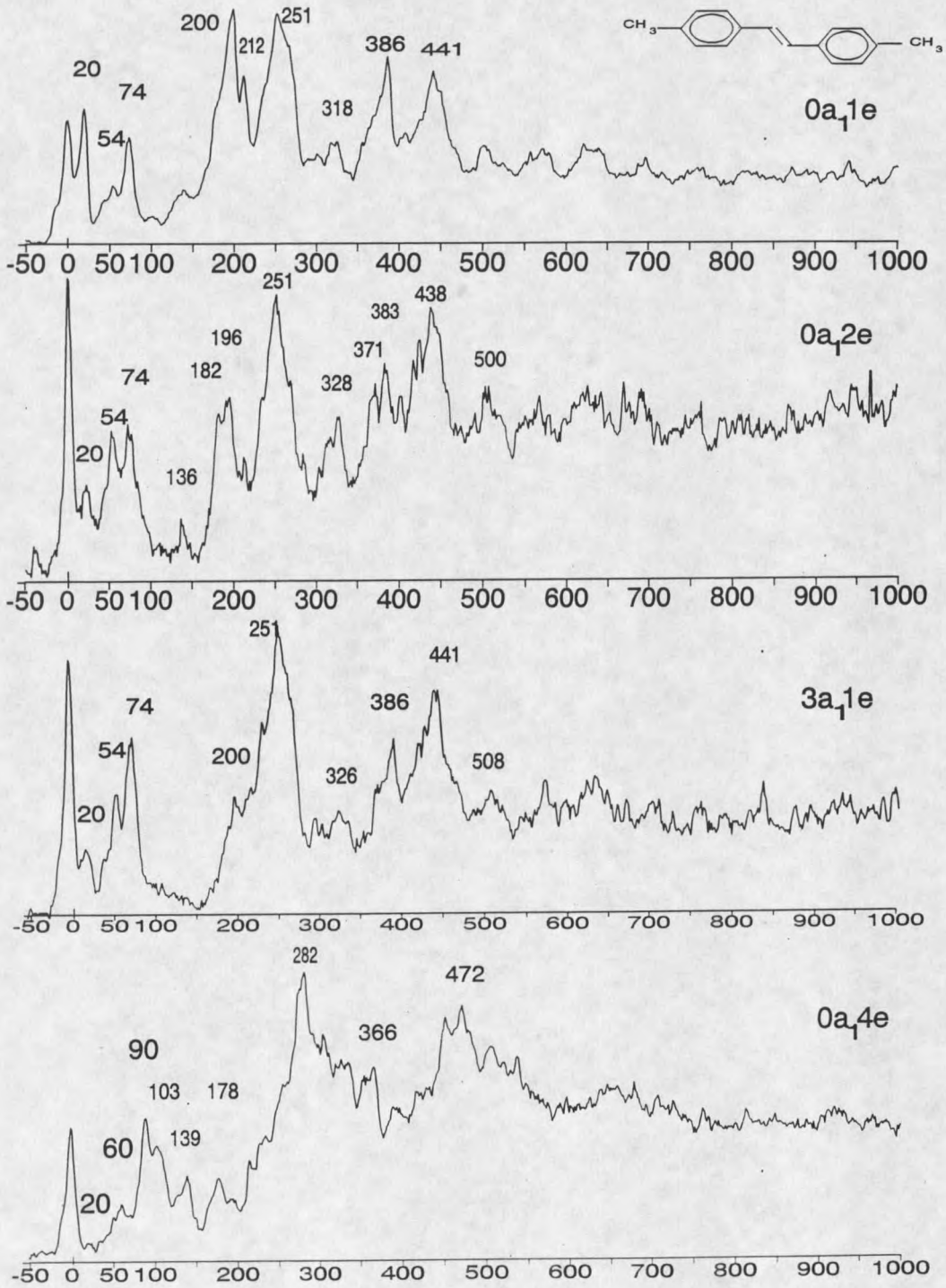

Figure 37. The dispersed emission from G symmetry levels of p'-p-dimethyl-trans-stilbene.

The methyl torsional frequencies associated with several fundamental modes in p'-p-dimethyl-trans-stilbene are given in Table 21. The coupling with modes other than ν_{37} has no great effect on the methyl torsional frequencies. The frequency separation between the methyl torsional modes for ν_{37}, however, indicates that the methyl torsional levels easily deform by the coupling with ν_{37}. Such a large anharmonic coupling plays an important role in IVR of trans-stilbene, which will be discussed in Chapter Five. On the other hand, the ground state frequency of 180 cm^{-1} for 25^0_1 can be ascertained from the dispersed emission of other levels.

Table 20. The major vibrational frequencies for the S_0 and S_1 states of p'-p-dimethyl-trans-stilbene.

Transition	S_0	S_1
ν_{36}, v=2	72	65
$\nu_{36} + \nu_{37}$		77
ν_{37}, v=2		89
ν_{24}		171
ν_{25} , v=1	180	177
ν_{25} , v=2	366	

Surprisingly, the intense peak after the assigned 2e gives a similar observed emission as A_1 symmetry. Further inspection reveals that this peak is part of the ν_{36} transition and is the $0a_10a_1$ peak. In fact, the 36^137^1 combination band can be found in between these two prominent peaks.

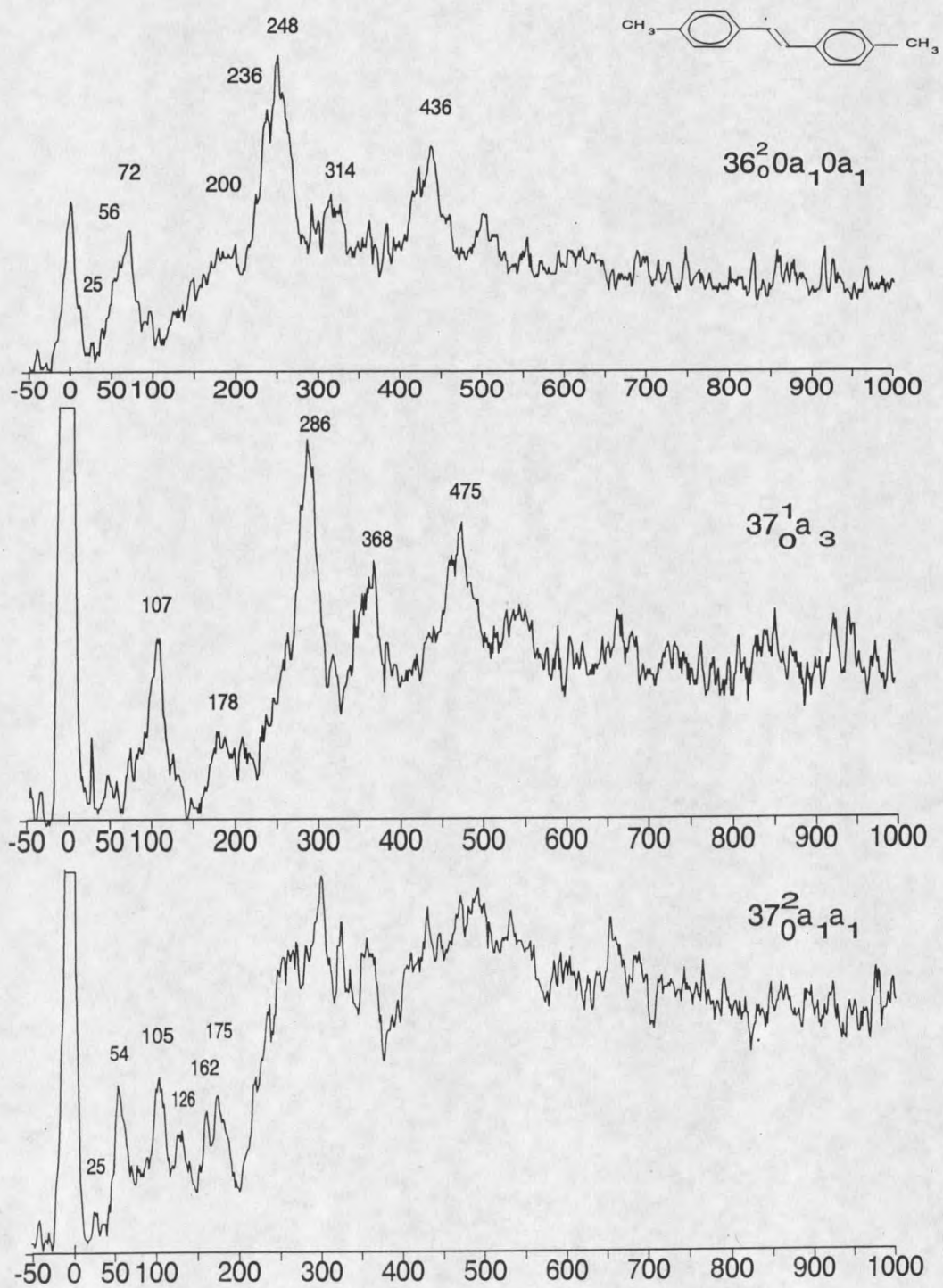

Figure 38. Dispersed emission spectra of transitions involving modes v_{36} and v_{37} in p'-p-dimethyl-trans-stilbene.

Table 21. Torsional frequencies for methyl rotation in p'-p-dimethyl-trans-stilbene.

	Ground State		Excited State	
Transition	Exp.	Calculated	Exp.	Calculated
$0a_1$	0 cm^{-1}	0 cm^{-1}	0 cm^{-1}	0 cm^{-1}
1e			-4	-3.4
2e	20	22.68	60	60.29
$3a_2$		49.15		73.77
$3a_1$	54	54.68	101	100.5
4e		89.45	119	120.5
V_3		32.67		132.12
V_6		-6.09		6.53

The two peaks surrounding 115 cm^{-1} could be possible candidates for internal rotor levels, such as the 1e4e and $0a_14e$ levels, since the 4e peak has strong intensity in p-methyl-trans-stilbene. The higher frequency transition at 119 cm^{-1} is assigned as the $0a_14e$ peak since it is broad and the dispersed emission identifies it as a G level. The peak at 112 cm^{-1} would be expected to be the 1e4e transition since the internal rotor levels have appeared as doublets thus far, however the dispersed emission displays A_1 character. The transition is clearly not a triplet and therefore is not likely to be a normal mode of the molecule. The transition is tentatively assigned as the combination band $37^1_03a_3$ for the following reasons. Both have A_3 symmetry in the G_{36} molecular symmetry group making the combination band totally symmetric and allowed. Also, the transition is approximately the correct frequency calculated to be 113 cm^{-1}.

Finally, a comparable transition was observed in p-methyl-trans-stilbene and assigned as a combination band between 37^1_0 and $3a_2$ based on similar evidence.

Since the methyl groups almost lie directly on the principle axis in trans-stilbene and this might encourage interaction between the two rotors, we start the methyl rotor analysis by ignoring the coupling between the two methyl groups. The energy levels for the methyl rotors in the ground state of p-methyl-p'-methyl trans-stilbene are listed in Table 20. The ground state frequencies fit a calculated barrier of V_3" = 32.6 cm^{-1} indicating the continuing trend of low barriers in the ground state of stilbenes. Table 20 also lists the energy levels for internal rotation in the S_1 excited state. The excited state frequencies fit a calculated barrier of V_3' = 132.12 cm^{-1}. The barrier to rotation is reduced relative to p-methyl-trans-stilbene, an indication of substituent effects. The approximation of two completely uncoupled, independent rotors for p'-p-dimethyl-trans-stilbene appears to be good since the calculated frequencies match the observed spectrum well. However, the methyl rotors may show small coupling behavior as they climb up the potential well. This coupling may show itself in the splitting of higher torsional levels and will be discussed in Chapter Five.

CHAPTER FIVE

DISCUSSION

This chapter will focus on several issues regarding the hindered internal rotation of the methyl group, including the ability to change the methyl torsional barrier by changing the substituent's conformation, hydrogen bonding the substituent, or by changing the substituent. Understanding the sensitivity of the methyl group in regards to substituent conformation will be discussed in light of the rotational coherence spectroscopy data; the spectra confirm the presence of the cis and trans conformers in p-methoxy-trans-stilbenes and provide information to differentiate their geometry. The changes in the methyl torsional barrier will also be discussed in terms of possible water complexes of the p-hydroxy-trans-stilbenes. The changes in the methyl torsional barrier relative to each functional group can be used to discuss the electronic effects of various remote substituents on the π electron density of the trans-stilbene system; a possible remote coupling between the two methyl groups in p'-p-dimethyl trans-stilbene illustrate the significant electronic interaction of two functional groups over an extended system. The chapter also includes an analysis of the methyl rotor in a vibrational state mixing, and observations of intramolecular vibrational redistribution.

The low frequency mode assignments discussed in this dissertation follow the proposed assignments of Spangler, Zee, and Zwier, which are generally agreed upon by others[29,57,62,92]. The trans-stilbene assignments are reviewed by Waldeck[51]. Recently, Laane published the excitation spectrum of trans-stilbene and methoxy trans-stilbene which we have investigated as well[58]. Laane's reinvestigation includes new assignments for the transitions including reassigning the generally accepted ν_{25} progression to a ν_{35} c=c torsion. The reassignments differ considerably from those of previous workers. In p-methoxy-trans-stilbene, Laane has only identified one electronic origin, assigning all the other transitions including the B conformer as vibrational modes and combinations built off the A origin[93]. Laane assigns the second conformer to ν_{24} (Ce-phenyl bend). This reassignment is also controversial considering our assignment of two electronic origins pertaining to the two conformers, and the general expectation of two conformers arising from the attachment of a methoxy (or hydroxy) group to an asymmetrical frame[22,94-97,115]. Although Laane's reassignments are based on additional vaporphase Raman data, we feel the previous assignments are accurate and choose to assign the spectra in this dissertation accordingly. The next section further addresses the presence of two conformers in the methoxy and hydroxy stilbenes.

The Methoxy Conformation in Para-Methoxy-Trans-Stilbenes

The conformation of phenyl methyl ethers has been under extensive investigation for many years. P-methoxy-trans-stilbene has two geometric isomers that differ in the orientation of the two O-CH_3 bonds with respect to the stilbene frame. Both p-hydroxy-trans-stilbene and p'-hydroxy-p-methyl-trans-stilbene also have two observed electronic origins identical to that of the para-methoxy trans-stilbenes recently reported in literature by Siewert and Spangler[22]. The existence of the two origins is attributed to the planar syn and anti conformers of the functional group against the rigid stilbene frame. The energy difference of 278 cm^{-1} between the two conformers is credited to the excited state stabilization from greater π electron density delocalization. Specifically, the stabilization is expected to come from the greater delocalization of the methoxy or hydroxy lone pair over the stilbene π system. Furthermore, Kruse and Coworkers have found that methyl ethers in aromatic systems prefer a planar s-cis orientation to the ortho position of highest electron density[98]. Therefore, the lower energy conformer will probably have the lone pair cis to the electron poor side of the ring.

This delocalization effect should be greater for the conformation that acts as the stronger electron donor. Therefore, the red-shifted origin (A conformer) is the methoxy/hydroxy conformer that acts as a better electron donor in their respective molecules. As mentioned in the experimental results, ν_{37} is sensitive

to the C_e-phenyl bond order and can be used to qualitatively measure the delocalization in the conjugated system. The higher ν_{37} frequency for the red-shifted conformer supports this rationale.

Additional evidence that supports the red-shifted conformers as better donors is the lower methyl torsional barriers found for them in the methylated species. Our research group has proven that strong electron donors lower the torsional barrier relative to p-methyl-trans-stilbene. The fitted barrier for the torsional progression built off the A origin, identical for both the methoxy and hydroxy, is 10% lower than the B conformer. In trans-stilbene, we suspect the cis side of the ring, with respect to the C=C, is slightly higher in electron density[22]. Thus, the red-shifted transition has been tentatively assigned to the origin of the syn isomer and the blue-shifted transition as the origin of the trans isomer[22]. This would place the methoxy cis to the electron rich side, which has been defined above as cis to the ethylenic double bond. However, this tentative assignment has not been confirmed.

We have stressed the fact that methyl torsional barriers in the S_1 state of para substituted trans-stilbenes are sensitive to secondary interactions between the methyl hydrogens and the π electron density in the meta positions. Given this, the ability to assign the origins to their respective conformers will give valuable insight into the exact nature of asymmetrical distribution of the π electron density in the meta positions of trans-stilbene.

The rotational constants of large molecules, such as trans-stilbene, demand an apparatus resolution approaching 10MHz, which exceeds the capabilities of our lab. The rotational constant is a function of the moment of inertia. Rotational coherence spectroscopy allows the use of time-domain equipment to measure the moments of inertia of molecules. Rotational coherence measurements were recently applied to the para methoxy trans-stilbenes to determine the rotational constants and the molecular geometry of each conformer[99].

Table 22. Rotational coherence data for S_1 para methoxy-stilbenes.

Species	recurrence time (ns)	Rotational constants (B+C) (MHz)	
	experimental	AMPAC calculation	experimental
p-methoxy-			
A conformer	2.990 ± 0.003	331.3	334.4 ± 0.3
B conformer	3.032 ± 0.003	328.0	329.8 ± 0.3
	diff.= 0.042 ± 0.006		
p'-methoxy-p-methyl-			
A conformer	3.668 ± 0.002	270.8	272.6 ± 0.3
B conformer	3.712 ± 0.003	268.2	269.4 ± 0.3
	diff.= 0.044 ± 0.005		

The polarized fluorescence time profiles for p-methoxy-trans-stilbene are shown in Figure 38. The time profiles were extended to 10 ns for both molecules and the relative precision is 5 ps. The J recurrence time (included in Table 22) can be extracted from the time profiles, and equals the inverse of the sum of the

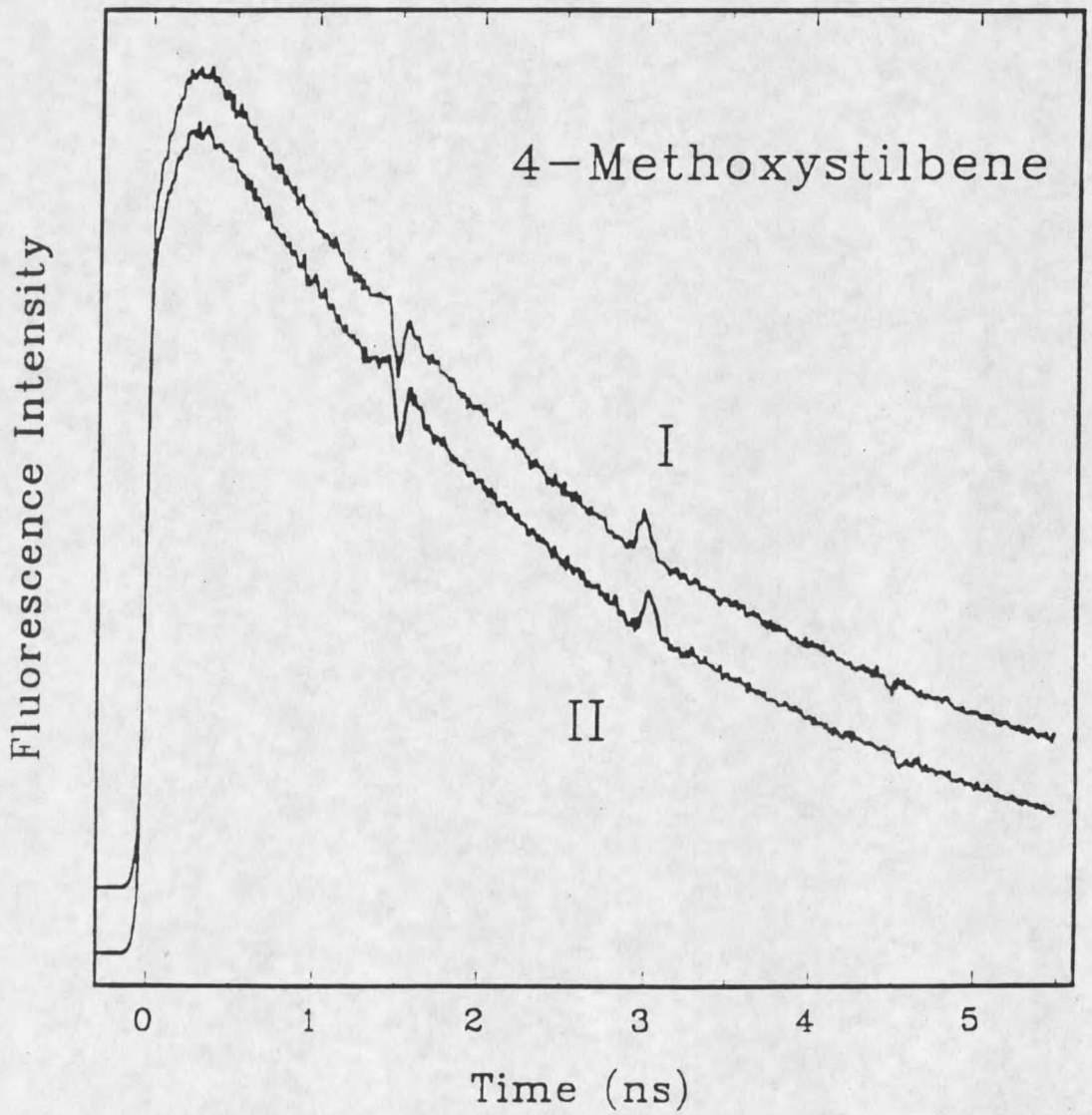

Figure 39. Polarized fluorescence time profiles for p-methoxy-trans-stilbene, showing displaced traces for two conformers.

rotational constants B and C. The discrepancy between the experimental and calculated rotational constants could be due to the AMPAC calculations, but does not affect the ordering of the results for the two conformers.

The existence of two conformers having significantly different S_1 energies in the para-methoxy-trans-stilbenes is supported by these independent experimental methods and is consistent with the previous knowledge of the trans-stilbene system. Using rotational coherence spectroscopy, the red-shifted origin in p-methoxy-trans-stilbene is found to be the syn conformer. In all probability, this conformer preference also exists in the para hydroxy-trans-stilbenes since the electronic properties of both functional groups are very similar. The lone pair electrons on the oxygen, which is in the plane of the aromatic ring, are cis to the more electron deficient meta position. This, in turn, suggests the anti meta position is relatively electron deficient and the syn meta position is relatively electron rich. It would seem plausible that the asymmetry in the π electron density must arise from the placement of the π-electron rich double bond and the remote aromatic ring off the para axis of the substituted ring. This explanation for the asymmetry is supported by the position of these groups on the side found to be electron rich. In summary, the asymmetry of the π-electron density in trans-stilbene is a natural consequence stemming from the geometry of the stilbene frame.

This must also be true in regards to the position of the remote substituent ring and double bond in relation to the methyl bearing ring in the methylated

trans-stilbenes. Specifically, the reason behind a preferred conformation and consequential torsional barrier for the methyl group is the placement of the pi-electron rich double bond and the remote substituent ring off the para axis of the methyl bearing ring. Given this, the varying methyl torsional barrier results found for the methylated species in this thesis point to how sensitive the methyl rotor is to the ability for the remote substituent to counterbalance the built-in π-electron density asymmetry through its electron donating or withdrawing properties. An elegant example of this sensitivity will be presented in the next section.

Remote Hydrogen Bonding Effects on the Methyl Rotor

Both the methoxy and hydroxy functional groups can accept a proton, but only a hydroxy group can donate a proton. It would be expected that p-hydroxy-trans-stilbene+H_2O and p-methoxy-trans-stilbene+H_2O would behave similarly if the functional groups behave as proton acceptors. Therefore, the dramatically different behavior suggests the hydroxy group in p-hydroxy-trans-stilbene donates a proton to the water molecule. The water complexation seen initially in the hydroxy-methyl spectrum was due to environmental contamination from air and serves to demonstrate the efficient hydrogen bonding. This behavior, which was not seen in working with the methoxy-stilbenes, points to the hydroxy group as a proton donor. This is not surprising considering the previous publications concerning water complexes of other molecules containing hydroxy groups[100-102].

The most notable change in the complex spectrum of p-hydroxy-trans-stilbene compared to the bare molecule is the drastic reduction in the frequency difference between the two conformer origins. Since the bare p-hydroxy-trans-stilbene and p-methoxy-trans-stilbene spectra are nearly identical, it is reasonable to suggest the position of the oxygen lone pair of electrons is the dominating influence for the different conformer energies. In a limiting case of complete removal of the proton, the electron density on the oxygen would increase and become symmetric about the para axis. The complete removal of the proton would change the molecular symmetry, such that only one distinct conformer would exist. As the proton is brought back, two distinct origins would begin to emerge from the degenerate peak. Since it is the lone pair that primarily determines the conformational energy difference, a more symmetric distribution reduces the energy difference and brings the origins closer in frequency. The spectrum shows that the two origins moved from 278 cm^{-1} to 24.5 cm^{-1} of each other, which is consistent with this model.

Proton donation by the hydroxy group will not only make the electron density around the oxygen more symmetric, but will also increase the overall density as well. Thus, $OH+H_2O$ should be a better electron donating group than OH. Previous work has found that strong electron donors in the para position on the distant ring into the π system reduce the S_1 methyl barrier relative to p-methyl-trans-stilbene. If the above model is correct, the complex formation should reduce the methyl barrier if the hydroxy group acts as a proton donor.

The lower methyl rotor barriers found for the water complexes, as compared to the uncomplexed p'-hydroxy-p-methyl-trans-stilbene, are consistent with this model.

Next, the structural possibilities for the second (red-shifted) complex will be considered. The red shifted complexes could either be a two water complex or one water attaching to a different site. As stated in Chapter Four, these transitions only became dominant at higher water concentrations, and only when the one water complex showed signs of depletion. For this reason, these red-shifted peaks are assigned to the two water complex. Saykally and coworkers using high resolution IR spectroscopy in a jet have suggested that the water trimer is likely a six-membered ring with each water acting as both a proton donor and acceptor[103]. Since the hydroxy group can function in the same manner, we speculate that a similar structure is formed in p-hydroxy-trans-stilbene$*(H_2O)_2$.

If this is the correct structure, it is interesting to consider what would be expected for the conformer energy differences and methyl barrier changes in p'-hydroxy-p-methyl-trans-stilbene. If the red shifted peaks are the result of a two water complex, with the hydroxy group donating a proton to one water and accepting a proton from the second water, the hydroxy group will have a partial bond to a hydrogen on both sides to the para axis. This creates a more symmetric electron density on the oxygen which reduces the conformer energy differences. The conformer energies are observed in the spectrum to be within

44.4 cm^{-1} to each other. The methyl barrier for p'-hydroxy-p-methyl-trans-stilbene$*(H_2O)_2$ should be similar to the bare p'-hydroxy-p-methyl-trans-stilbene since the effects of an electron density increase at the oxygen caused by donating a proton, and a density decrease caused by accepting a proton should approximately cancel. The observed methyl barriers for both conformers of the p'-hydroxy-p-methyl-trans-stilbene$*(H_2O)_2$ are 96 cm^{-1} and 98 cm^{-1}, which are nearly the average values of the two p'-hydroxy-p-methyl-trans-stilbene conformer barriers at 92 cm^{-1} and 104 cm^{-1}.

By reference to the positions of the 0,0 bands, we notice interesting spectral shifts of the one water complexes relative to the 0,0 bands of the two bare conformers. Specifically, the A conformer shifts to a higher frequency by 258 cm^{-1}, whereas the B conformer increases by only 16.5 cm^{-1}. Although different spectral shifts for the cis and trans conformers are common, the direction of the spectral shift is not[104]. There is a generally held belief that the addition of the first water as a proton acceptor has a net red-shift affect. There is disagreement, however, as to whether the hydrogen bonding stabilizes the LUMO or destabilizes both the HOMO and LUMO to achieve the net red shift[100,102]. While the spectral shifts seen in the p-hydroxy-trans-stilbene and the p'-hydroxy-p-methyl-trans-stilbene spectra run counter to previously observed proton donor/acceptor shifts, the assignments are justified based on the following evidence. The hydroxy functional group attached to an aromatic ring is a better acid than water and should be the proton donor[105-107]. P-hydroxy-trans-

stilbene and p-methoxy-trans-stilbene show completely different water complex behavior. It would be expected that p-hydroxy-trans-stilbene+H_2O and p-methoxy-trans-stilbene+H_2O would behave similarly if the functional groups behave as proton acceptors. Since only the hydroxy group can function as a proton donor, donation would account for the different behavior. Finally, the p'-hydroxy-p-methyl-trans-stilbene$*(H_2O)_1$ methyl barrier behaves as predicted if the hydroxy group is the proton donor.

While we are certain in our assignment, we are unable to form a consistent explanation for the complex shifts that occur. It is worth noting that the helium complexes of all the stilbenes investigated thus far show a red shift, which is opposite to the blue shift observed in most molecules. The large increase in the delocalization that occurs in excitation to S_1 is suspected to play a role in the complex shift behavior of the stilbenes.

p'-p-dimethyl-trans-stilbene

In p'-p-dimethyl-trans-stilbene, a unique substituent-substituent interaction between the two methyl groups may occur. The methyl rotor is well known for its coupling to the low frequency modes of trans-stilbene, in particular the ν_{37} mode, thus the stilbene frame may be involved in the interaction[15]. The rotor-ring-rotor coupling may be important given the results between p-xylene (CH_3-Ph-CH_3) and biacetyl ($CH_3COCOCH_3$)[44,86]. Both contain two rotors that are remote from each other and lie in completely symmetrical planar environments. In S_1 p-xylene, the

two rotors behave as free rotors similar to the methyl group in toluene; they act independently even though the rigid benzyl ring and the two methyl groups on the same axis should be a perfect environment for methyl rotor-overall rotational coupling. In S_1 biacetyl, however, the torsional levels of the two rotors were fit to a high methyl torsional barrier potential containing a significant coupling term of 9 cm^{-1}. The coupling between the methyl rotors seems to correlate with the presence of a potential barrier. Additionally, the motion in biacetyl where the methyl groups rotate in the direction of the $COCH_3$ wagging coordinate or against the wagging displacement is deemed important to induce coupling.

Since p'-p-dimethyl-trans-stilbene possesses a significant methyl torsional barrier in the excited state, and since the methyl groups show coupling to the phenyl ring torsion, it would be anticipated that a small methyl-methyl coupling would exist. Insight into the dynamics of the torsional modes comes from a comparison of the torsional energy levels for each rotor. The torsional-torsional hamiltonian interaction term affect states with E_i symmetry more than a state with A_1 or G symmetry[108,109]. Therefore, changes in the methyl rotor splittings at higher torsional levels could indicate a small torsional-torsional perturbation involving the E_i symmetry levels. A simple difference of 2-3 cm^{-1} in the 2e or $3a_1$ doublets is enough to suggest a small amount of coupling exists.

Figure 39 shows the low frequency region for p'-p-dimethyl-trans-stilbene. The methyl torsional splittings are observed to increase slightly with increasing torsional energy from 4 cm^{-1} to 6 cm^{-1} at the $3a_1$ torsional levels. The increased

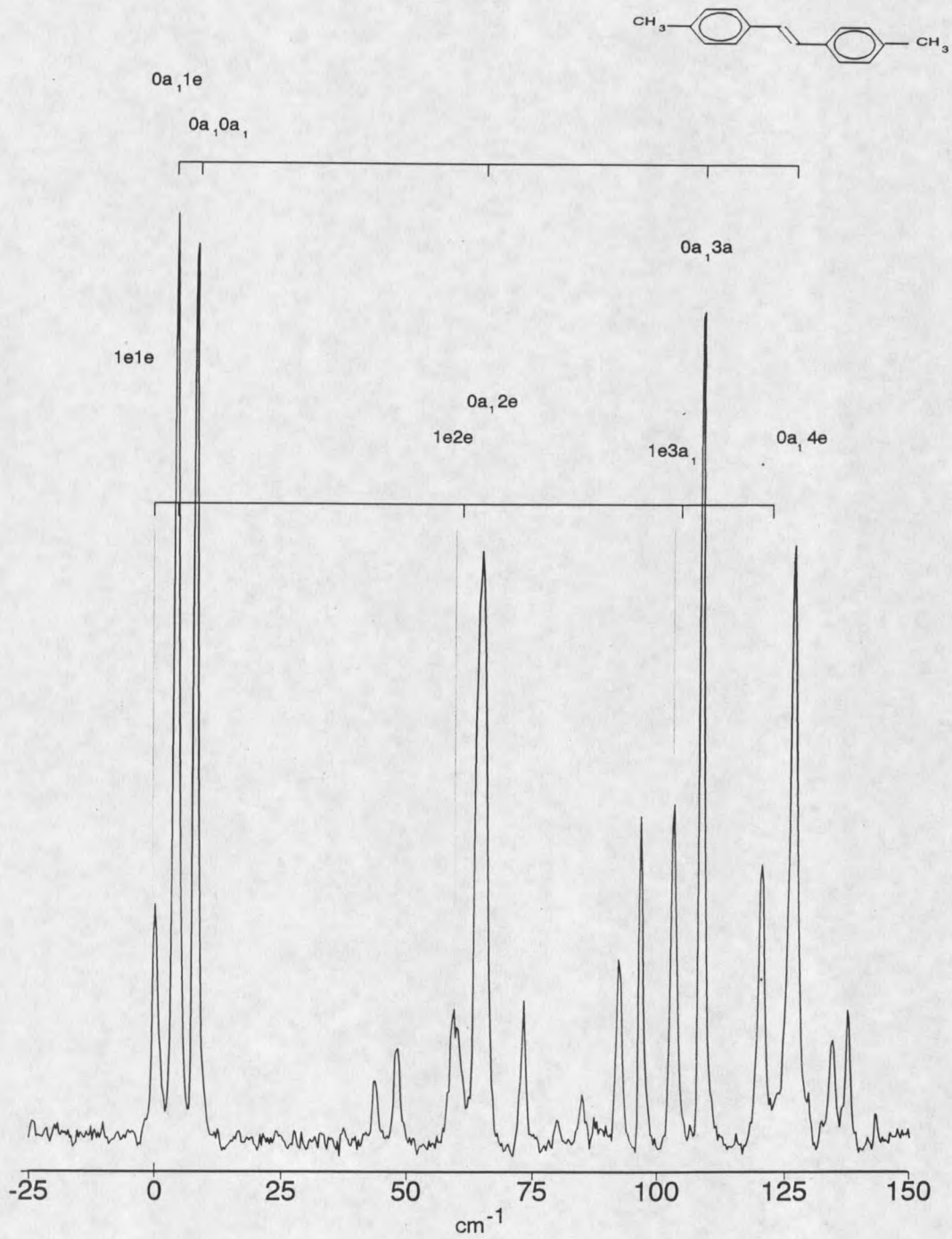

Figure 40. The low frequency region of p'-p-dimethyl-trans-stilbene. The tie lines aid in comparing the different internal rotor frequencies for the two methyl groups. The different frequencies suggest a possible rotor-rotor coupling.

splitting can be rationalized by the fact that rotor-rotor coupling involves angular momentum from both rotors. Since there is a large change in the kinetic energy associated with torsional motion, the magnitude of the coupling would be expected to increase as the kinetic energies of the two methyl rotor motions increase[109]. The measurable interaction in the excited state is then explained by the rigidity in the stilbene frame as well as the increased coupling with the phenyl torsion.

Table 23. Comparison between the methyl torsional levels for the two methyl groups in p'-p-dimethyl-trans-stilbene. The different energies for the higher torsional levels may imply increased coupling at the higher levels.

Methyl torsion	Calculated	First CH_3 rotor	Second CH_3 rotor
$0a_1$		0 cm^{-1}	0 cm^{-1}
1e		-4	-4
2e		57	56
$3a_1$		101	99

In most cases where significant methyl rotor coupling is observed, the coupling is associated with direct steric interaction. The motion of an "egg beater" is figuratively used to describe the gearing and anti-gearing of the sterically hindered methyl groups. Since the methyl rotors are attached at opposite ends of the molecule, the presence of coupling in p'-p-dimethyl-trans-stilbene is an elegant illustration of how the methyl group is sensitive to π electronic interactions of remote substituents.

Methyl Rotor Analysis

In all the methylated stilbenes studied in this thesis, the ground states have low three-fold torsional barriers because the π system is not very delocalized. Consequently, the central bond and distant ring would have a small influence on the methyl substituted ring and the methyl substituted ring should behave similar to toluene[44]. Conversely, the excited states of the trans-stilbene derivatives are known to have greater delocalization, and all display higher barriers. This higher barrier is caused by the pi density difference in the two positions adjacent to the methyl group.

As can be seen from Table 24, the para'-para-substituted stilbenes all have barriers lower than p-methyl-trans-stilbene. The most intriguing evidence regarding the methoxy and hydroxy barriers is they are exactly identical. The similarity in the barriers between the two functional groups is evidence that the molecular orbitals of the methyl group are influenced more by the position of the electron density on the oxygen atom caused by the conformation of the substituent ten carbons away from the rotor.

The data compiled in Table 24 provides concrete evidence that the stilbene π system is localized in S_0, significantly more delocalized in S_1, and that the methyl barrier is sensitive to the increased delocalization. Since the mechanism for the interaction between the π system and the CH_3 group is still in debate, including whether steric interaction or π-bonding is the determining factor

in barriers to methyl internal rotation, it is beneficial to discuss our data in terms of the established models.

Table 24. Methyl rotor barriers upon excitation for methylated stilbenes.

Species	V_3"	V_6"	V_3'	V_6'
p-methyl-trans-stilbene[a]	28cm^{-1}		150	
p'-trifluoromethyl-p-methyl-t-stilbene	30		134	-24.0
p'-methyl-p-methyl t-stilbene			132.1	6.53
p'chloro-p-methyl t-stilbene[b]	25		104.3	4.9
p-fluoro-p-methyl t-stilbene[b]	28		100.5	12
p'-cyano-p-methyl-t-stilbene	22.9	-10.5	87.4	8.8
p'-methoxy-p-methyl t-stilbene B[b]	15		103.4	
p'-methoxy-p-methyl t-stilbene A (syn)	17		91.8	
p'-hydroxy-p-methyl t-stilbene B			103.9	10.5
p'-hydroxy-p-methyl t-stilbene A			91.3	16.1
p'-hydroxy-p-methyl stilbene $(H_2O)_1$ A	31.03	-14	77.7	-9.9
p'-hydroxy-p-methyl stilbene $(H_2O)_1$ B	32.2	5.7	74.	-9.0
p'-hydroxy-p-methyl stilbene $(H_2O)_2$ A			96.4	15.1
p'-hydroxy-p-methyl stilbene $(H_2O)_2$ B			97.8	21.3
p'-dimethylamino-p-methyl-t-stilbene	28.62		68.08	4.36
p'-amino-p-methyl-t-stilbene[c]	27		54	-2.7

[a] reference 15. [B] reference 64. [C] reference 23.

First, the selection of the extended conjugated system found in trans-stilbene was intentional, so as to rule out any possible steric interactions between the remote substituent and the methyl group. Thus, the discussion will focus on the π-bonding model. As discussed in Chapter Two, the consideration

of the π-like orbitals of the CH_3 group is important in terms of the electronic interactions between a methyl group and the π system of aliphatic systems (see Figure 4). Moreover, it is the methyl hydrogen interaction with the secondary atom, X, that is the deciding factor in conformational preferences. In all likelihood, when considering the $C\text{-}C_{Ph}$ bond order and length, the carbon p orbital in π_{CH3} does indirectly affect the overlap between the methyl hydrogens and the secondary atom.

In applying these ideas to the stilbene system, which has π density on either side of the methyl group, the π interactions are similar, yet become complicated since there are more π_{CH3} - π interactions to consider. In the case where the stilbene π MOs are symmetric on either side of the methyl group, the opposing forces on the methyl tend to cancel to a large degree. An incomplete cancellation would result in a three-fold barrier and a C-H bond eclipsing the plane.

In p-methyl-trans-stilbene (CH_3-Ph-CH=CH_2-Ph), the low methyl torsional barrier ($V''_3 \cong 30$ cm^{-1}) in the ground state is comparable to that of p-methylstyrene (CH_3-Ph-CH=CH_2). This implies that the ethylenic bond in both species, and the unique remote ring in trans-stilbene create only a small density difference in the carbons adjacent to the methyl substituted position. On the other hand, the excited state barrier in p-methyl-trans-stilbene is significantly higher ($V'_3 \cong 150$ cm^{-1}), whereas the excited state barrier for p-methylstyrene has not changed. Hence, it is the remote ring and not the ethylenic bond that has a

much greater influence in the excited state due to the greater delocalization in S_1. If this were not true, implying instead that the ethylenic bond is the dominant influence, then substitution on the remote ring would be expected to have little effect on the S_1 barrier. The fact that the S_1 methyl barrier changes with different remote substituents (Table 24) confirms the influence of the remote ring.

The next issue to consider is why the methyl barrier decreases with substitution of remote substituents. A qualitative explanation for the observed methyl torsional barriers could be that electron donating groups substituted in the para position of the remote ring will cause a π density increase in both positions adjacent to the methyl group, but cause a greater increase in the position that was originally more electropositive. This will lessen the difference in the π density of the meta positions and produce a lower barrier as observed for the electron donating groups. There is a pattern in the reduction of the barrier suggesting that the stronger the electron-donating group, the lower the barrier.

On the same note, electron withdrawing substituents substituted in the para position of the remote ring will cause a π density decrease in both positions adjacent to the methyl group, but cause a greater decrease in the position that was originally more electronegative. This also reduces the difference in the π density at the meta positions and lowers the asymmetry of the meta positions. The decreasing barrier heights in the order of p'-chloro-, p'-fluoro-, and p'-cyano-p-methyl-trans-stilbene is strong support for the mechanism presented here.

Two considerations, however, might suggest that this concept is too simple. The methyl torsional barriers for both p'-trifluoromethyl-p-methyl-trans-stilbene, and p'-dimethylamino-p-methyl-trans-stilbene are expected to be the lowest in their respective category based on the above model, but do not behave accordingly. The cause for the disparate behavior could be the inability for the electron donating or withdrawing properties of the remote substituent to be effectively transferred through the conjugated system. Evidence pertaining to p'-trifluoromethyl-p-methyl-trans-stilbene may be found in the electronic origin frequency, where the introduction of the CF_3 group does not produce a lower frequency shift of the fluorescence excitation spectrum than p-methyl-trans-stilbene. In other words, the small decrease in the methyl torsional barrier for p'-trifluoromethyl-p-methyl-trans-stilbene relative to p-methyl-trans-stilbene may be related to the poor ability of the trifluoromethyl group to conjugate with the π electron system[74].

The reason for the non-conforming behavior observed for p'-dimethylamino-p-methyl-trans-stilbene may be due to a twisting of the functional group about the c_{aryl}-ring axis creating a twisted intramolecular charge transfer "tict" state against a relatively inflexible stilbene conjugated frame. In a "tict" state, the twisting can in principle decouple the nitrogen lone pair from the π electrons of the phenyl rings. This leads to localization of the positive charge on the dimethylamino group and a larger value of the dipole moment of the charge transfer state[110]. Evidence for a "tict" state has been found in the solution

studies of p'-dimethylamino-p-cyano-trans-stilbene, and recent RCS data indicates that p'-dimethylamino-p-cyano-trans-stilbene is nonplanar under free expansion conditions as well[78,111]. The dispersed emission spectra of p'-dimethylamino-p-methyl-trans-stilbene, including the electronic origin, show a broad congestive background underlying the discrete emission.

Fermi Resonance

At approximately or near 40 cm^{-1} above the origin in para'-p-methyl-trans-stilbenes examined by this group, there is a relatively strong transition that has no analog in trans-stilbene. There is no $0a_1$-1e splitting expected for a skeletal mode and the transition only appears when a methyl group is present, so it seems reasonable to assign this transition to the motion of the methyl group. However, the methyl rotor torsional frequencies are accounted for, and 40 cm^{-1} is too low for any functional group bends or stretches of the methyl group. Careful backing pressures have ruled out the assignment as a hot band. This leaves the possibility that the 40 cm^{-1} transition is due to a *low* frequency stilbene vibration that is given allowed character; only ν_{36}, ν_{37}, and ν_{48} out-of -plane vibrations are likely to have such a low frequency. A vibration that would possibly appear in this region is the 1e level of 37^1_0, which would have e x a_2 = e symmetry and be accessible from the ground state. Strong evidence that the *e* torsional levels in out of plane modes have allowed character can be found in 5-methylindole[112]. Therefore, this transition is assigned as 37^1_0-1e,

since the common axis of internal rotation for the methyl rotor and phenyl torsion should induce angular momentum coupling. Further evidence that supports this assignment as an "e" only transition is the spectrum of p'-p-dimethyl-trans-stilbene. The 2e peak in this molecule appears as a doublet representing the $0a_1$-2e and 1e-2e transitions. The "37^1_0-e only" transition also appears as a doublet.

Dispersed emission from the 37^1_0-1e transition in p'-fluoro-p-methyl-trans-stilbene[64] and in p'-cyano-p-methyl-trans-stilbene (see Figure 21) display similar characteristics as the 2e level. Furthermore, it appears that as the 2e moves to lower frequency, the 37^1_0-1e transition gains intensity. Figure 40 shows the intensity of the 37^1_0-1e increasing relative to the proximity of the 2e. This would suggest the peaks are tied to one another through angular momentum coupling. After looking at several species we have identified a fermi resonance with this transition and the 2e peak. Fermi resonance represents the simplest mechanism for the transfer of energy between vibrational modes. The simple two level fermi resonance between the two peaks allows us to determine the coupling matrix element from the positions and intensities of the two transitions.

Therefore, this transition is assigned as 37^1_0-1e, since the common axis of internal rotation for the methyl rotor and phenyl torsion should induce angular momentum coupling. Further evidence that supports this assignment as an "e" only transition is the spectrum of p'-p-dimethyl-trans-stilbene. The 2e peak in

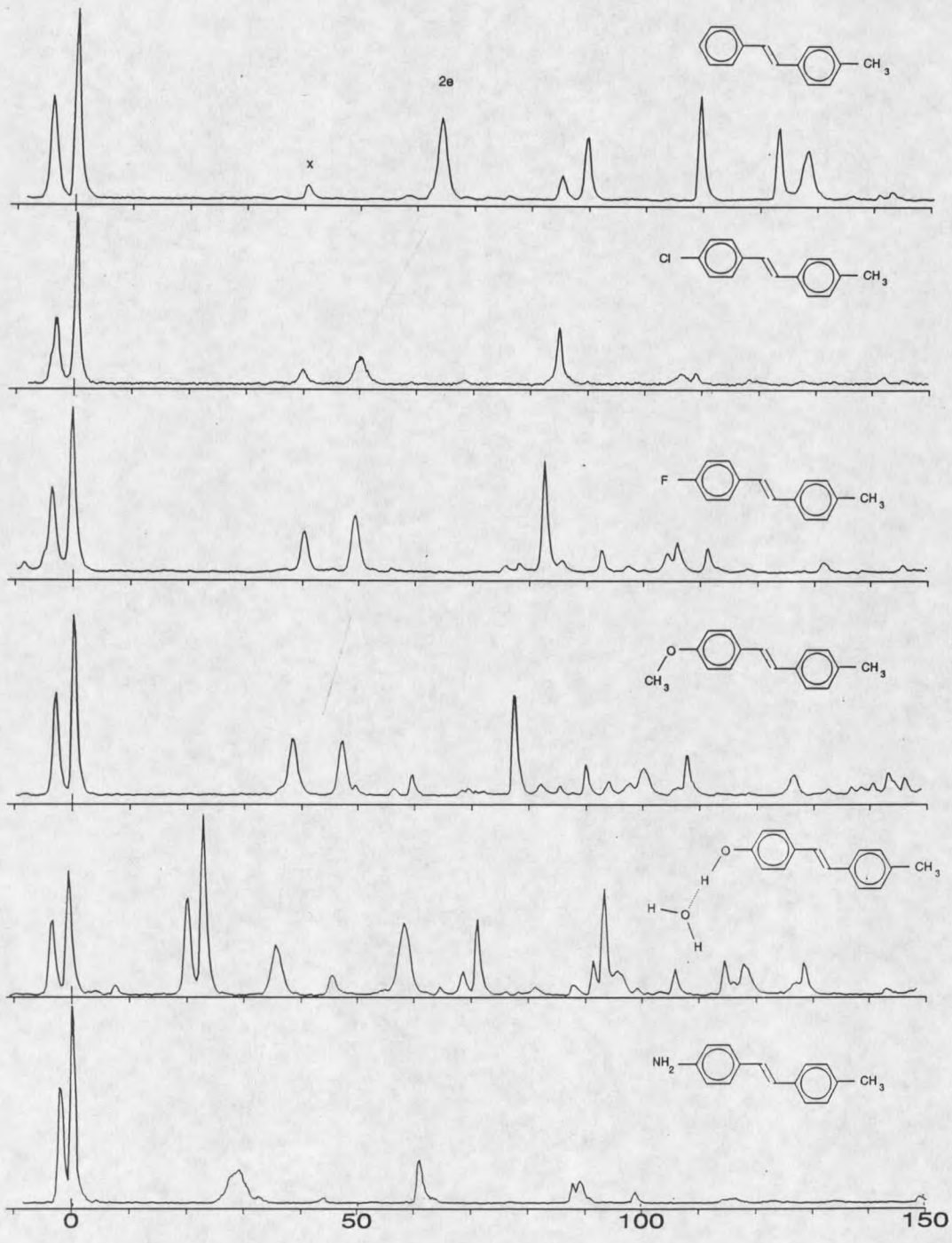

Figure 41. The comparison of the 2e-37^{1}_{0}1e fermi resonance in several methylated stilbenes. An example of complete mixing can be seen in the p'-methoxy-p-methyl-trans-stilbene spectrum.

this molecule appears as a doublet representing the $0a_1$-2e and 1e-2e transitions. The "37^1_0-e only" transition also appears as a doublet.

Dispersed emission from the 37^1_0-1e transition in p'-fluoro-p-methyl-trans-stilbene[64] and in p'-cyano-p-methyl-trans-stilbene (see Figure 21) display similar characteristics as the 2e level. Furthermore, it appears that as the 2e moves to lower frequency, the 37^1_0-1e transition gains intensity. Figure 40 shows the intensity of the 37^1_0-1e increasing relative to the proximity of the 2e. This would suggest the peaks are tied to one another through angular momentum coupling. After looking at several species we have identified a fermi resonance with this transition and the 2e peak. Fermi resonance represents the simplest mechanism for the transfer of energy between vibrational modes. The simple two level fermi resonance between the two peaks allows us to determine the coupling matrix element from the positions and intensities of the two transitions.

Table 25. The energy separation and intensity ratio for the fermi resonance in selected methylated stilbenes.

Stilbene	Perturbation ΔE (2e-X)	Intensity ratio
p-methyl	23 cm-1	0.152
p-chloro	11	0.402
p-fluoro	9	0.66
p-methoxy	8.8	0.97
p-hydroxy*H20	9.4	0.3959
p-amino	17	0.059

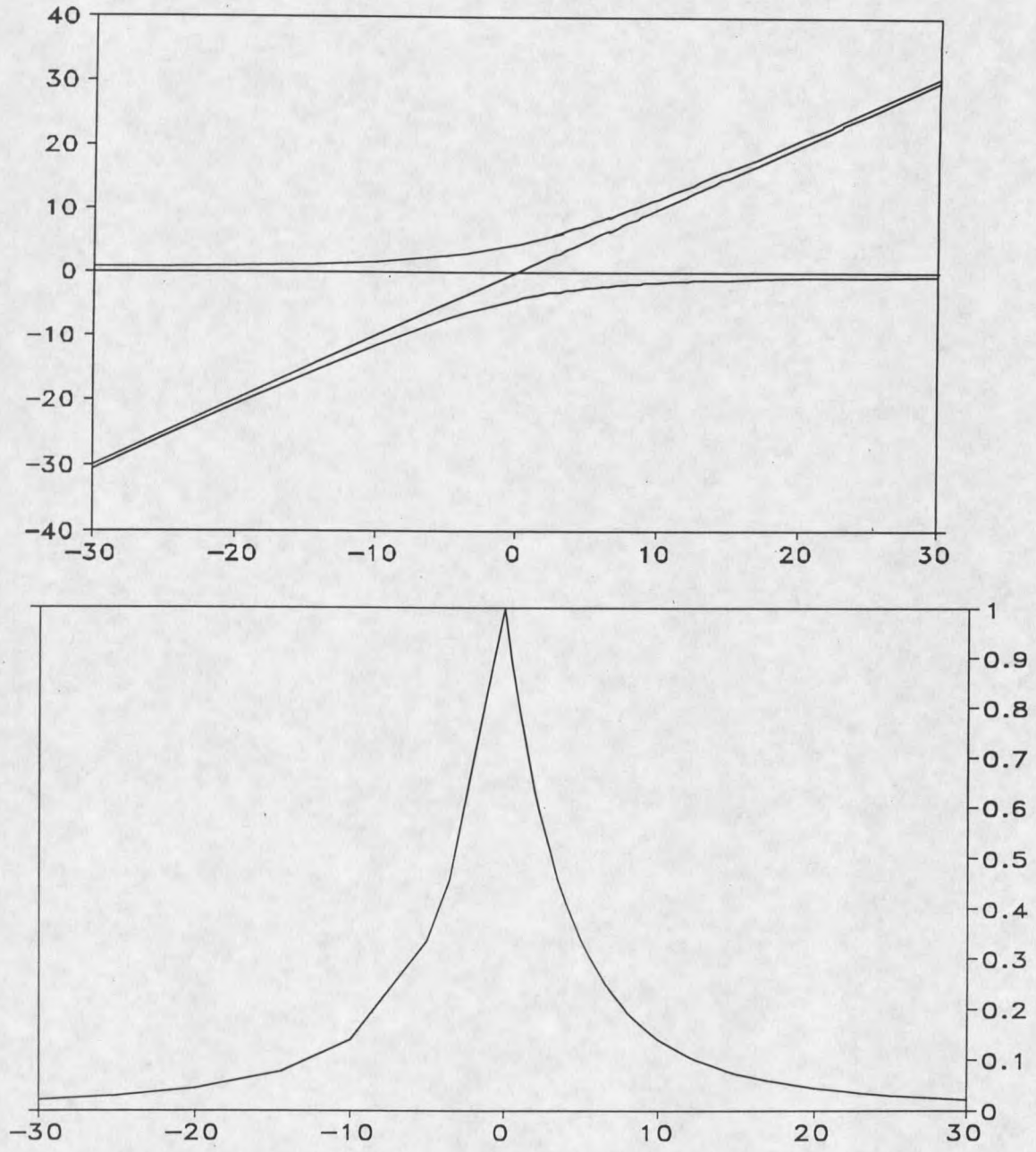

Figure 42. The calculated internal perturbation between the 2e and x transition showing a characteristic avoided crossing. Bottom trace: The calculated intensity ratio for a simple fermi resonance with 4.5 cm^{-1} mixing coefficient.

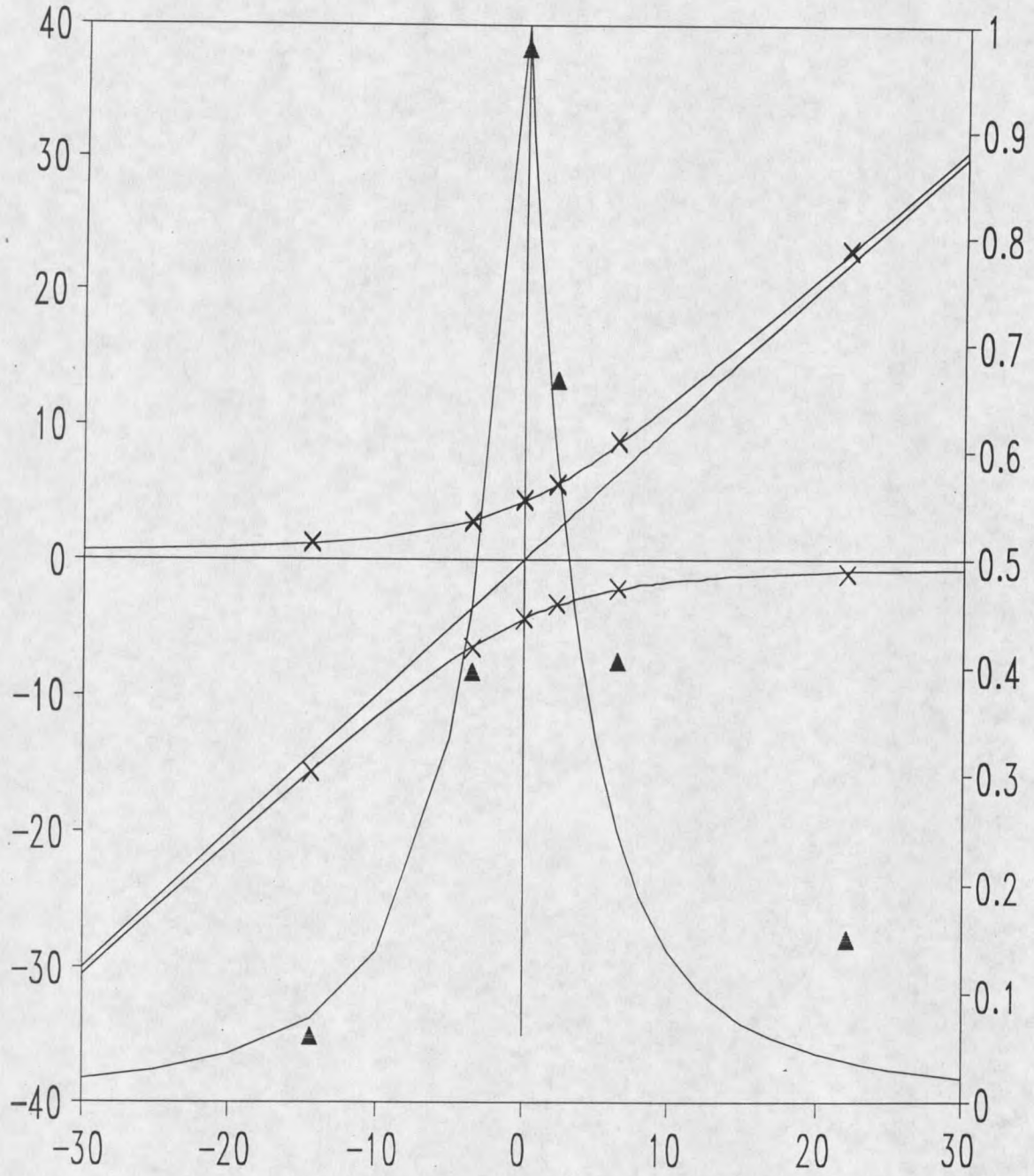

Figure 43. The fitting of the experimental intensities and frequency differences of the fermi resonance between the 2e and e-only phenyl torsion to the calculated internal perturbation.

It is highly unlikely that the transition would have significant intensity apart from the coupling. Perturbation theory can then be used to calculate modifications of the vibrational states caused by the coupling. In regards to a fermi resonance, the degenerate energy states will have an intensity ratio of one, and the energy splitting between the states will be $2b$, where b refers to the coupling matrix element. The five molecules used as an example in Figure 40 have been summarized in Table 25. We have used the para methoxy species as the degenerate level due to the intensity ratio near one. The energy splitting of 8.8 cm^{-1} would suggest a coupling matrix element of 4.4 cm^{-1}. Thus, a perturbed energy difference and an intensity ratio between the two states, shown in Figure 41, can be calculated from the spectroscopic data. The experimental frequencies and intensity ratios are compared to the calculations in Figure 42. The 37^1_0-1e intensities for the electron-donating groups seem to correlate well with the calculations. This is surprising giving the rough approximation of the mixing coefficient. However, the matrix element does not accurately fit the experimental intensities of the electron withdrawing modes as well. Uncertainties aside, the fermi resonance does provide an excellent illustration of new types of internal perturbations opened for the vibrational state mixing in a molecule following methyl substitution.

Photoisomerization

Stilbene is a prototypical molecule to look at the model and mechanism of photoisomerization. Stilbene is a representative of molecules that exhibit a unimolecular reaction, specifically cis/trans isomerization. At first, the photoisomerization of stilbene was recognized as a simple example of a fundamental photochemical process[113]. Presently, it is more acceptable to believe that the photoisomerization process in trans-stilbene is a multidimensional potential energy surface with several key vibrations involved.

The mechanism for the isomerization of stilbene has been extensively studied in solvents and in the gas phase. The isomerization process can be measured quantitatively since a reduction in quantum yield is due to energy being lost to nonradiative transitions. The quantum yield depends on the rate constant and barrier height of the isomerization process.

Focusing on the gas phase, the photoisomerization of stilbene under collisionless conditions requires energy to be moved from excited modes to reactive modes through intramolecular vibrational redistribution (IVR)[114]. IVR plays a crucial role in isomerization in that it is the mechanism by which the energy of the initially excited mode flows into the reactive modes. The onset and extent of IVR can be examined qualitatively in dispersed emission spectra recorded from single vibrational level fluorescence (SVLF) excitation[114]. If a laser is tuned to pump a S_1-S_0 absorption terminating in a level that does not undergo IVR, say a level relatively low in the S_1 manifold, discrete vibrational structure will

be observed in dispersed fluorescence. The broadening occurs since the fluorescence excitation spectra from redistributed modes generally differ from the spectrum of the initially excited SVL. Since the rate and extent of IVR is expected to depend on the density of accepting modes at the initial mode and the coupling strength between the initial modes and accepting modes, it is plausible to relate the broadening to the extent of IVR. The broadening is induced by the extensive coupling among states of different vibrational character. The broadening occurs since the fluorescence from the redistributed modes differ from the spectrum of the initially excited SVL[114].

Studies have shown a connection between the CH_3 group as an accelerating feature in certain photophysical processes such as IVR because the methyl rotor increases the density of states[26]. The acceleration of the IVR by the methyl torsional modes result from the low frequency, great anharmonicity, and its strong anharmonic coupling with other vibrational modes, especially with the phenyl torsional mode of ν_{37}. Spangler has discussed previously that the coupling of methyl rotor levels to phenyl torsion is reasonable since they are twisting on the same axis and the meta positions on the phenyl ring determine the potential barrier of the methyl group. It has been reported recently of the importance of the phenyl ring torsion, ν_{37}, in the photocyclization process of cis-stilbene[28]. The increased density of states in dimethyl-trans-stilbene and the lowering of the barrier to methyl rotation relative to p-methyl-trans-stilbene may

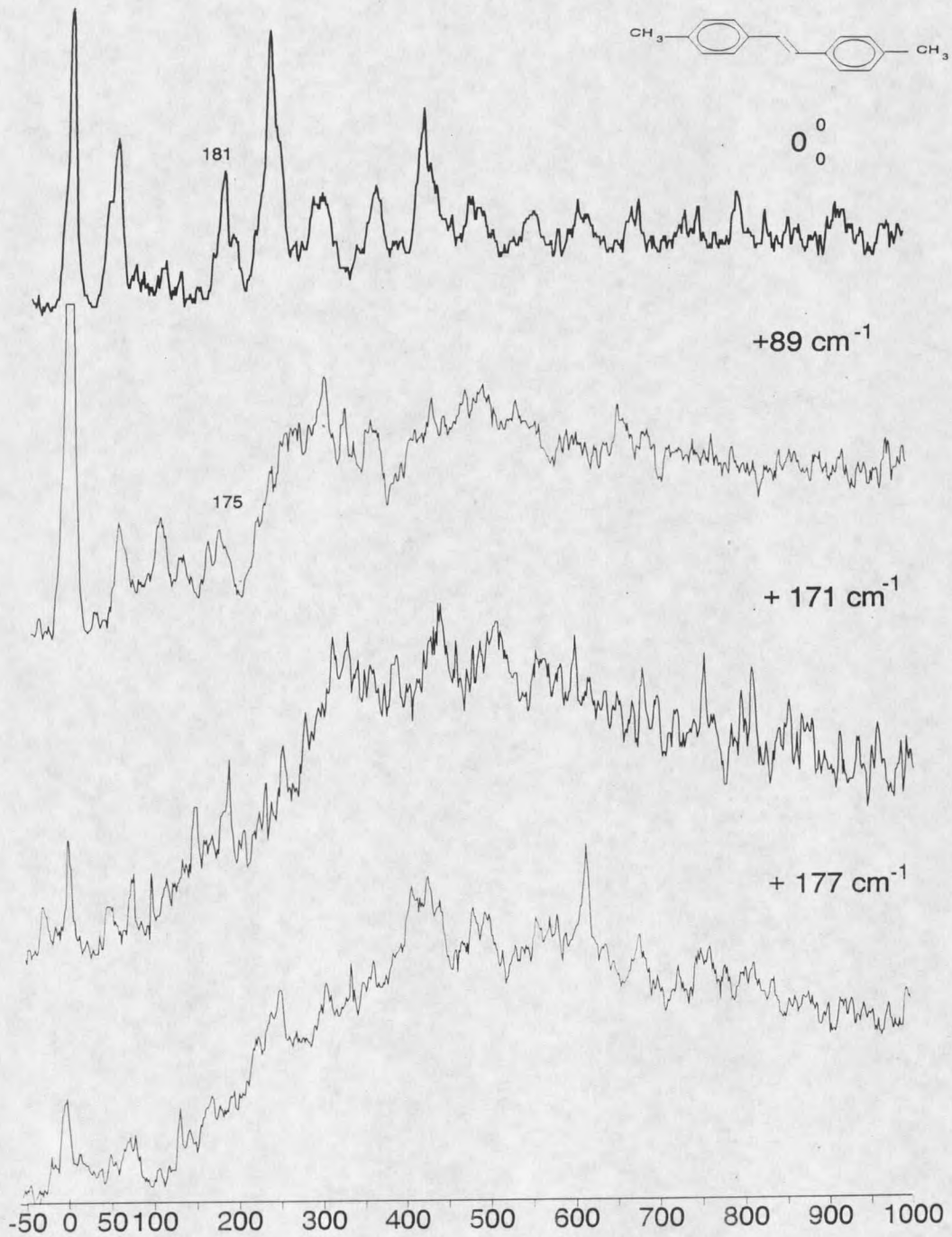

Figure 44. Dispersed emission spectra of p'-p-dimethyl-trans-stilbene recorded for different excitation energies. Note the increase in broad continuum-like fluorescence with increasing energy, indicative of IVR.

allow for efficient coupling to the ring torsions, thus inducing a lower competitive pathway to trans-cis isomerization.

The dispersed fluorescence spectra enables one to examine qualitatively the onset and extent of IVR. An indication of possible IVR dynamics in p'-p-dimethyl-trans-stilbene is shown in Figure 43 which contains SVL emission spectra resulting from excitation into vibronic states at the origin, 89, 171, and 177 cm^{-1}. The discrete emission at the electronic origin gives way to rising congested background near the frequency range of ν_{25}. The diminished intensity of the ν_{25} peaks in the excitation spectrum and the unresolvable dispersed emission from these peaks may indicate the onset of photoisomerization at a low frequency of 170 cm^{-1}. Unique photoisomerization behavior was also found for p'-p-dimethyl-trans-stilbene in solution[116]. Thus in both the gas and liquid phase, the coupling to ν_{37} to the methyl torsional levels might change the reaction coordinate in the isomerization process .

CHAPTER SIX

CONCLUSIONS

The goal of this research was to investigate the effect of remote substituents on the methyl torsional barrier and π electron density in methylated stilbenes. Because of the sharpness of the jet-cooled excitation and emission spectra, accurate assignments for the methyl torsional modes can be given. In all the methylated stilbenes studied in this thesis, the asymmetry in the π density is primarily due to the remote ring not being coaxial with the methyl rotor. Nonetheless, the ground states have low three-fold torsional barriers because the π system is not very delocalized so the central bond and distant ring have a small influence on the methyl substituted ring. Conversely, the excited states of the trans-stilbene derivatives are known to have greater delocalization, and all display higher barriers.

Two electronic origins were found in the spectra of p-hydroxy-trans-stilbene and p-hydroxy-p'-methyl-trans-stilbene, and these origins are due to the two preferred conformers of the hydroxy group. It was observed that the methyl torsional barrier is sensitive to the conformation of the hydroxy group ten carbons away. A 12 cm^{-1} difference between the methyl barriers for the two conformers of the hydroxy group suggests the conformation of the hydroxy group

significantly alters the π electron density ten carbons away in the conjugated system. The nearly identical frequencies that have been observed for p-hydroxy-trans-stilbene and p-methoxy-trans-stilbene and for p'-hydroxy-p-methyl-trans-stilbene and p'-methoxy-p-methyl-trans-stilbene in the excited state and ground state suggests that both molecules act the same under supersonic expansion.

Excitation spectra of the p-hydroxy-p'-methyl-trans-stilbene van der Waals complexes with water show that the excited state methyl barrier is sensitive to hydrogen bonding over ten atoms away. The dramatically different water complexation behavior between p'-hydroxy-p-methyl-trans-stilbene and p'-methoxy-p-methyl-trans-stilbene suggests the hydroxy group donates a proton to the water molecule. Previous work has found that strong electron donors in the para position on the distant ring into the π system reduce the S_1 methyl barrier relative to p-methyl-trans-stilbene. The lower methyl rotor barriers found for the water complexes, as compared to the uncomplexed p'-hydroxy-p-methyl-trans-stilbene, are consistent with this model. Accordingly, this work proves the use of methyl rotors as powerful tools in understanding subtle hydrogen bonding mechanisms in excited states of stilbenes.

The influence of the electronic effects of substituents and their mode of transmission through the aromatic system can be measured by the changes in the barrier to internal rotation relative to 150 cm^{-1} methyl barrier found for p-methyl-trans-stilbene. The fact that the S_1 methyl barrier changes with different remote substituents confirms the influence of the remote ring. There is a pattern

in the reduction of the barrier suggesting that the stronger the electron-donating group, the lower the barrier. This research is one of the first to provide evidence towards a sophisticated mechanism in explaining the sensitivity of the methyl rotor to remote substituents.

The torsional mode plays the most important role in the IVR process of trans-stilbene. We do not see a change in the dynamics of the photophysical properties by changing the potential of the methyl group. Increasing the density of states, however, dramatically increases the congestion and reduces the quantum yield of the fluorescence in these species. The methyl group seems to be at the center of the issue in its' ability to combine with normal modes suspected as agents in dynamics relating to photoisomerization in trans-stilbene.

This thesis gives a comprehensive overview of the electron-donating and withdrawing remote substituent effects on the methyl rotor and the trans-stilbene molecule in general. This work points to the sensitivity of the methyl rotors to the delocalization and asymmetry of the π electronic system via excitation. The data in this thesis may also help in efforts aimed at improving excited state calculations. We have validated the use of methyl barriers as a probe of π electron effects in excited states of moderately sized molecules. The ability to change the barrier by changing the substituent, the substituent's conformation, or by hydrogen bonding the substituent demonstrates the sensitivity of the methyl group.

by hydrogen bonding the substituent demonstrates the sensitivity of the methyl group.

REFERENCE CITED

1. K. Pitzer, Chem Revs., 27, 39 (1940).

2. J. Lowe, Science, 179, 527 (1973).

3. D. Harris, and M. Bertolucci, Symmetry and Spectroscopy, Oxford University Press, 1978.

4. S. Mizushima, Structure of Molecules and Internal Rotation, Academic Press, New York, 1954.

5. K. Umemoto, and K. Ouchi, Proc. Indian Acad. Sci., Chem. Sci. 94, 1 (1985).

6. D. Herschbach, and L. Krisher, J. Chem. Phys. 28, 728 (1958).

7. P. Groner, J. Durig, J. Chem. Phys. 66, 1856 (1977).

8. M. Ito, T. Ebata, N. Mikami, Annu. Rev. Phys. Chem. 39, 123 (1988).

9. W. Hehre, J. Pople, and A. Devaquet, J. Am. Chem. Soc. 98, 664 (1976).

10. M. Baba, U. Nagashima, and I. Hanazaki, J. Chem. Phys. 83, 3514 (1985).

11. J. Murakami, M. Ito, and K. Kaya, Chem. Phys. Lett. 80, 203 (1981).

12. K. Okuyama, N. Mikami, and M. Ito, J. Phys. Chem. 89, 5617 (1985).

13. J. Cable, The Spectrum: Center for Photochemical Sciences, Bowling Green State University, 16-19, Summer 1990.

14. A. Dorigo, D. Pratt, and K. Houk, J. Am. Chem. Soc., 109, 6591 (1987).

15. L. Spangler, W. Bosma, R. VanZee, T. Zwier, J. Chem. Phys., 88, 6768 (1988).

16. J. Hollas, and P. Taday, J. Chem. Soc., Faraday Trans. 86, 217 (1990).

17. S. Larsson, and M. Braga, Chemical Physics, 176, 367 (1993).

18. P. Sautet, and C. Joachim, Chemical Physics, 135, 99 (1989).

19. T. Pascher, J. Chesick, J. Winkler, and H. Gray, Science, 271, 1558 (1996).

20. K. Ohkata, K. Yamamoto, M. Ohsugi, M. Ohsawa, and K. Akiba, Heterocycles, 38, 1707 (1994).

21. M. Zhao, and S. Rice, J. Phys. Chem. 98, 3444 (1994).

22. S. Siewert, and L. Spangler, J. Phys. Chem., 99, 9316 (1995).

23. S. Yan, and L. Spangler, J. Phys. Chem. 99, 3047 (1995).

24. C. Parmenter, and B. Stone, J. Chem. Phys. 84, 4710 (1986).

25. D. Moss, C. Parmenter, and G. Ewing, J. Chem. Phys. 86, 51 (1987).

26. P. Timbers, C. Parmenter, and D. Moss, J. Chem. Phys. 100, 1028 (1994)

27. V. Vachev, J. Frederick, B. Grishanin, V. Zadkov, and N. Koroteev, Chem. Phys. Lett. 215, 306 (1993).

28. J. Frederick, Y. Fujiwara, J. Penn, K. Yoshihara, and H. Petek. J. Phys. Chem. 95, 2845 (1991).

29. T. Suzuki, N. Mikami, and M. Ito, J. Phys. Chem., 90, 6431 (1986).

30. K. Rademann, U. Even, S. Rozen, and J. Jortner, Chem. Phys. Lett, 125, 5 (1986).

31. W. Flygare, Molecular Structure and Dynamics, 2nd ed., Prentice Hall, Englewood Cliffs, NJ, 1978.

32. P. Bunker, Molecular Symmetry and Spectroscopy, Academic Press, New York, NY., 1979.

33. H. Longuet-Higgins, Molecular Physics, 6, 445 (1963).

34. L. Spangler, and D. Pratt, Jet Spectroscopy and Molecular Dynamics, Chapman and Hall, ltd. (1995)

35. W. Gordy, and R. Cook, Microwave Molecular Spectra, 3rd ed., Wiley Interscience, New York, NY 1984.

36. J. Coon, R. DeWames, and C. Loyd, J. Mol. Spectroscopy. 8, 285 (1962).

37. E. Heller, Acc. Chem. Res. 14, 368 (1981).

38. M. Orchin, and H. Jaffe, Symmetry, Orbitals, and Spectra, Wiley Interscience, New York, NY 1971.

39. J. Laane, J. Mol. Struct., 12, 427 (1972).

40. L. Spangler, Ph.D Thesis, University of Pittsburgh 1984.

41. R. Kilb, C. Lin, and E. Wilson, Jr., J. Chem. Phys., 26, 1695 (1957).

42. G. Sorenson, T. Pederson, H. Dreizler, A. Guarnieri, and A. Cox, J. Mol. Struct. 97, 77 (1983).

43. J. Murakami, M. Ito, and K. Kaya, Chem. Phys. Lett. 80, 203 (1981).

44. P. Breen, J. Warren, and E. Bernstein, J. Chem. Phys. 87, 1917 (1987).

45. K. Okuyama, N. Mikami, and M. Ito, J. Phys. Chem. 89, 5617 (1985).

46. R. Bandy, A. Garrett, H. Lee, and T. Zwier, J. Chem. Phys. 96, 1667 (1992).

47. R. Smalley, D. Levy, and L. Wharton, J. Chem. Phys., 64, 3266 (1976).

48. A. Maercker, Organic Reactions, 14, 270 (1965).

49. W. Wadsworth, and A. Emmons, J. Am. Chem. Soc., 83, 1733 (1961).

50. P. Williard, and C. Fryhle, Tet. Lett. 21, 3731 (1980).

51. D. Waldeck, Chem. Rev. 91, 415 (1991).

52. J. Saltiel, and J. Charleston, Rearangments in Ground and Excited States. Mayo Ed.; Academic Press, New York 1980; Vol 3.

53. H. Gorner, and H. Kuhn, Advances in Photochemistry, 19, 1 (1995).

54. G. Fischer, G. Segar, K. Muszkat, and E. Fischer, J. C. S. Perkin II, 1569, (1975).

55. A. Aviram, and M. Ratner, Chem. Phys. Lett. 29, 277 (1974).

56. T. Zwier, E. Carrasquillo, D. Levy, J. Chem. Phys., 78, 5493 (1983).

57. L. Spangler, R. Zee, and T. Zwier, J. Phys. Chem. 91, 2782 (1987).

58. W. Chiang, J. Laane, J. Chem. Phys. 100, 8755 (1994).

59. B. Champagne, J. Pfansteil, D. Plusquellic, D. Pratt, W. Van Herpen, and W. Meerts, J. Phys. Chem. 94, 6 (1990).

60. H. Abe, N. Mikami, and M. Ito, J. Phys. Chem. 86, 1768 (1982).

61. E. Berstein, H. Im, M. Young, H. Secor, R. Bassfield, and J. Seeman, J. Org. Chem. 56, 6059 (1991).

62. J. Syage, P. Felker, and A. Zewail, J. Chem. Phys. 81, 4685 (1984).

63. S. Kim, W. Lee, and D. Herschbach, J. Phys. Chem. 100, 7933 (1996).

64. Sonja Sue Siewert, Ph.D. Thesis, Montana State University 1994.

65. L. Wade, Organic Chemistry , 2nd edition, Prentice Hall.

66. Gibson, A. Jones, and D. Phillips, Chem. Phys. Lett. 136, 454 (1987).

67. A. Warshel, J. Chem. Phys., 62, 214 (1975).

68. Beilsteins Handbuch Der Organischen Chemie Vierte Auflage Vol 644, p 311.

69. A. Marshall, A. Clark, R. Jennings, K. Ledingham, J. Sander, and R. Singhal, Int. J. Mass Spect. and Ion Proc., 116, 143 (1992).

70. J. Zhu, D. Iustig, I. Sofer, and D. Lubman, Anal. Chem., 62, 2225 (1990).

71. D. Bent, and D. Schulte-Frohlinde, J. Phys. Chem. 78, 451 (1974).

72. H. Gorner, Ber. Bunseges. Phys. Chem. 88, 1199 (1984).

73. A. Neckers, Adv. in Photochemistry.

74. Sugiyama, Y; Suzuki, Y.; Mitamura, S.; and Nishiyama, T. Bull. Chem. Soc. Jpn., 66, 687 (1993).

75. R. Gordon, J. Hollas, P. Ribeiro-Claro, and J. Teixeira-Dias, Chem. Phys. Lett. 211, 392 (1993).

76. H. Gruen, H. Gurner, Z. Naturforsch. 38a, 928 (1983).

77. R. Weersink, S. Wallace, J. Phys. Chem. 97, 6127 (1993).

78. R. Daum, T. Hansson, R. Norenberg, D. Schwarzer, and J. Schroeder, Chem. Phys. Lett. 246, 607 (1995).

79. E. Gibson, A. Jones, A. Taylor, W. Bouwman, D. Phillips, and J. Sandell, J. Phys. Chem. 92, 5449 (1988).

80. D. DeHaan, A. Holton, and T. Zwier, J. Chem. Phys. 90, 3952 (1989).

81. T. Zwier, J. Chem. Phys. 90, 3967 (1989)

82. R. Howell, H. Petek, D. Phillips, and K. Yoshihara, Chem. Phys. Lett. 183, 249 (1991).

83. V. Grassian, J. Warren, and E. Bernstein, J. Chem. Phys. 90, 3994 (1989).

84. R. Gordon, J. Chem. Phys. 93, 6908 (1990).

85. S. Lunak, M. Nepras, R. Hrdina, and H. Mustroph, Chem. Phys. 184, 255 (1994).

86. M. Senent, D. Moule, Y. Smeyers, and F. Penalver, Chem. Phys. Lett. 221, 512 (1994).

87. L. Pierce, J. Chem. Phys. 31, 547 (1959).

88. J. Meier, A. Bauder, and H. Günthard, J. Chem. Phys. 57, 1219 (1972).

89. M. Senent, D. Moule, and Y. Smeyers; J. Phys. Chem. 99, 7970 (1995).

90. J. Durig, P. Groner, M. Griffin, J. Chem. Phys. 66, 3061 (1977).

91. L. Spangler, and D. Pratt, J. Chem. Phys. 84, 4789 (1986).

92. T. Urano, H. Hamaguchi, M. Tasumi, K. Yamanouchi, S. Tsuchiya, and T Gustafson. J. Chem. Phys. 91, 3884 (1989).

93. W. Chiang, and J. Laane, J. Phys. Chem. 99, 11823 (1995).

94. P. Breen, E. Bernstein, H. Secor, and J. Seeman, J. Am. Chem. Soc. 111, 1958 (1989).

95. S. Humphrey, and D. Pratt, J. Chem. Phys. 99, 5078 (1993).

96. J. Smith, X. Zhang, A. Thompson, C. Lakshminarayan, and J. Knee, J. Phys. Chem. 97, 3990 (1993).

97. V. Grassian, E. Berstein, H. Secor, and J Seeman. J. Phys. Chem. 93, 3470 (1989).

98. L. Kruse, C. DeBrosse, C Kruse, J. Am. Chem. Soc., 107, 5345 (1985).

99. T. Troxler, M. Topp, B. Metzger, and L. Spangler, Chem. Phys. Lett., 238, 313 (1995).

100. R. Knochenmuss, and S. Leutwyler, J. Chem. Phys. 91, 1268 (1989).

101. A. Oikawa, H. Abe, N. Mikami, and M. Ito, J. Phys. Chem., 87, 5083 (1983).

102. M. Pohl, M. Schmitt, and K. Kleinermanns, J. Chem. Phys. 94, 1717 (1991).

103. N. Pugliano and R. Saykally, Science, 257,1937 (1992).

104. A. Oikawa, H. Abe, N. Mikami, and M. Ito, J. Phys. Chem., 88, 5180 (1984).

105. Lahmani, A. Douhal, E. Breheret, A. Zehnacker-Rentien, Chem. Phys. Lett. 220, 235 (1994).

106. S. Kim, S. Li, and E. Bernstein, J. Chem. Phys. 95, 3119 (1991).

107. S. Kim, S. Hsu, S. Li, and E. Bernstein, J. Chem. Phys., 95, 3290 (1991).

108. P. Haag, R. Spooren, M. Ebben, L. Meerts, and J. Hougen, Molecular Physics, 69, 265 (1990).

109. X. Tan, W. Majewski, D. Plusquellic, and D. Pratt. J. Chem. Phys. 94, 7721 (1991).

110. A. Gorse, and M. Pesquer, J. Chem. Phys. 99, 4039 (1995).

111. E. Gilabert, R. Lapouyade, and C. Rulliere, Chem. Phys. Lett.145, 262 (1988)

112. D. Sammeth, S. Siewert, P. Callis, and L. Spangler, J. Chem. Phys., 96, 5771 (1992).

113. A. Olsen, Trans. Faraday Soc. 27, 69 (1931).

114. J. Syage, P. Felcker, and A. Zewail, J. Chem. Phys. 81, 4706 (1984).

115. S. Yamamoto, K. Okuyama, and M. Ito, Chem. Phys. Lett. 125, 1 (1986).

116. N. Park, and D. Waldeck, J. Chem. Phys. 91, 943 (1989).

117. Rediington, T. Redington, B. Rajaram, and R. Field, J. Chem. Phys. 97, 1624 (1992).